SURVEY OF INSTRUMENTATION APPLICABLE TO THE STUDY OF ROCKET EXHAUST PLUMES

C. H. Fisher
ARO, Inc.

May 1971

VON KÁRMÁN GAS DYNAMICS FACILITY
ARNOLD ENGINEERING DEVELOPMENT CENTER
AIR FORCE SYSTEMS COMMAND
ARNOLD AIR FORCE STATION, TENNESSEE

NOTICES

When U. S. Government drawings specifications, or other data are used for any purpose other than a definitely related Government procurement operation, the Government thereby incurs no responsibility nor any obligation whatsoever, and the fact that the Government may have formulated, furnished, or in any way supplied the said drawings, specifications, or other data, is not to be regarded by implication or otherwise, or in any manner licensing the holder or any other person or corporation, or conveying any rights or permission to manufacture, use, or sell any patented invention that may in any way be related thereto.

Qualified users may obtain copies of this report from the Defense Documentation Center.

References to named commercial products in this report are not to be considered in any sense as an endorsement of the product by the United States Air Force or the Government.

SURVEY OF INSTRUMENTATION APPLICABLE TO THE STUDY OF ROCKET EXHAUST PLUMES

C. H. Fisher
ARO, Inc.

FOREWORD

The research reported herein was sponsored by Arnold Engineering Development Center (AEDC), Air Force Systems Command (AFSC), Arnold Air Force Station, Tennessee, under Program Element 921E and NASA-Defense Purchase Request No. H-58562A.

The results of the research were obtained by ARO, Inc. (a subsidiary of Sverdrup & Parcel and Associates, Inc.), contract operator of AEDC, AFSC, Arnold Air Force Station, Tennessee, under Contract F40600-71-C-0002. The work was performed from November 1969 to March 1970 under ARO Project No. ST 1027, and the manuscript was submitted for publication on October 20, 1970.

The following individuals have made significant contributions to the text of this report: Mr. W. N. MacDermott for Section 2.2, Mr. H. T. Bentley III for Section 5.1.2, and Dr. J. D. Trolinger for the preliminary VKF (AEDC) Tunnel F test report on holographic velocimetry in Section 5.2.2.

This technical report has been reviewed and is approved.

Emmett A. Niblack, Jr.
Lt Colonel, USAF
AF Representative, VKF
Directorate of Test

Joseph R. Henry
Colonel, USAF
Director of Test

ABSTRACT

A review of measuring techniques and instrumentation which may be of use in the study of rocket exhaust plumes is presented in a twofold manner. The most practical techniques which have proven successful through actual application in rocket exhaust studies or related environments are treated in an integrated fashion within a plume analysis framework. An additional descriptive collection of appropriate techniques and instrumentation have been compiled into an appendix. This report is organized around those measurements considered most important: temperature. pressure, density. and velocity.

CONTENTS

Page

ABSTRACT iii
I. INTRODUCTION 1
II. TEMPERATURE
2.1 Translational Temperature Measurements 3
2.2 Rotational and Vibrational Temperature Measurements 4
2.3 Total Temperature Measurements 8
2.4 Electron and Ion Temperature Measurements 9
III. PRESSURE
3.1 Absolute or Direct Pressure Measurements 12
3.2 Nonabsolute or Indirect Pressure Measurements 15
IV. DENSITY
4.1 Molecular or Gas Density Measurements 15
4.2 Electron and Ion Density Measurements 24
4.3 Particle (Micron Size) Density Measurements 27
V. VELOCITY
5.1 Gaseous or Molecular Velocity Measurements within the Flow Field of a Compressible Media 28
5.2 Measurement of Micron-Size Particle Velocities 30
VI. SUMMARY
6.1 Temperature 36
6.2 Pressure 38
6.3 Density 39
6.4 Velocity 40
REFERENCES 41

APPENDIXES

I. ILLUSTRATIONS

Figure

1. Intensity Ratio of (0,1) and (1,0) Bands versus T_{vib} 59
2. Sample Log I_K' Plot 60
3. Robben/Talbot Calibration Curve 61
4. Effect of Nonlinear Log I_K' Plot 62
5. Static Temperature in Hypersonic Nozzle for p_o = 10 atm and T_o = 4000°K 63
6. Construction Details of the Boundary-Layer Total Temperature Probe 64
7. Simple Tare-Measurement Probe for Enthalpy, Impact Pressure, and Gas Composition in Extremely High Heat-Flux Environments 65
8. Cross Section of Pitot-Static Tube 66
9. Strain-Gage Transducers 67
10. Simplified Schematic of a Differential Capacitance Diaphragm Pressure Sensor 68

Figure | Page

11. Schematic Arrangement for Attenuation or Absorption Measurements 69
12. Typical Component Arrangement for Measuring Electron-Beam-Induced Fluorescence 70
13. Principle of Density Measurement by Electron Scattering 71
14. Calibration Curve Obtained in the Low Density Wind Tunnel 72
15. Density Profile Measured in the Low Density Wind Tunnel
    a. Cold Flow 73
    b. Hot Flow 73
16. Typical Measuring Arrangement for the Bremsstrahlung Technique 74
17. Basic Cosmic Dust Sensor Schematic 75
18. Antenna Geometry for Free-Stream Velocity Measurement Using the Doppler Radar Technique 76
19. Line Broadening 77
20. Display of Typical Doppler-Shifted Lines
    a. Two Single Lines 78
    b. Composite of Lines 1 and 2 78
21. Absolute Line Shift 79
22. Comparison of the Shifted and Unshifted Argon Line as Recorded with Standard Iron Lines 80
23. Rotating Refractory Plate 81
24. Block Diagram for System for Measurement of Velocity Distributions in a Highly Expanded Plume 82
25. Schematic Diagram of Typical Single Component Laser Anemometer System . . 83
26. Typical Three-Dimensional Laser Doppler Anemometer 84
27. Laser Doppler Particle Velocity System with Fabry-Perot Interferometer 85
28. Typical Holography (Recording Phase)
    a. In-Line 86
    b. Off-Axis 86
29. VKF Tunnel F Holocamera Arrangement 87

II. TECHNICAL BRIEFS
Temperature 88
Pressure 94
Density 97
Velocity 109

SECTION I
INTRODUCTION

The objective of this report has been to review, evaluate, and consolidate, in a condensed compilation, existing techniques which may be applicable to the measurement of aerodynamic properties of rocket exhaust plumes. As a word of caution, each technique should be studied carefully by means of the references provided to fully determine the degree of relevance when a particular environmental measurement is considered.

The body of the report concerns itself with those techniques that have been chosen from the standpoint of their proven value in extracting the desired parameter. Discussion, although not elaborate, is entertained in sufficient detail to allow a competent decision to be reached on the applicability of a technique to a particular analysis. References are cited for each technique as an assurance of the completeness of the evaluation process.

An appendix (Appendix II) of additional techniques, presented in brief categorized form for ease in scanning, concludes the report. The abstract of each outline is taken directly from the referenced report.

In the body and also in Appendix II the techniques are listed under four main parameter classifications: temperature, pressure, density, and velocity. Many of the methods offer a multiparameter analysis; in these cases an attempt has been made to categorize the technique under the most appropriate parameter heading.

SECTION II
TEMPERATURE

In addition to their internal energies, basic particles, such as free electrons and atomic nuclei, primarily exhibit translational (kinetic energy of a particle associated with the translation of its mass through space) and spin energies. As the atomic structure becomes more complex, atoms have, in addition to the complex energies associated with the atomic nuclei, energies associated with the orbital electrons. Since molecules consist of two or more atoms, they may have, in addition to translational, spin, and electronic energies, rotational and vibrational energies. These energies are a result of the vibratory reaction of the nuclei with the internuclear binding forces and a whole body rotation of the molecule. Therefore the total energy of the molecule in general can be represented by a summation consisting of the following elements: (1) the translational energy, (2) the nuclear binding energies, (3) the rest mass energies, (4) the sum of the electron orbital energies, (5) the sum of the rotational energies, (6) the sum of the vibrational energies, (7) the sum of the electron-spin energies, (8) the sum of the nuclear-spin energies, and (9) the sum of the interaction energies among these modes. In brief, the total energy of a particle in a particular state can be expressed as the sum of the translational energy and the internal energy. Translational energies of all particles occur in a continuum and may be the result of random or directed velocities. All the other energy modes are quantized (occur only in discrete magnitudes).

An important extension of this molecular hypothesis of finite energy partitions is the kinetic theory of heat which assumes that molecules move more or less rapidly corresponding to the degree of hotness or coldness exhibited by the body of which the molecules are a part. The kinetic theory of heat postulates that the heat energy of the body is in reality mechanical energy consisting of the kinetic and potential energies of the associated molecular motions relative to the body as a whole. This was shown by Joule in his experimental studies of the mechanical equivalent of heat to indeed be the case. Since heat energy is regarded as hidden mechanical energy it must be expressible in terms of mechanical units. The fact that heat is not a material substance, but that its presence in a body is related to the energy resident in the random motions of the particles of which the body is composed, was first suggested by Francis Bacon in 1620.

Any mode of energy can serve as the basis for the measurement of a particular temperature, subject to the condition that statistical equilibrium prevails for storage within this mode. This defines a unique rotational temperature, a unique vibrational temperature, and so on.

A temperature of considerable interest to the aerodynamicist is the temperature associated with the mean translational kinetic energy of the gas molecules. This is the temperature most often used to describe the thermal energy or aggregate thermal content of a gas. In kinetic theory this temperature, T, referred to as the kinetic-theory temperature, is defined directly in terms of the peculiar speeds of the molecules by the relation (Ref. 1)

$$1/2\, m\overline{C^2} = 3/2\, kT$$

where k is a constant which is the same for all gases. The peculiar speed denoted by C is explained in Ref. 1. In the equation m is representative of the molecular mass.

Another closely related temperature, the thermodynamic temperature, arises from the various attempts that have been made to express temperature on an absolute numerical scale. Probably the most illustrative of these solutions is based on a thermodynamic principle first proposed by William Thomson (later Lord Kelvin) in 1848. Lord Kelvin showed that the efficiency of a reversible engine working between two temperatures is a function of the temperatures only and is completely independent of the physical properties of any material substance. The quantities of heat given off or taken in by a reversible engine working between the two temperatures are assumed to be proportional to the temperatures. Values of temperatures on this scale are close to those obtained with the hydrogen thermometer (the change in pressure of a constant volume of hydrogen under specified conditions can serve as a fundamental measure of the temperature change). Since hydrogen does not completely ascribe to the conditions of an ideal gas, small corrections must be made. Temperatures expressed on an absolute numerical scale are referred to as absolute temperatures.

It is shown in Ref. 1 that it is possible to establish the fact that the kinetic-theory temperature is proportional to the temperature of the thermodynamic scale. In other words, the thermodynamic temperature is proportional to the mean translational kinetic

energy per molecule which is relative to the general motion of the gas. The constant of proportionality depends on the units of energy and temperature and not on the gas.

In aeronautical nomenclature temperature is often defined by a particular state of the gaseous system in question. An example is the static temperature, which is a temperature taken where the bulk gas velocity is zero.

Up to this point the properties discussed have been related to molecular or microscopic systems. For completeness a brief comment on the statistical link between these microscopic systems and the thermodynamic properties is necessary. The connection between thermodynamics and statistical mechanics is the H-theorem or a postulate relating entropy to the thermodynamic probability which is related to the partition function. The partition function describes a relationship between the thermodynamic coordinates of a macroscopic system and the coordinates of the constituent microscopic systems.

A complete treatment of these basic concepts can be found in Refs. 1 through 9. Recommended reading for anyone involved in temperature measurements should include Refs. 10 and 11 which provide an excellent treatment of the basic concepts, standards, and techniques. With these thoughts in mind, the most applicable temperature measurement techniques for rocket exhausts will be explored in the following sections.

2.1 TRANSLATIONAL TEMPERATURE MEASUREMENTS

The movement of gas molecules as a result of thermal energy produces an optical emission line broadening with a half-width proportional to $(T/M)^{1/2}$, where M is the molecular weight of the element. Since T is the translational temperature, Doppler broadening should be a suitable technique for measurement of this parameter, especially for the lighter elements and at elevated temperatures. Doppler broadening of an emission line is attributable to the parallel or antiparallel component of motion of the atom or molecule to the line of sight, which allows a $T_{perpendicular}$ and a $T_{parallel}$ measurement of T in a rarefied flow.

The technique is based on the dependence of the width of a discrete spectral line upon the translational velocity distribution of the emitting species. The half-width, α_D, is given in terms of the gas temperature, T(°K), the wave-number of the radiant energy, ν, and the molecular weight, M (Ref. 12).

$$\alpha_D = [8 (\ell n\, 2)\, RT/Mc^2]^{1/2}\, \nu$$

where R is the gas constant and c is the velocity of light. This equation applies only for the case of Doppler broadening.

For a range of low pressures (at high densities spectral line broadening is density dependent) the dominant factor in spectral line widths (excluding fine and hyperfine structure) is attributable to Doppler broadening. Although a direct measurement of the half-width determines the temperature, this is an extremely difficult measurement to make because of the high wavelength resolution that is required.

Although the Doppler broadening technique is presently the most hopeful prospect for translational temperature measurements in low density gases, this is not the only method available. For example, the wings of the Rayleigh line of Raman scattering depend upon the translational temperature and the number density.

Since spectrum lines can be broadened by other mechanisms, a thorough analysis should be made to determine if other sources of line broadening are present before a temperature measurement is attempted.

A system which has successfully measured velocity distributions of molecular beams separated from rocket plume flow fields (Ref. 13) is presently being investigated as a feasible means of measuring translational temperature. Since the probe samples only one component of the velocity distribution, a study is being conducted by the Aerospace Division of the von Kármán Gas Dynamics Facility (VKF) at AEDC to define a relationship between this singular measurement and the translational temperature.

2.2 ROTATIONAL AND VIBRATIONAL TEMPERATURE MEASUREMENTS

2.2.1 Original Work

The first quantitative study of temperature measurements in a flowing gas by means of spectral analysis of the emission produced by electron beam excitation was that of E. P. Muntz (Ref. 14). In that work, the relation between gas vibrational and rotational temperatures and intensity of emission of the various vibrational bands and rotational lines, respectively, of the N_2^+ first negative band spectrum produced by electron beam bombardment of the gas was established theoretically and verified experimentally for a limited range of temperature. The theory for both the vibrational band and rotational line intensity was based on an excitation-emission model which allowed for only direct excitation to the emitting state ($N_2^+ B_2\ \Sigma$) of the nitrogen molecular ion, followed by spontaneous emission to the ionic ground state ($N_2^+ X^2\ \Sigma$). Effects of population of the emitting state by any other processes were considered to be negligible.

The intensity of emission in a given vibrational band (v',v'') was determined for this excitation-emission model using Franck-Condon factors for both excitation and emission for the transitions involved. Here, v' is the vibrational quantum number of the emitting state and v'' that for the final state of the emission process. The ratio of intensity of certain vibrational bands, $(Iv'_1,v''_1)/I(v'_2,v''_2)$, was found to be a convenient function of the temperature (T_{vib}) characterizing the vibrational energy distribution of the target nitrogen molecules. A large number of such band intensity ratios are usable, but practical considerations of the absolute band intensities limits this number to four or five. In Fig. 1 (Appendix I) the intensity ratio for the (0,1) and (1,0) bands of the N_2^+ first negative system as a function of T_{vib}, as given in Ref. 14, is presented. These two bands are found at 4278 and 3582Å, respectively.

The intensity of a given rotational line, I_K', within a given vibrational band (v',v'') was derived for the same excitation-emission model. using the relative transition probabilities normally associated with optically allowed transitions (Honl-London factors).

Here, K′ is the rotational quantum number of the emitting state and, for optically allowed transitions, $\Delta K' = \pm 1$, $\Delta K' \neq 0$. The functional dependence was given as

$$I_{K'} = C\nu_{K'}^4 \, K'[G] \exp\left[-\left(\frac{\theta_{rot}}{T_{rot}}\right) K'(K'+1)\right]$$

where $\nu_{K'}$ is the wave number of the K′ line, θ_{rot} is the rotator constant (2.891°K for N_2), T_{rot} is the temperature characterizing the distribution of rotational energy states in the target N_2, and the constant of proportionality, C, is determined by the gas density and beam parameters. The presence of the product of K′ and the exponential indicates that the $I_{K'}$ distribution with respect to K′ will be similar to an equilibrium Maxwell-Boltzmann distribution of rotational states. The factor [G], tabulated in Ref. 14 as a function of K′ and T_{rot}, allows for a perturbation of the Maxwell-Boltzmann distribution in the excited states produced by the electron beam. The use of this relation for $I_{K'}$ follows standard spectral diagnostic practice: a plot of $-\log \{I_{K'}/(\nu_{K'}K'[G])\}$ versus $K'(K'+1)$ for a number of rotational lines in the same vibrational band will give a straight line with a slope of θ_{rot}/T_{rot}, Fig. 2. For practical reasons, almost all applications of this technique have been confined to the most intense vibrational band (0,0) of the first negative system, located at 3914Å.

By application of this technique to various experimental flows of nitrogen having known static temperatures, it was found that log $I_{K'}$ plots were linear for K′ out to 18 and that the reduced temperatures were correct within ±2 percent. Muntz thus concluded that his excitation model was correct and that the technique was a 2-percent technique at least for pressures from 150 to 500 microns, temperatures from 170 to 373°K, beam voltages from 12 to 20 kev, and beam currents from 85 to 250 μamp. Measurements of both T_{rot} and T_{vib} were also demonstrated in a small uncalibrated arc jet in which self-radiation was present.

This work was carried out with a grating spectrograph and photographic emulsions for recording of the spectral data. In subsequent work, a technique was developed for T_{rot} measurements in short-duration shock tunnel flows in which the rotational structure of the band was not fully resolved. The spectrograph was replaced by properly tailored narrow-band interference filters which isolated separate regions of the vibrational band, and detection was by photomultiplier tubes (Refs. 15, 16, and 17).

2.2.2 Subsequent Applications

Muntz' pioneering work was extensively adopted by a number of wind tunnel laboratories as the first practical means of direct measurement of temperature in a flowing gas. Petrie (Ref. 18) and Sebacher (Ref. 19) both applied the rotational and vibrational temperature measurement in arc-heated wind tunnels operating at sufficiently high stagnation temperature that nonequilibrium effects in the nozzle expansions were expected. Measured rotational temperatures were in the range from 150 to 400°K, in apparent equilibrium with translational temperature, and vibrational temperatures were in the range from 1600 to 3500°K, frozen at some large fraction of the stagnation temperature. These measurements were used to infer the nonequilibrium effects in the

flow by comparison with complete equilibrium and frozen flow models. Marsden (Ref. 20) made a unique application of the technique in a study of the energy accommodation of rarefied nitrogen on a solid surface in a static test chamber. The vibrational band structure was recorded by photomultiplier technique rather than by the cumbersome and inaccurate photographic emulsion, and this practice has now been almost universally adopted in the field. Also, for the first time, evidence of possible shortcomings in the Muntz theory was reported. Careful measurements in the static chamber indicated that the measured T_{rot} was equal to the supposed gas temperature above 400°K, but below this temperature a systematic increase of T_{rot} over the gas temperature was found which reached 3 percent at 300°K.

The accuracy of the measurement below 300°K subsequently came under even more serious question with publication of Ref. 21 by Robben and Talbot and Ref. 22 by Marrone. These experiments marked the extension of the rotational temperature technique to unheated low density expansions in which static temperatures fell to very low levels (5 to 10°K). The results of these two independent laboratories were in direct contradiction. Marrone reported no difference between measured rotational temperature and temperature inferred from aerodynamic flow calibration for temperatures as low as 55°K. Robben and Talbot, on the other hand, reported an increasing trend towards excessive measured rotational temperature as the temperature level was lowered. A calibration curve was given in Ref. 21 with which it was recommended that all T_{rot} data be corrected (Fig. 3). This curve agrees with Marsden's observation at 300°K and may be regarded as a continuation of the trend first noted in Ref. 20. In addition to these primary results, Refs. 21 and 22 both reported evidence of non-Maxwellian distributions of rotational states at low temperatures in the form of nonlinear log I_K' plots. Robben and Talbot found this to be generally characteristic of low temperature flowing gases, but Marrone found the nonlinearity to occur only after a certain point in any given low density expansion.

2.2.3 Accuracy of the Method

It is important to consider that for rotational temperatures above 300°K, the electron beam measurement technique as interpreted by Muntz' theory is accurate[1] to 3 to 6 percent and is, therefore, the most precise spectrometric temperature measurement available. Even at temperatures as low as 100°K the inaccuracy is no more than 8 percent, and for many purposes measurements of sufficient accuracy can be made at this temperature.

Below about 80°K, however, the uncertainty becomes prohibitive for almost all purposes. Naturally, research groups working in this temperature range have been especially active in attempting to clarify the status of the technique. Ashkenas, Ref. 23, using a liquid-nitrogen-cooled static calibration channel to eliminate uncertainties in aerodynamic calibration, uncovered information which complicated the situation even

[1] Hunter at NASA (Langely) performed T_{rot} measurements from 300 to 1100°K and found an increasing discrepancy, rising to 6 percent at 1100°K.

more. Nonlinear log I plots were found at 77°K and, upon close inspection, even at 300°K. This led to a definite ambiguity in the measured rotational temperature, that is, a dependence of T_{rot} on the number of rotational lines used (Fig. 4). Agreement with Robben and Talbot's data is observed if only 21 rotational lines are used at 300°K and 8 lines at 78°K. An apparent dependence of T_{rot} on the static gas density was also observed; however, this may have been a manifestation of dependence on electron/molecule collision rate.

Hickman, Ref. 24, suggested that Muntz' excitation model, based on optically allowed transitions, was inadequate and re-derived the rotational intensity distribution function for a different excitation model in which transitions of $\Delta K' = \pm 3$ as well as ± 1 were allowed. The result is functionally similar to Muntz' relation, shown above, except that the [G] function is much more complex. In some experimental applications, Hickman's model appears to give appreciably better results than does Muntz', but there are others in which it does not. As a result, the status of the rotational measurement technique is still uncertain for temperatures below 80°K.

The accuracy of determination of nitrogen vibrational temperature by the foregoing method is no better than the precision of the vibrational transition probabilities used—approximately 10 percent. So far, no efforts have been reported to calibrate the vibrational temperature measurement although this appears to be a badly needed experiment. Since Muntz' initial publication, new and presumably more accurate values of the transition probabilities have become available which should increase the accuracy of the vibrational temperature measurements. Further study of this problem indicates that judicious selection of vibrational bands circumvents the need for accurate band strengths and the Franck-Condon factors can be used instead. If the excitation cross sections are correct, 1-percent accuracy is expected.

An example of the fruitful utilization of the rotational temperature measurement even in the range where its accuracy is only 8 percent is given in Fig. 5. The static temperature at the exit of a hypersonic wind tunnel nozzle operated with arc-heated air at a supply pressure of 10 atm and supply temperature of 4000°K is plotted versus area ratio in the nozzle expansion. Calculated curves are shown for the two limiting cases of complete equilibrium and completely frozen flow as well as for two expansions having chemical reactions and vibrational energy transfers occurring at finite rates. Clearly, since the total nonequilibrium effect on the static temperature of the flow is of the order of 200°K, the 8-percent experimental temperature measurement is entirely adequate for evaluation of the finite-rate calculations.

The electron beam temperature measurement technique offers a unique method of measuring static temperatures in a flowing low density gas containing large amounts of molecular nitrogen. In determination of rotational temperatures, it is sufficiently accurate (3 to 6 percent) at temperatures of 300°K and above. Because of uncertainties in the underlying theory of the measurement, the accuracy is degraded as the temperature is decreased, reaching 8 percent at 100°K.

The electron beam vibrational measurement technique is generally considered to be about 10-percent accurate. Recent developments have introduced the possibility of improving the accuracy of this method.

2.2.4 Analysis of Metastable Beam Fluorescence

A study is presently under way in the Engine Test Facility (ETF) T Cells Special Projects Branch of ARO, Inc., at AEDC to determine the feasibility of utilizing metastable beam fluorescence to measure variables of low density gas flows including the rotational and vibrational temperatures. Results thus far indicate that metastables, because of their larger collision cross section, offer a distinct gain in sensitivity and resolution over the electron beam excitation technique, particularly at lower densities. As the density increases, the problem of beam spreading becomes quite pronounced because of the large elastic cross section of metastable atom/molecule collisions. It should be noted that at sufficiently low densities, electron beam diagnostics can be employed to much better advantage than metastable atomic beam diagnostics by lowering the electron beam energy to increase the excitation cross section.

2.3 TOTAL TEMPERATURE MEASUREMENTS

The total temperature can be regarded as that temperature which would prevail if all the energy states of the gas were in equilibrium with the translational energy states. Various techniques have been developed to measure free-stream total temperature. Typical of these methods are spark velocity (Ref. 25) and wave velocity measurements (Ref. 26) which produce an average velocity over a comparatively large scale from which the temperature can be deduced. Since the spatial resolution of these measurements is limited, these techniques are unsuited for high resolution measurements in the vicinity of boundary effects as encountered in an expanding exhaust plume.

Another, and most popular, approach to the direct measurement of a total temperature is the insertion of a small physical probe, instrumented with heat sensing devices, into the flow. In Ref. 27, features which can limit the application of probes of this type in the measurement of a total temperature are considered. Primary among these considerations is the probe response time.

With these criteria in mind a miniature short-time-response total temperature probe has been developed based on the shielded thermocouple principle (Ref. 28). This instrument as shown in Fig. 6 is typical of the general trend which exists in direct total temperature measurements utilizing a physical probe.

A general description of this device is as follows. A heated shield minimizes radiative and conductive losses from a thermocouple formed from 0.025-mm-diam wires. The probe operates as a null measuring device; two runs at temperatures spanning the flow temperature enable estimation of the flow temperature to within ±3 percent. With a prototype probe, a full temperature-time history of the flow was obtained from a minimum of three hypersonic gun tunnel runs. The shield temperatures were set up before each run to span the expected range of flow temperature. The temperature at any

given time was obtained by joining the three thermocouple temperatures by a straight line through the three shield temperatures. Unfortunately rocket exhaust flow parameters vary considerably from run to run. This problem could be eliminated by using multiple probe rakes to define a profile during one run.

In Ref. 28 a theoretical model of the probe operation is presented which demonstrates the physical parameters affecting the response time and accuracy limitations of this type of probe. In addition, experimental results of total temperature measurements are described. A Mach number range from 8 to 11.5 and a Reynolds number range from 5×10^6 to 2.7×10^7 were investigated. The wall-to-free-stream total temperature ratios were between 0.26 and 0.36. The tunnel stagnation temperature was within the range from 800 to 1100°K.

For measurements under extreme temperature (15,000°K) and high enthalpy (typical: 10,000 Btu/lb) conditions there are the miniature, high-pressure, liquid-cooled calorimetric probes (Refs. 29 through 33). A typical probe configuration is shown in Fig. 7. Since the total temperature is determined from the total enthalpy, a word of caution should precede the use of these probes as sensors of the total temperature. Implicit in the enthalpy measurement is the assumption that the probe external heating remain constant for both the flow and no-flow conditions of probe operation. For this reason these instruments are under scrutiny as to their applicability as a means of high temperature measurement.

Total temperature measurements have also been performed using a pulse heated wire technique (Ref. 34). The wire recovery temperature is deduced from certain measured temperature-time histories of a thin wire pulse heated in the flow and in a vacuum. Temperatures up to 1100° K have been measured indirectly using this method.

2.4 ELECTRON AND ION TEMPERATURE MEASUREMENTS

Various configurations of electrostatic probes have long been used to determine the electron and ion temperatures of ionized gases or plasmas. Basic among these is the well-known Langmuir probe.

The Langmuir probe is a charged particle collector, which, when exposed to an ionized gas and operated at varying potentials with respect to the surrounding gas, allows the calculation of electron and ion temperatures from current-potential relationships. The conceptual application and mathematical formulation were developed in the early 1920's by Irving Langmuir and H. M. Mott-Smith (Refs. 35 through 38). Extensive theoretical and numerical analysis of the Langmuir probe technique complete with experimental results has been recorded throughout the field of scientific literature (Refs. 39 through 43).

When the probe is used to obtain electron and ion temperature, careful attention to the analysis of the data is required. The largest single source of error is a result of the alien disturbance the mass of the probe induces into the surrounding ionized region. This effect is extended and complicated by the probe potential and suggests the necessity of a

two- or three-dimensional treatment rather than the usual one-dimensional analysis. Smaller size and double probes are used to reduce the disturbance problem and the undefined influence on the properties being measured, but even with the miniature double probes the effect is still present. Finally, the mechanism of probe operation under the prevailing conditions must be fully understood to properly interpret the temperature measurement.

Electrostatic probes have been used extensively to measure properties such as electron and ion temperatures within ionized gases at both high and low densities. Because accuracy, range resolution, and measuring time are complex functions of geometry, procedure, and analysis techniques, a detailed discussion of the measurements will be left to Refs. 39 through 43 and Ref. 44 in particular.

SECTION III
PRESSURE

It is a matter of common experience that fluids and gases exert forces on material solids with which they are in contact; common examples are the forces that tend to burst a high pressure air tank and those that support a floating boat or balloon. Experience justifies the assumption that in static equilibrium these forces are normal to the surfaces in question and are usually of a positive nature.

It is a fact that in static equilibrium at a given point in a fluid or gas the pressure exerted on a real or imaginary surface is independent of the orientation of the surface through this point.

Torricelli, in 1643, first devised a method for measuring the pressure of the atmosphere by his invention of the mercury barometer. Fundamental to most pressure measurements is a knowledge of atmospheric pressure. The reason for this is because most pressure measuring devices use the pressure of the atmosphere as a reference level and measure the difference between an actual pressure and atmospheric pressure. Therefore a definition of absolute and gage pressures is in order.

Absolute pressure: The actual pressure at a point in the fluid or gas.

Gage pressure: The difference between absolute pressure at a point in a fluid or gas and the pressure of the atmosphere.

While on the subject of definitions a brief lexicon of aeronautical pressure terminology commonly encountered in the literature follows. These definitions are taken from the NASA Aeronautical Dictionary.

1. Impact Pressure: That pressure of a moving fluid brought to rest which is in excess of the pressure the fluid has when it does not flow, i.e., total pressure less static pressure. Impact pressure is equal to dynamic pressure in incompressible flow, but in compressible flow impact pressure includes the pressure change owing to the compressibility effect.

2. Total Pressure: Same as stagnation pressure. The pressure a moving fluid would have if it were brought to rest without losses.

3. Static Pressure: The unit force that a fluid exerts, excluding that due the (relative) motion of the fluid.

4. Pitot Pressure: The pressure received in a pitot tube. It is the stagnation pressure at the tube.

5. Dynamic Pressure: The pressure of a fluid resulting from its motion equal to one half the fluid density times the fluid velocity squared. In incompressible flow, dynamic pressure is the difference between total pressure and static pressure.

6. Partial Pressure: That part of the total pressure of a mixture, such as a gas mixture or gas-vapor mixture, that is contributed by one of the constituents.

To illustrate these concepts a schematic cross section of a pitot-static tube is presented in Fig. 8. If the motion of a compressible fluid relative to the tube is such that Bernoulli's law is applicable, the velocity and pressure of the free stream at point 3 are P and v. In the pitot tube (connected to the right-hand side of the differential manometer) at point 1 the velocity is reduced to zero and the full pitot pressure, stagnation pressure, or total pressure P_1 is developed (assuming no energy losses). In the static tube, connected to the left side of the manometer, the entry holes are set far enough back so that the velocity and pressure outside the holes have the free-stream values. The pressure inside the static tube, like the pressure at a surface inside a boundary layer, will also be the free-stream pressure. The difference between the pitot pressure or total pressure and the static pressure as illustrated by the manometer is, as definition 5 states, the dynamic pressure. For a compressible fluid a small compressibility effect must be neglected for this statement to be true. The dynamic pressure, as its name implies, is related to the energy or physical force associated with the motion of the fluid by means of the following formulation:

$$v^2 = 2(P_1 - P)/\rho,$$

where

v = speed of the fluid

P_1 = pitot pressure

P = static pressure (free-stream pressure)

ρ = density of fluid

Remember this formula does not account for the compressibility effect encountered in a compressible fluid.

In addition, three other very important effects must be considered when making pressure measurements in rarefied flow: the orifice effect, the viscous effect, and the thermal transpiration effect.

The orifice effect problem is, in general, associated with rarefied local (orifice) flows embedded in either continuum or noncontinuum flow fields. The relation between pressure in an orifice cavity and the true pressure on the surface of a cooled or heated body in rarefied, but not necessarily free-molecular, flow is discussed in Ref. 45. The existence of an "orifice effect" is demonstrated using data derived from impact pressure probes in low density hypersonic flows. Combined analytical and experimental results are applied to predict the orifice effect in impact and static pressure measurements.

Viscous effects in the free jet are of four types (Ref. 46): (1) Boundary-layer growth on the converging nozzle. This effect is seen in the variation of nozzle discharge coefficient with Reynolds number and in a shrinking of the scale of the flow downstream, and is generally very small if the nozzle Reynolds number is more than a few hundred. (2) Mixing-layer growth at the free jet boundary. This has no effect on the flow inside the shock barrel until, under circumstances of low Reynolds number and high pressure ratio, the mixing layer begins to overlap with, and eventually to eradicate, the downstream portions of the shock barrel and the Mach disk. (3) Thickening of the shock waves that form the sides and bottom of the barrel. This, in combination with the growth of the mixing layer, is the most prominent qualitative feature of the observed transition from the typical nearly inviscid flow pattern to free-molecular effusion, but it presumably does not influence the flow upstream of these shocks, as long as any such flow exists. (4) Viscous dissipation in the core of the flow, arising from the slight but nonvanishing velocity and temperature gradients in that region. These effects may be of experimental significance at points on or near the jet axis and far downstream from the orifice, at Reynolds numbers so large that the first three classes of effects are insignificant!

There is also an effect known as the thermal transpiration effect. A difference in temperature between two spatially separated points of measurement can result in a pressure gradient between these two points. This condition and the resulting effects are discussed in Ref. 47.

The remainder of this section will concentrate directly on the actual measuring techniques and their associated devices. These measurements can be grouped into two categories: absolute, or the direct inference of pressure as a result of the measurement, and nonabsolute, where the pressure is inferred indirectly from the measured parameters.

3.1 ABSOLUTE OR DIRECT PRESSURE MEASUREMENTS

A technique which senses the direct measurement of a normal force per unit area is by definition an absolute pressure measurement. This implies that the measurement will be the same for all ideal gases at the same pressure. Devices which fall into this category are, by necessity, mechanical or electromechanical in nature. In most applications these methods require monitoring the deflection of an incompressible fluid column or an elastic

element within the device. Included in this classification are the mercury and oil manometers, the aneroid or capsule-bellows manometers, the metallic and quartz Bourdon tube elements, and a variety of diaphragm transducers. These devices are discussed with regard to their principle of operation and application in Ref. 48.

Tensioned diaphragms have been used for many years as force collectors in pressure sensing devices. The movement of the diaphragm is a result of a normal force per unit area and hence constitutes an absolute reaction or direct measure of pressure. Two problems must be dealt with in the application of this technique: (1) the fidelity and sensitivity of the diaphragm in detecting an applied force, and (2) the accuracy, resolution, and sensitivity of the device which senses the diaphragm movement.

In practical applications the dynamic response of the diaphragm with regard to the imposed force is of utmost importance. An ideal diaphragm would exhibit no hysteresis, be perfectly elastic, have negligible mass, produce a linear response, be thermally insensitive, and possess infinite resolution. Obviously, perfection of this magnitude cannot be achieved in actual practice. However, a close approach has been accomplished by utilizing state-of-the-art manufacturing techniques, i.e., ultra-thin, low-mass diaphragms constructed of highly elastic materials mounted under considerable radial tension.

The most common pressure measuring device of this type utilizes a strain gage to transduce the mechanical movement of the diaphragm into an electrical signal. Strain-gage transducers can be categorized into two general classes: bonded and unbonded. Figure 9 is a schematic representation of these two classes of strain gages.

The bonded strain gage is physically attached to a strain member by an adhesive. The free end of the strain member is fastened to the diaphragm while the other end is securely anchored to a stationery support. Strain within the member as a result of diaphragm movement is therefore sensed by the attached strain gage.

The unbonded strain gage consists of a strain-sensitive wire which acts both as strain member and strain gage. It is attached between the diaphragm and a fixed reference point.

Both the bonded and unbonded strain gage operate on the principle that a pressure upon the diaphragm causes it to move: this movement changes the length of the strain gage element which produces a corresponding change in resistance.

Since the magnitude of the force requirement on the unbonded strain gage is minimal (only necessary to displace the small strain-sensitive filament), this allows the design of smaller size and more sensitive transducers as compared with the bonded type.

A recent improvement in strain-gage design is the thin-film strain-gage transducer, Ref. 49. The thin-film strain gage is applied directly to the strain member by means of a vacuum deposition process. Specifications of interest of a typical thin-film strain-gage transducer, Statham Instruments, Inc., Model PA 822 are:

Maximum overload:	200 percent of rated range through 500-psi range; 150 percent for 1000 psi and above
Resolution:	Infinitesimal
Nonlinearity:	Less than ±0.3 percent full scale (terminal)
Hysteresis:	Less than 0.1 percent full scale
Thermal Sensitivity Shift:	Less than 0.005 percent per °F
Range (psia):	0 to 15, 0 to 20, 0 to 25, 0 to 50, 0 to 100, 0 to 200, 0 to 500, 0 to 1000, 0 to 2000, 0 to 5000.

The model PA 822 utilizes a vacuum-deposited, fully active strain-gage bridge.

A technique which employs a capacitive sensor to detect deflections of the tensioned diaphragm (instead of a strain-gage sensor) has resulted in the most accurate absolute pressure gage for the 1000 to 10^{-4} torr range of pressures. The gage, shown in Fig. 10, utilizes a highly tensioned metal membrane (diaphragm) securely clamped between two insulating disks which also support a set of capacitive electrodes. The electrodes are vacuum deposited on concave, spherically ground surfaces of two ceramic disks. Pressure displaces the diaphragm, increasing the capacitance between the diaphragm and one electrode and decreasing the other capacitance. The capacitors form a two-arm AC bridge circuit. The bridge is sensitive to diaphragm deflections as small as one billionth (10^{-9}) of an inch.

The gage operates in a differential mode and is equipped with a test pressure input port and a reference pressure input port. A simplified readout (Fig. 10) allows the differential pressure (test pressure minus reference pressure) to be displayed on a center-zero meter. The gage can be operated in an absolute mode by reducing the reference pressure to a very small fraction of the test pressure.

Interesting performance factors of the MKS Instruments, Inc., series 77 differential capacitance diaphragm pressure sensor are:

Maximum overpressure (differential): All units will withstand 1000 mm or greater overpressure, and will withstand full atmosphere on vacuum operation.

Resolution: Infinite (voltage output)

Hysteresis: Less than 0.003 percent of pressure cycle applied for 30-mm Hg range, 0.015 percent for 100-mm Hg range, 0.04 percent for 300-mm Hg range, and 0.08 percent for 1000-mm Hg range.

Accuracy (Digital Readout): The bridge is balanced by four decade dials which can be read at higher pressures to five places. Lighted decimal point is fixed by head in use. The accuracy of this system in combination with the series 77 sensor head is: 0.02 percent of full range plus 0.15 percent of dial reading taken direct from dials or 0.02 percent of full range plus 0.05 percent of dial reading with reference to a calibration chart (furnished). At very low pressures additional accuracy can be obtained by valving the two ports together and adjusting zero before the measurement is started (0.02 percent factor in accuracy reduced to 0.005 percent or better).

Range: 10^{-5} to 1000 mm Hg (2×10^{-7} to 20 psi)

Sensitivity: 0.00001 of full scale over entire operating range.

Speed of Response: DC output—less than 10 msec for 63 percent response to a step of pressure of 30 mm Hg at 760 mm Hg. AC output is faster.

Detailed information concerning the operating principles and applications of capacitance diaphragm pressure sensors can be found in Refs. 50 through 53.

A recent concept is being investigated and as a result of feasibility studies and preliminary work, pressure measurements as low as 10^{-12} mm Hg are theoretically feasible using a tensioned diaphragm-type pressure sensor. The design of this instrument places the diaphragm displacement sensor in a closed loop electromechanical servosystem. The differential pressure is opposed by an equal electromagnetic pressure with an identical force per unit area distribution to reduce the net operating strain on the diaphragm sensor to a negligible value. Monitoring the current or voltage required for the diaphragm restoring force produces a highly resolved readout of the applied differential pressure.

Over its dynamic range the diaphragm capacitance manometer is the most satisfactory absolute pressure gage available. It allows pressure measurements in the vacuum range independent of the nature or composition of the gas. Actual pressure (normal force per unit area on the diaphragm element) is measured as opposed to thermal or ionization equivalents of pressure. In addition, the gage (such as the MKS Baraton®) is passive with no pumping action to affect the pressure being measured.

3.2 NONABSOLUTE OR INDIRECT PRESSURE MEASUREMENTS

Unfortunately, absolute (direct) pressure measurements using mechanical or electromechanical devices become inaccurate or impossible at pressures less than 10^{-5} torr. This limitation has necessitated the development of nonabsolute or indirect pressure

measuring techniques for use in the high vacuum range (10^{-3} to 10^{-8} torr), and in the ultra-high vacuum range (10^{-8} to 10^{-12} torr).

3.2.1 Thermal Conductivity Gages

Thermal conductivity gages are often used within their range from 10^{-3} to 1 torr (these gages are nonlinear and have poor resolution outside this interval). Several configurations of the basic operating principle are available. All of these configurations depend on the effect of gas pressure on the temperature and resistance of one or more heated elements. Measurements with these devices are qualitative, and the devices are sensitive to contamination by condensates and to gas composition. A thorough treatment of thermal conductivity gages can be found in Refs. 54 and 55.

3.2.2 Ionization Gages

This classification covers a broad assortment of devices whose range encompasses the pressure spectrum from atmospheric to 10^{-14} torr. These instruments all share a common characteristic: instead of sensing pressure directly they detect a function of the molecular density. The subject of ionization gages has been extensively examined (Refs. 53, 54, and 56). For this reason extensive categorizing and explanations will not be presented in this report. However, it is important to understand the operating principles of the particular ionization gage chosen for a pressure measurement so that an accurate and representative estimate can be made concerning the pressure involved.

SECTION IV
DENSITY

Of basic interest in the study of media such as rocket exhaust plumes is a knowledge of the density of the species involved within the flow field. These densities can be divided into four basic categories according to the nature of the matter to be measured: (1) molecular or gas density, (2) electron density, (3) ion density, and (4) particle density. The term particle will be used in this section to mean particulate matter with a characteristic dimension on the order of microns.

Techniques for each of the four density measurements have been chosen based on their practicability, fidelity of measurement, and applicability to the environs encountered within the exhaust plume flow field.

4.1 MOLECULAR OR GAS DENSITY MEASUREMENTS

Because of the large volume of successful experimental and theoretical work that has been accomplished using the electron beam probe as a diagnostic tool in low density gas flows, techniques based on electron interaction phenomena have been chosen for elaboration in this section.

Although an electron beam projected across a low density gas flow does not produce aerodynamic disturbances, the electrons lose energy and are scattered from their original

course. Various observables which can be traced to a beam electron-gas molecule interaction are utilized for molecular density diagnostic purposes.

During the last decade. molecular density measurements using the electron beam probe have been developed following four distinct approaches:

1. The attenuation or absorption measurement.
2. The fluorescence or electroluminescence measurement.
3. The electron scattering measurement.
4. The bremsstrahlung measurement.

The fluorescence, electron scattering, and bremsstrahlung density measurement techniques are similar except that for each method, a different particle emanating from the sensitive volume is observed.

4.1.1 The Attenuation or Absorption Measurement

Measurements of gas density using the principle of beam attenuation were first accomplished by C. Ramsauer (Ref. 57) and von Engel and Steenbeck (Ref. 58). The attenuation or absorption method was further investigated at the University of California Los Alamos Scientific Laboratory, Los Alamos, New Mexico, by Douglas Venable and Daniel E. Kaplan (Ref. 59). Their desire was to perfect a technique of measuring shock thickness utilizing a probe of radiation which would not disturb the flow in question. Although this particular method of gas density measurement has been extensively labeled as an absorption method, this may be somewhat misleading since the beam electrons are not in reality absorbed by the gas.

As the electron beam traverses a rarefied, gaseous medium, the primary electrons are scattered by elastic and inelastic processes. The result of this scattering reduces the beam to a fraction of its initial intensity. This effect is evident within a distance along the beam of several electron mean free paths. Also, a cylindrical halo surrounds the beam which contains singly and multiply scattered electrons. To apply this method, it is necessary to design a beam collector with a sufficiently small angular aperture that only the beam core, or those primary electrons that have traversed the entire medium without a deflection, are measured. If this is the case, then the measured beam intensity can be related to the original beam intensity by the linear absorption law. In an application where the flow field in question possesses axial symmetry, an Abel integration scheme can be applied to obtain a density profile (Ref. 60).

The attentuation method has been successfully employed in shock tubes for the measurement of density distributions within shock fronts and boundary layers by several investigators (Refs. 61, 62, and 63). To measure shock thickness accurately, the beam of particles must conform to the following specifications (Ref. 64):

1. The de Broglie wavelength of the particles must be small compared to the molecular mean free path of the gas in question.

2. The beam diameter must be small as compared to a molecular mean free path.

3. The excitation cross section must be negligible compared with the total collision cross section.

4. The beam intensity and total scattering cross section should be great enough so that transmission measurements can be made that are statistically significant.

At sufficiently low pressures (approximate range from 0.01 to 1.0 mm Hg) a beam of electrons meets all of the above requirements for a fairly large spread of energies. In most cases, beam accelerating voltages from 5 to 50 kv are quite satisfactory. Electron beam currents from 10 to 500 μamp have been utilized. Figure 11 illustrates a typical application of this measurement.

4.1.2 Fluorescence or Electroluminescence Measurement

The electron beam fluorescence probe was developed by B. W. Schumacher and A. E. Gruen (U.S. Patent No. 2952776, German Patent No. 1 102 442, 1955). The first report published on the use of this method for measuring local gas density was by B. W. Schumacher and E. O. Gadamer (1958) (Ref. 65). The principle of the measurement is based on the fact that for a range of sufficiently low densities, the intensity of the fluorescence or electroluminescence from gas particles excited to elevated electronic energy states by a beam of high energy electrons is a linear function of the molecular number density.

Application of the technique consists of injecting a collimated beam of high energy electrons through the flow field under investigation. Inelastic collisions of the electrons with the gas particles produce a radiating, concentric cylinder of gas nearly coincident with the electron beam. A measurement of the intensity of the radiation may be related directly to the density of the radiating species present in a small volume for chosen locations throughout the flow. A typical component arrangement is shown in Fig. 12.

The simplest detection system consists of a photocell and collimator arranged to view the total radiated light from a small portion of the beam (sensitive volume). Unfortunately, problems usually arise during practical applications which necessitate a more complicated analysis of this radiation. The problems most frequently encountered are (1) the presence of intense background radiation, (2) the radiation from metastable energy states present in some gases, and (3) the presence of vibrational molecular excitation. In order to overcome these difficulties and extend the scope of the measurement, a spectroscopic analysis is most often used to observe radiative transitions of the gas particles. Visible and near-ultraviolet electroluminescence spectra of helium, argon, oxygen, nitrogen, and nitric oxide have been studied by Muntz and Marsden (Ref.

66). Results of this study indicate that transitions suitable for application in high velocity, rarefied gas flows were present in all spectra except oxygen.

In general, not all the spectral lines and bands that contribute to the fluorescence are suitable for density measurements. The excitation-emission process should involve direct excitation to an excited state immediately followed by a spontaneous emission to the ground state (average lifetime of 10^{-8} to 10^{-7} sec). This is necessary to prevent the observed emission from being dependent on the stream velocity.

The predominant radiation resulting from inelastic collisions of electrons with air or molecular nitrogen at low density is a product of the first negative emission system of N_2^+. This system fulfills the requirement of a lifetime of 10^{-8} to 10^{-7} sec. In addition, no residual radiation resulting from metastable energy states in molecular nitrogen excited by an electron beam has been observed in sufficient quantity to affect the measurement of molecular number density. This is indeed a fortunate situation since molecular nitrogen constitutes a large percentage of the rocket exhaust composite.

Several observables exist in the emission produced by the electron beam probe from which a determination of molecular nitrogen number density can be obtained. The three most often used are (1) a measurement of the total radiation intensity, (2) a measurement of the intensity of a vibration-rotation band, and (3) a measurement of the intensity of a particular rotation line in a vibration-rotation band. The thermal state of the flow field under investigation will dictate which method or methods can be applied to produce accurate and valid results. In addition, the effect of elevated rotational and vibrational temperatures on the measurement of molecular concentrations cannot be ignored (Ref. 67). Depending on the degree of excitation, the effect of elevated temperatures in the flow may or may not require vibrational (in the case of a band intensity measurement) or both vibrational and rotational (in the case of a line intensity measurement) temperature data to be taken simultaneously with the intensity measurement. A theoretical and experimental analysis of the measurement of molecular nitrogen number density can be found in recent literature (Ref. 18).

This measurement is presently confined to a pressure range where the emission intensity is approximately a linear function of gas density. The lower limitations depend upon the sensitivity of the detection equipment, the resolution desired, and the available photon flux. On the other hand, the fluorescence phenomenon itself restricts the upper limits of the measurement.

As the density increases, a nonlinearity in the variation of light intensity with density occurs as a primary result of collision quenching. In the process of collision quenching a colliding particle absorbs the excess energy from the excited ion (interaction time on the order of the lifetime of the excited state) allowing the ion to pass to its ground state without the emission of radiation. For this reason the upper boundary for a valid measurement is obscure, although density measurements are possible in the presence of quenching provided the appropriate quenching cross sections are known. Further investigations of the phenomena involved are necessary to produce valid data in this region of nonlinearity. Approximate upper limits for accurate density measurements using

this method have been quoted as being on the order of 0.25 mm Hg for argon and 0.35 mm Hg for nitrogen at room temperature (Ref. 68). These limits are based on the interpretation of results obtained from the measurement of density ratios across the shock waves in these gases. It is reported in Ref. 67 that experimental studies indicate no significant quenching for densities corresponding to a pressure of 0.40 mm Hg at room temperature. For pressures above 5 mm Hg (room temperature), sensitivity to further increases in gas density is almost nonexistent in air (Ref. 69).

A spectroscopic analysis of the fluorescence from a narrow electron beam has been used to determine the component densities in rarefied helium-argon flows (Ref. 70). This method could be extended to other mixtures in cases where the excitation-emission processes involved are understood. In another application of this method, point densities in the near wake of a freely flying model have been measured in a three-dimensional hypersonic flow (Ref. 15). The use of this technique for the measurement of densities in shock tunnels has been discussed in detail (Refs. 16 and 17).

As with all of these methods the conditions under which the measurement is to be performed will determine the accelerating potential and current requirements of the beam-generating apparatus. Beam voltages have ranged from approximately 10 to 200 kv. A wide range of beam current has also been utilized (10 μamp to 10 ma).

4.1.3 Electron Scattering Measurement

When an electron penetrates matter it is deflected from its trajectory because of interaction with the atomic electrons and associated nuclei. For a considerable range of primary electron energies and sufficiently low molecular densities, the deflection or scattering of the primary electrons is almost entirely a result of elastic collisions with the atomic nuclei. The effects of these elastic collisions have been divided into four classes: (1) single or Rutherford scattering, (2) multiple scattering, (3) plural scattering. and (4) diffusion. For the purpose of measuring local densities in a rarefied gas, the phenomenon of single scattering is most attractive. The basic principle of this type of measurement is shown in Fig. 13. A collimated beam of monoenergetic electrons (approximate energy range: 20 to 200 kev) is injected into the test gas. At large angles the total collision cross section is almost entirely attributable to the single scattered primary beam electrons. The measurement is obtained using a collimated detector which is exposed to a small cylindrical volume of the beam (sensitive volume). The length of this sensitive volume is determined by the collimator, and the diameter corresponds to the overall diameter of the beam. Since the probability that a collision will occur is proportional to the number of molecules exposed to the beam, the rate at which particles are detected from this sensitive volume is proportional to gas or molecular density. The theory of Rutherford scattering is sufficient to describe this mechanism for the range of electron energies and gas densities involved in the measurement.

A large-angle (90-deg) electron scattering densitometer has been used to measure density profiles in a low density, arc-heated wind tunnel (Ref. 71). A calibration curve of this particular installation is shown in Fig. 14. Two density profiles were measured and are reproduced in Fig. 15a (cold flow) and Fig. 15b (arc heater operating). In these tests

the arc heater was operated at a chamber pressure of 10 atm and a stagnation temperature of 3800°K. Free-stream Mach number was estimated to be 14.8 at a static pressure of 17 μ Hg, based on nonequilibrium flow calculations. Cold flow data were taken at an arc-heater chamber pressure of 2.7 atm, which resulted in the same mass flow obtained with the arc heater operating. The density during arc-heated runs as estimated by nonequilibrium flow calculations was 10 percent higher than the density actually measured by the scattering method. Measurements made using this technique were found repeatable to within 1.0 percent. At the present time, the scattering techniques can be applied at higher densities and probably also at lower densities than the fluorescence method.

Density measurements in rarefied gas flows using the method of large-angle, electron scattering from an injected beam have been reported in a recent publication by Grodski and Schumacher (Ref. 72). Also discussed in this report is an interesting extension of the method into a two-dimensional picture-forming system.

A practical application of the basic technique has been described by Camac (Ref. 73). By measuring the intensity of large-angle scattered electrons from a 100-kev electron beam, the density variation during translational adjustment in argon shock waves was determined.

4.1.4 Bremsstrahlung Measurement

When an electron interacts with matter, energy losses are observed which result from the processes of excitation, ionization, and the emission of bremsstrahlung (German for braking radiation). Bremsstrahlung or emission of X-ray photons occurs when the electron undergoes acceleration during deflection when passing through the field of a nucleus (or atom). This phenomenon has been discussed in detail in Refs. 74 and 75.

The X-ray flux emitted from an electron beam traversing a gaseous media is a function of: (1) electron beam current and voltage, (2) atomic number density, (3) average atomic number, and (4) average atomic weight. Knowing the average atomic number and weight and the current and accelerating voltage of the beam. it is possible to determine density directly from the counting rate of the X-ray photons reaching the detection system. A typical measuring arrangement is shown in Fig. 16.

A prototype system has been developed based on this principle of density measurement (Ref. 76). After a static calibration in air at 22°C for a range of pressures from approximately 0.05 to 1.0 mm Hg, local gas densities within an arc-heated plasma were determined over a range from 0.1 to 0.4 $\mu gm/cm^3$. For these measurements the electron beam was operated at 40 kv, 3 μamp. The overall accuracy of this particular system was estimated to be within 10 percent.

4.1.5 Resolution, Accuracy, and Measuring Time

The spatial resolution in two dimensions for all four methods is dependent upon the diameter of the electron beam probe. Degradation of the spatial resolution along the

beam diameter is primarily caused by beam spreading. The principle cause of beam spreading is small-angle multiple scattering; the cumulative effect of this scattering results in small angular deflections of the primary electrons. There are two net effects of many random small-angle scatterings. First, the beam becomes broader as it traverses the media. Second, the individual electrons no longer travel exactly parallel to the beam axis.

Calculations by Rossi and Greisen predict that the electron density along the beam axis and the angles which individual electron paths make with the beam axis have a gaussian distribution (Ref. 77). In addition, an expression is given for the rms beam radius at any point along the beam axis. Current densities in an electron beam have been measured experimentally at energies from 30 to 50 kev over beam lengths up to 60 cm for pressures ranging from 0.02 to 1.0 mm Hg (Ref. 71). Experimental measurements of beam width have also been performed by Camac (Ref. 73). In both instances, the measured beam spread was less than that predicted by the Rossi and Greisen theory. It should be noted that although the measured beam spread in Ref. 71 was lower than the values based on the theoretical calculations at the lower densities, the variation of measured beam spread as a function of density was actually greater.

In the case of the fluorescence measurement, radial resolution is ultimately affected by the soft emission surrounding the primary beam attributable to secondary electrons. However, for the lower densities this is usually a short range effect, slightly larger than the diameter determined by beam spreading. In addition, if the light is emitted as a result of emission from an electronic level of the neutral species, the fluorescence can spread because of resonance diffusion.

Second-order effects attributable to beam spreading may take place in the measurement of large-angle scattered electrons. These effects would arise when (1) scattering occurs where the detector solid angle is larger, (2) the scattering angle is no longer the same for all electrons, the reason for this being that the small-angle scattered electron paths will be inclined at a small angle to the beam axis, and (3) multiple scattering takes place between the point of measurement (sensitive volume) and the detector.

It is evident that spatial resolution along the axis of the primary beam is relevant in any method of measurement which allows a segment of the beam to be examined. When measuring fluorescence, axial resolution along the beam path depends on the distance required to establish an equilibrium between the primary and secondary electrons. This has been quoted as being on the same order of magnitude as the beam diameter (Ref. 65). However, there are factors involved which may invalidate this assumption (Ref. 66). As compared to the fluorescence method, there is a slight improvement in spatial resolution along the beam axis in the measurement of electron scattering for comparable measuring times. In order to preserve system accuracy at low densities, it is necessary to observe a longer portion of the beam for the bremsstrahlung measurement (to gain higher counting rates) than is the case for the fluorescence or electron scattering measurements made in the same time period under identical conditions.

If an exact analysis of the physical phenomena were available, and if the geometry and efficiency of the equipment were precisely known, an absolute density measurement would be possible using these techniques. In addition, an accurate, absolute measure of beam voltage and current would be required. Unfortunately, this is not the case; therefore, a calibration of the apparatus must be made in the media under investigation over a range of known static parameters. For most applications the errors induced during calibration will be predominant because of the extreme difficulty in obtaining a measure of density under low pressure conditions comparable to the statistical accuracy available from the detection system. Briefly, this means that although the statistical error of the measurements, in most instances, can be held to values on the order of 1 percent or less, the calibration errors are usually on the order of 5 percent.

Since the data producing mechanism of all these systems is a statistical phenomenon, the accuracy with which an observable can be measured is a function of the measuring time. In other words, measurements must take place over a time span of necessary length to produce statistically significant results. The investigator should realize that resolution, accuracy, and measuring time are dependent; therefore, a compromise must be accepted for each application of these techniques.

4.1.6 Concluding Remarks Concerning Density Measurements Using the Electron Beam Probe as a Diagnostic Tool

Upon comparison of these density measuring techniques, it is immediately evident that no one method can be acclaimed most practical in all cases. Instead, each individual application should determine which technique or techniques will be used depending upon the specific requirements and conditions involved. It is impossible to develop a complete scheme of classification concerning each of these techniques since each measurement program imposes its own requirements and restrictions.

The attenuation method is probably the least expensive and easiest to apply. This type of measurement is incapable of the spatial resolution necessary to obtain a direct measure of point or local density distributions. In other words, all the beam attenuation methods generate integral values over beam path length for the density; therefore, the actual differential values can never be regained. This technique should be helpful in exploring relaxation phenomena behind shocks where the time scale is large compared with the density rise time of the shock front.

The other three methods (fluorescence, electron scatter, and bremsstrahlung) overcome the major limitations of the attenuation measurement because these methods allow the investigator to perform localized measurements of densities over small increments of the electron beam. The fluorescence method utilizing spectrographic analysis can measure the concentration of certain selected species. On the other hand, the electron scatter and bremsstrahlung techniques are independent of the degree of dissociation, ionization, excitation, and thermochemical state of the gaseous medium.

Since all methods utilize a beam of charged particles, the effects of any stray magnetic fields should be investigated for each particular application of these techniques.

In general, a magnetic field would affect the fluorescence and bremsstrahlung methods by causing an uncertainty in the location of the measurement. In the case of the electron scattering method a second effect may also be present. This is because a magnetic field with flux lines perpendicular to the plane defined by the beam and the line of sight of the collimator will change the scattering angle in addition to the location of measurement.

4.2 ELECTRON AND ION DENSITY MEASUREMENTS

Because of the similarity of the techniques involved in electron and ion density measurements which have been developed for investigating hot ionized gas flows, these two parameters will be treated in a simultaneous manner from an instrumentation standpoint.

Investigations of charged, subatomic element densities can be classified into two groups which are broadly categorized by the type of experimental probing technique employed. For convenience these groupings will be denoted by the nomenclature (1) electrostatic probes and (2) electromagnetic probes. Obviously, the electrostatic probes, for example the Langmuir probe, have been in existence as measurement techniques considerably longer than the methods which rely on electromagnetic radiation phenomena. These latter methods have developed concurrently along with the tools which have made such measurements possible, e.g., lasers, microwave generators, and spectroscopic techniques.

4.2.1 Electrostatic Probe Measurements

Electrostatic probes have evolved and exist in a variety of configurations. Basic to their operation is the fact that they are limited to the analysis of ionized gases. This is because the probe relies on an imposed potential to induce a charge flow in the surrounding gas.

The classical electrostatic probe was developed by Langmuir for use in low density gas discharges. The theory and performance of this basic configuration has been extensively investigated (Refs. 78 and 79). Expanded theories have increased the scope and understanding of this instrument (Refs. 80, 81, and 82).

To obtain reliable measurements in hypersonic flows with Langmuir probes it is necessary to understand in detail the physics of their operation. Of primary consideration is probe size. The size of the probe should be smaller than the electron or ion mean free paths within the plasma. If the characteristic probe dimension is much greater than the electron or ion mean free paths, the current drawn by the probe tends to be reduced by local plasma drainage effects.

When using the Langmuir probe to study high velocity flows, such as rocket exhausts, it is necessary to relate the properties measured to the undisturbed flow properties. This is most reliably accomplished if the probe is also made free molecular with respect to the neutral particles in the flow, i.e., the ratio of the electron or ion

mean free paths to the characteristic dimension should be equal to or greater than an approximate magnitude of five.

Measurements of electron density of a low density supersonic plasma jet by means of a stagnation point Langmuir probe have been reported (Ref. 83). As an extension of this investigation a series of experiments has been conducted consisting of both microwave transmission and Langmuir probe measurements in a low density plasma for comparison purposes (Ref. 84). A typical operating condition in argon for the Langmuir probe installation was free-stream Mach number of 6.2, static pressure of 425 microns, jet centerline stagnation temperature of 5000°K, mean stagnation temperature of 3500°K, flow rate of 1.16 gm/sec, and a power input to the plasma generator of 11.4 kw. The ionization indicated by the probe measurements was 2.7×10^{13} ions/cm^3. Agreement between the microwave transmission and Langmuir probe measurements was only fair because the electron densities required by the microwave equipment were so low that the assumption of a sheath thickness less than a mean free path was not true.

In Ref. 85 the application of a free-molecular Langmuir probe to the investigation of the hypersonic plasma flow generated in a shock tunnel is described. This study indicates that practical Langmuir probes (diameter $\geqslant 0.025$ mm) will be free molecular at least up to densities corresponding to an altitude in the vicinity of 200,000 ft for typical shock tunnel flow velocities. An example of the experimental test section conditions under which a series of tests were conducted using the free-molecular Langmuir probe are static temperature, 150°K; free-stream density, 2.42×10^{-8} gm/cm^3; free-stream velocity, 4870 m/sec; Mach number, 17.33; electron concentration, 8.3×10^8/cm^3 (these values were obtained using nonequilibrium nozzle calculations). Measuring times were less than 5 msec. It is concluded that the free-molecular Langmuir probe may be used to obtain valid measurements (under certain restrictions outlined in the text) of plasma density in the free stream, in shock layers, and in boundary layers with an excellent degree of resolution.

Experiments have been carried out to measure electron density fluctuations using single coaxial electrostatic probes, a floating triple electrostatic probe and arrays of electrostatic probes (Ref. 86). Signals from an array of five coaxial probes, which were produced when the probes were swept by the wake of a high velocity projectile, were cross-correlated to produce a family of spatio-temporal correlations. From these data the wake convection velocity, space correlations, and temporal decay of the turbulence pattern were estimated.

Attempts have been made to measure the time history of gas temperature and electron density at a point in a flowing turbulent plasma (Ref. 87). The device to be used consists of a hot-wire and Langmuir probe mounted close together on the same holder. Typical operating ranges of the plasma wind tunnel over which this probe configuration is to be applied are electron density, to 10^{13}cm^{-3}; nozzle Mach number, 3.5; type of working gas, argon, nitrogen, and nitrogen/air; enthalpies, to 10,000 Btu/lb.

Further applications, feasibility studies, and theoretical investigations of electrostatic probes and the chemistry of charged matter are reported in Refs. 88 through 91.

The electrostatic probe measurement is open to the objection that it introduces a physical obstacle into the flow, and thus introduces some distortion; however, if intelligently pursued, this low-cost simple measurement can be an extremely useful tool in the study of ionized gases.

4.2.2 Measurements Utilizing Electromagnetic Probing Techniques

These methods all have the advantage of producing noninterfering measurements on ionized gases, but the instrumentation involved is complex and expensive.

Microwave probing is a technique which is often used to determine electron densities within an ionized gaseous media. In particular, this parameter has been measured successfully in the 1000-ft Hyperballistic Range (G) of the von Kármán Gas Dynamics Facility (VKF) at AEDC by monitoring the effects of high velocity projectile wakes on the microwave transmission properties of a series of collimated and focused beams.

It is well known that microwaves are not transmitted through a plasma if their frequency is less than the plasma frequency, which is proportional to the square root of the electron number density in the plasma. Therefore, measuring the cutoff frequency for transmission yields the plasma electron number density.

In the VKF application five broadside probing systems operating over a full four octaves of frequency (4.32, 8.6, 17, 35, and 70 GHz) provide microwave transmission and reflection properties of ionized gases. The axial location within the plasma at which effective cutoff electron densities are realized can be determined using this system. Typical measuring times are on the order of milliseconds. Important operating parameters are shown below.

Operating Frequency, GHz	Typical Beam Width, in.	Electron Cutoff Density, electrons/cm^3
4.32	10.0	2.3×10^{11}
8.6	8.0	9.1×10^{11}
17.0	7.0	3.6×10^{12}
35.0	6.0	1.5×10^{13}
70.0	6.0	6.1×10^{13}

Also in operation in Range G are two dual-channel, focused, phase-quadrature microwave interferometers which are operated at each of two frequencies—35 and 70 GHz. Typical beamwidths at range centerline (10-db points) are, for 35 GHz, 0.70 in., and for 70 GHz, 0.35 in. Performance characteristics are listed below.

Operating Frequency, GHz	Electron Cutoff Density at Operating Frequency, electrons/cm^3	Measurable Range Electron Density for 1.0-cm Path Length, electrons/cm^3
70.0	6.1×10^{13}	8×10^{11} to 3×10^{13}
35.0	1.5×10^{13}	3×10^{11} to 7.5×10^{12}

Electron density within a plasma has also been measured by laser interferometry (Ref. 92). The plasma was probed axially producing an averaged value of the electron density.

Finally, electron densities can be determined by observation of the profile of Stark-broadened lines. The effects of magnetic fields on Stark-broadened hydrogen Balmer lines along with a new method for measuring electron densities from these line profiles in strongly magnetized plasmas has been proposed (Ref. 93). The range of electron densities investigated were from 3×10^{15} to 1×10^{16} electrons/cm^3.

4.3 PARTICLE (MICRON SIZE) DENSITY MEASUREMENTS

A unique instrument which was designed as a cosmic dust sensor (Ref. 94) could be applied to the measurement of concentrations of micron and submicron size particles present in the far field region of an expanded rocket exhaust plume. In operation the impact of a particle upon a surface is measured by the sensor and recorded by electronic monitors. In addition to the particle's direction, the speed and mass are determined.

The sensor performance is based upon two measurable phenomena which occur when a hypervelocity particle impacts upon a surface: a transfer of momentum and ionization. The basic sensor (the instrument is composed of an array of these sensors) is shown schematically in Fig. 17.

Three probable particle types have been considered in the operation of this device: (1) a high energy, hypervelocity particle (>1.0 erg); (2) a low energy hypervelocity particle (<1.0 erg); and (3) a relatively large high velocity particle (>10^{-10} gm).

The physics and geometry of the experiment in addition to sensor controls, calibrations, electronics, and telemetry bit layout are described in detail in Ref. 94.

Although optical techniques tend to stress the determination of particle size rather than particle concentration or density, it is obvious that these methods could produce a measure of micron size particle densities throughout a flowing optically transparent media. These techniques are too numerous to list but are described in detail in chapter 7 of Ref. 95.

SECTION V
VELOCITY

The general definition of velocity states that it is a vector quantity equal to speed in a given direction. In the analysis of flowing ionized gases there are many vector quantities present which fit this description—electron velocities, ion velocities, and sonic velocities, to mention a few. As far as the science of aerodynamics as applied to expanding rocket exhausts is concerned, the velocity measurements of prime interest are gaseous or mean molecular velocity and the corresponding velocity profiles of the free stream and the particulate velocities and their velocity distributions as encountered in the stream. Pertinent velocity measurements applicable to the study of rocket exhaust plumes will be discussed and catalogued under these two general headings.

5.1 GASEOUS OR MOLECULAR VELOCITY MEASUREMENTS WITHIN THE FLOW FIELD OF A COMPRESSIBLE MEDIA

5.1.1 Doppler Radar System

The physics of the technique is based on the classical Doppler effect using probe frequencies in the radar spectrum. The equipment used in the investigation considered herein (Ref. 96) was a 1-nsec, coherent, x-band, pulse, Doppler radar instrument. This instrument could be applied to the near field region of a rocket exhaust plume to examine velocities of the ionized gas.

Figure 18 illustrates the arrangement used in Ref. 96 as applied to a typical rocket plume expansion. The principle of operation is based on the fact that the backscattered electromagnetic radiation is shifted in frequency because of the Doppler effect as a result of the motion of the scatterer. Since the scattering results from clustered electron number density irregularities which will be present in the ionized region of the plume, the Doppler shift is proportional to the gaseous or molecular velocity if it is assumed that the positive ions and electrons have translational velocities of the same magnitude as the neutral molecular velocity in the flow field.

For the past four years a 35-GHz oblique Doppler radar system has been in operation at Range G. This system has been used to measure the velocities of reflecting media contained within the wakes of hypervelocity spheres.

5.1.2 Spectroscopic Doppler-Shift Technique

Molecular velocity measurements by a spectroscopic Doppler shift technique in iron arcs (about 2000 m/sec) have been performed by laboratories in the past and found to be in good agreement with other spectroscopic measurements (Ref. 97). This technique is presently being applied at AEDC by the Staff Research Section of ARO, Inc., to a self-radiating gaseous environment as a means of obtaining the velocity of the radiating species.

The fact that a spectral line will be shifted in frequency by the Doppler effect composes the basis of the technique used. A comparison is made between the frequency of the radiation as viewed from two angles relative to the local flow. To date, three methods have been used. They are labeled (1) line broadening, (2) absolute line shift, and (3) rotating refractory plate. A fourth method utilizing an interferometer either scanned mechanically or by pressure scanning will be used later. The advantage of an interferometer is found in its ability to increase resolution and also in its potential as a rapid scanning device.

Figure 19 shows the line broadening method. Here, two beams can be superimposed upon a photographic plate. Figure 20a shows two Doppler-shifted lines separated by $\Delta\lambda$, which is the Doppler shift. The halfwidths of this line can be measured separately by exposing a single beam at a time. The composite line as shown in Fig. 20b consists of the Doppler shift plus the halfwidth. This value when measured gives a direct measure of the Doppler shift. The shift was indeed readily seen in the experiments. Although the shift is only about twice the resolution of the equipment, good statistical accuracy could be expected by using enough different lines from the spectrum.

Figure 21 indicates an absolute line shift method. Again, a photographic plate is used; however, an iron line is also recorded with the argon line, or any other emitting spectral radiation. The iron arc is used as a standard because of the many sharp, well-defined lines in its spectrum. Figure 22 shows a comparison of these lines. Here the absolute values of the shifted and unshifted argon lines were obtained again providing the Doppler-shift measurement.

The principles used on the two previous methods can also be applied to an electronic readout method shown in Fig. 23 and is perhaps the most versatile technique of the three. Here, a rotating refractory plate (an optical flat) located in the spectrometer scans the lines across the photomultiplier tube. The output of this photomultiplier tube is fed to an oscilloscope which is triggered by a microswitch on the rotating plate. In this manner, the spectral lines are displayed on the face of the oscilloscope allowing a more direct readout. If the signal-to-noise ratio becomes low, a signal averager could electronically smooth the data allowing a line to rise above the noise level. As with the previous method, iron lines are used to determine the absolute frequency shift.

These methods, while not affording a high degree of accuracy, are applicable in those regimes where addition of particles to the flow is prohibited or where particles will not follow the flow field accurately as in very low density facilities. Velocities > 1000 m/sec can be measured using these techniques; however, velocity resolution as low as 200 m/sec is possible with interferometric techniques.

The flow should be stable, radiative, optically thin, and of sufficient duration to expose a photographic plate. For the electronic techniques the time requirement may be reduced to a fraction of a second. The resulting Doppler shift is, of course, integrated along an optical path through the plume. The Abel inversion for circular cross sections, which converts integrated data from several positions to a radial profile, cannot be applied in this case. Techniques for inverting elliptic cross sections for parallel flow have been developed. However, this capability has not at this time been established at AEDC.

The three methods outlined are being compared as to accuracy, ease of data reduction, and acquisition time at AEDC, and none of the results have yet been published.

5.1.3 Laser Schlieren Method

A method referred to as the method of forced similarity which proposes the possibility of obtaining direct measurements of the most probable preferred[2] angular velocity locally within turbulent flows by optical correlation of laser schlieren signals is introduced in Ref. 98. The report utilized simple two-dimensional models to describe the theory, systematic analysis, and practical application of the method. Although sufficient data verifying the theory do not exist at this time, the theory is indeed plausible, and the technique is practical to the extent that further investigation is justified toward the application of this method for the study of turbulent structures in high velocity, high enthalpy rocket exhaust components.

5.1.4 Orifice-Generated Molecular Beam

Mass spectrometry combined with sampling probe techniques have been adapted for gas species (molecular) velocity distribution measurements throughout an expanded plume. The operating principle of the system is based on a time-of-flight analysis of a collimated molecular beam within the probe. Figure 24 illustrates the total system. An impulse function is applied to the beam by a rotating chopper wheel. As these molecular impulses traverse axially within the probe, a distribution of the individual molecules takes place according to their respective velocities. Thus, since the distance traveled is a known constant, and the time of flight is a measured parameter, a molecular velocity distribution of the individual gas species is determined by the system. Further exploration of this technique is described in Ref. 99.

5.2 MEASUREMENT OF MICRON-SIZE PARTICLE VELOCITIES

The determination of the velocity of micron-size particles within the flow field of a chemical propulsion system, such as a rocket exhaust plume, would be considered a significant contribution to the theoretical and experimental evaluation of the phenomena involved.

Of particular importance in the study of nonequilibrium, two-phase, rocket exhaust plume expansions is the velocity lag of the metallic fuel constituents or possible solids in liquid-propellant rocket plumes. Micron-size particulate matter is accelerated in the rocket exhaust by frictional forces exerted by the expanding gas upon the particles. Because of the definite effect of the velocity lag of particulate matter on rocket performance a determination of this parameter is of utmost value.

---

[2]The author of Ref. 98 uses preferred in the context that the statistical process involved does not produce angular velocity components which are based on statistical averages of absolute values.

5.2.1 Velocity Analysis of the Frequency Shift of Scattered Light as a Result of the Doppler Effect

Two distinct effects must be considered when velocity measurements are to be obtained from the interaction and resultant scattering of electromagnetic radiation with matter: (1) the scattering process, and (2) the perturbation or frequency shift with regard to the scattered wave.

Familiar light scattering processes of interest as far as plume studies are concerned are (1) Raleigh scattering from atoms and molecules, (2) Thompson scattering from free electrons, (3) resonant scattering from atoms and molecules, and (4) Mie scattering from particulate (micron-size) mass.

An extensive treatment of the theory of the scattering of electromagnetic radiation in addition to recent practical applications and a comprehensive list of references can be found in Refs. 100 and 95.

A number of techniques based on an analysis of scattered photons which have experienced a shift in frequency directly proportional to the velocity of the particulate scattering center in a flow field can be utilized to obtain both single and multiple component velocity measurements. Two important considerations concerning these methods are (1) the media must be transparent to the photon beam, and (2) micron- or submicron-size particles must be available to scatter a sufficient portion of the incident beam for effective detection. A new theoretical model describing the frequency shift of scattering light is explored in Ref. 101.

The most widely practiced optical velocity measurements are based on the Doppler effect and use the laser as a source of monoenergetic photons. The original laser Doppler technique was first conceived in 1963 by Dr. Edward Fisher at United Technology Center. The technique involved optically homodyning particle scattered (Doppler-shifted) light signals with unscattered source light and analyzing the beat frequency to determine particle velocities.

Two basic optical arrangements have evolved as a result of practical applications of the Doppler effect. These two approaches will be described separately because they differ widely in their range and resolution.

5.2.1.1 Detecting the Frequency Shift by Means of the Square Law Response of a Photodetector

An instrument of this type was first developed by Yeh and Cummins (Ref. 102) to provide a measure of the velocity of a fluid. This technique was expanded by Foreman, George, and Lewis (Refs. 103 and 104) to obtain a localized measurement of velocity in a gas flow. Subsequent work at AEDC and elsewhere (Refs. 105 through 114) has produced various modifications and improvements.

A simple optical arrangement of the laser Doppler velocimeter (LDV) which illustrates the basic principles currently being used in flow measurements typical of those in Refs. 105 through 114 is illustrated in Fig. 25 (only one component of velocity is measured for clarity in explanation). A beam of monoenergetic photons from a CW gas laser is focused by lens L1 at the point of measurement P. Unscattered radiation passes through the flow and is eventually focused on the photocathode surface of a photomultiplier tube by lens L2. After passing through lens L2, the unscattered beam is reflected by the surface of the beam splitter. Light scattered at an angle θ in relationship to the incident beam by particles in the flow within the neighborhood of point P are focused by lens L3 onto the photocathode after passing through the beam splitter. The optical path lengths of the scattered and unscattered beam are adjusted to equalize the distance between point P and the photocathode for each case.

The frequency shift attributable to the Doppler effect is given by

$$\Delta f = \frac{1}{2\pi} (\bar{k}_s - \bar{k}_i) \cdot \bar{v} \tag{1}$$

where $\bar{k}_s$ is the wave vector of the scattered beam and $\bar{k}_i$ is the wave vector of the incident beam. The term $\bar{v}$ is the local flow velocity vector at the point P, which in general has arbitrary magnitude and direction. With this in mind, the arrangement of Fig. 25 allows the measurement of the x_1 component of velocity provided the direction of vector $(\bar{k}_s - \bar{k}_i)$ is taken along the x_1 axis. Making use of the approximation $|\bar{k}_s| = |\bar{k}_i|$ this constrains the x_2-axis to bisect the scattered angle θ as shown in Fig. 25. Now we can express Eq. (1) as

$$\Delta f = k_i/2\pi (\bar{i}_s - \bar{i}_i) \cdot \bar{v} \tag{2}$$

where $\bar{i}_s$ and $\bar{i}_i$ are unit vectors in the direction of the scattered beam and incident beam, respectively.

When Eq. (2) is applied to the optical arrangement of Fig. 25 we have

$$\Delta f = \frac{2nV_{x_1}}{\lambda_i} \sin \theta/2 \tag{3}$$

where k_i has been replaced by $2\pi n/\lambda_i$, n is the index of refraction of the media corresponding to the incident laser wavelength λ_i in vacuo, and v_{x_1} is the magnitude of the velocity vector along the x_1 axis.

Expansion of this principle to three dimensions results in the representative electro-optical arrangement shown in Fig. 26. In addition, there are many other configurations which utilize both forward and back scattering applications of this principle.

The frequency Δf of the Doppler heterodyne signal can be recorded several ways. One of the methods most often used is to display the photomultiplier output on a spectrum analyzer. A direct spectrum analysis readout is adequate for measurement of

mean flow velocities in steady laminar flow, and in steady turbulent flow if the magnitude of the turbulence remains slight. Unfortunately, when the measurement is extended to velocity fluctuations in unsteady flow or turbulent flow no information can be obtained with a spectrum analyzer. It is suggested (Ref. 105) that under these conditions the instantaneous Doppler shift Δf be converted into an analog voltage and recorded on a magnetic tape or strip-chart recorder. Consideration of this problem by other investigators has produced new methods of electronic processing which have proved valuable in extracting information on turbulent flow (Ref. 113, pages 38 and 39). An up-to-date review of the techniques involved in laser Doppler measurements of velocity is presented in Section 5.1 of Ref. 113.

5.2.1.2 Detecting the Frequency Shift by Means of a Narrow Passband Interferometer

As in the preceding discussion, this instrument also monitors the change in frequency of the scattered light as a result of the Doppler effect. The significant difference is the utilization of a Fabry-Perot scanning interferometer which acts upon the optically homodyned photon beam as a variable-frequency, narrow passband filter, limiting the signal to the photon counter tube at any moment to those photons whose Doppler-shifted frequency coincides with the interferometer transmission frequency. The arrangement is illustrated in Fig. 27.

A collimated continuous beam from a helium-neon gas laser operating in a single axial mode (wavelength 6328Å) passes through a beam splitter and is reflected from a stationary mirror and also from individual moving particles within the flow field. The objective lens has a dual function in that it focuses the source light in a small region about the particle and also focuses the scattered rays at a point where the adjustable slit (for spatial resolution) is located. The collimating lens also has a twofold function as it collimates the scattered light and focuses the source beam at the location of the slit. Finally the scattered rays mixed with the reference rays return through the beam splitter into the interferometer. The interferometer functions as a very high resolution spectrometer to measure the wavelengths of the shifted and unshifted radiation.

It is common practice to display the amplified data from the photon counter tube on a storage oscilloscope. Because of the storage ability, after a short time the presentation consists of a distribution of maximum signals versus velocity. A one-to-one correspondence between Doppler-shifted frequency (velocity) and the horizontal displacement of the oscilloscope is obtained by coupling the interferometer mirror movement to the scope horizontal circuit. By sweeping the Doppler-shifted frequency an oscilloscope presentation is generated that is representative of the locus of maximum signals versus velocity. It has been suggested that this locus represents the largest particle with this particular velocity (Ref. 115).

The first successful application of the integration of a Fabry-Perot interferometer into a velocity measuring device based on the Doppler effect was reported by James, Babcock, and Seifert (Ref. 116). Further endeavors have developed a prototype instrument that has produced a measurement of particle velocities in a typical solid-propellant rocket exhaust (Ref. 117)

5.2.1.3 Comparison of Detection System Performance

The following information is presented in tabular form to facilitate a quick comparison of the two basic detection systems used in Doppler velocimetry.

	Narrow Passband Optical Filter (Fabry-Perot Interferometer)	Photomultiplier (Square-Law Response)
Velocity Range	200 to 20,000 ft/sec (see Note 1)	3×10^{-6} to 3000 ft/sec. An upper maximum of 6000 ft/sec (equivalent to Doppler-shifted frequency of 200 MHz at $\theta = 4$ deg using the formulation given by Eq. (3) of this report) has been suggested, but not measured (Ref. 105).
Spatial Resolution (Probe volume)	10^{-6} cm^3 (Diffraction-limited Lenses)	10^{-6} cm^3 (Diffraction-limited Lenses)

NOTE 1: Resolution and maximum velocity depend on the relationship:

$$d = \frac{2\lambda}{2V_{max}\,[\cos\theta - \cos(\theta + \phi)]}$$

where

d = interferometer mirror separation distance

c = speed of light

λ = wavelength of incident light

V_{max} = maximum velocity of particle

θ = angle between the particle path and the direction of the source of illumination referenced to the particle.

ϕ = angle between the direction of propagation of the incident light and the scattered light.

For example, if $\lambda = 6328$Å, $\theta = 30$ deg, and $\phi = 180$ deg

$d = 9.1$ cm for 600 m/sec

$d = 0.91$ cm for 6000 m/sec

5.2.2 Holographic Velocimetry

Since there has been considerable interest generated recently by the advent of new methods in holography utilizing the laser as a source of coherent radiation, a brief summary of the basic technique as applied to a particulate velocity measurement will be discussed in terms of applicability to rocket exhaust environs.

In general, holography is a technique based on the interference properties of electromagnetic radiation with matter. Three-dimensional quantitative information concerning particulate matter in a flow field can be recorded on and recovered from a two-dimensional medium (usually photographic film). Two optical arrangements are utilized for data recording purposes: in-line (Fig. 28a), and off-axis (Fig. 28b).

The application of holography is limited by constraints placed upon parameters such as laser power and coherence length. film resolution and sensitivity, optical transfer functions, subject motion, subject size, subject physical characteristics, and system vibration. An in-line arrangement is considerably less physically restrictive; consequently, this configuration is most often encountered in subsonic holographic velocimetry. The presence of turbulence or shock boundaries in supersonic flows may disturb an in-line reference beam to the extent that an off-axis reference could be required.

The most widely practiced recording scheme obtains three-dimensional velocity data by exposing a film plane to successive pulses from a Q-switched ruby laser. Each object (particle) will produce a Fraunhofer interferogram for each incident light pulse. Individual interference patterns (singlets) as recorded on the film contain the position and size in three dimensions of the particle. Two separate light pulses (time-wise) produce a pair of interference patterns or (doublet). A holographic doublet record contains unique information in the form of interference patterns on the location of a particle at the two different times of exposure. Since the time between exposures is a known parameter, the average velocity components can be determined if the three-dimensional displacement components can be extracted from the record.

A serious limitation of the holographic technique with regard to a high velocity flow is the progressive degradation of the fidelity of the interference pattern (smearing), which occurs as a direct result of the particle motion during the time of the exposing pulse (nominally 20 nsec for a Q-switched ruby laser). Consequently, the axial velocity component of the particulate flow should not exceed 1000 m/sec for particles which have characteristic diameters of less than 80 microns.

The holographic doublet technique along with important system considerations are fully reviewed from a state-of-the-art viewpoint in Ref. 118. An associated paper, Ref. 119, considers data processing methods applicable to holographic velocimetry. A modified approach concerning the development of flow-field holograms is presently being investigated by the Experimental Research Group of ARO, Inc., at AEDC. An interesting objective of this work is the study of high velocity particles such as those encountered in rocket exhausts. Extensive background information leading up to this phase of the program can be found in Refs. 120 through 126. A preliminary report on the experiment and initial results follows.

A holocamera was designed, tested, optimized, and then installed at the VKF Tunnel F test section for a series of experiments aimed at attempting to record small particles travelling at hypervelocities generated by electrode erosion in the arc heater of the tunnel. Particle velocities on the order of 10,000 ft/sec were expected. The significance of the high velocities lies in the fact that smaller particles (less than 75 microns) will produce streaks, instead of images, in reconstructed holograms because of the movement during the 20-nsec exposure time characteristic of the pulsed ruby laser.

The experimental arrangement for the test is shown in Fig. 29. As the light leaves the laser, it is spatially filtered with a 50-micron pinhole and allowed to diverge as it crosses the test section. An f/4, 4-in.-diam, diffraction-limited collimating lens collects the scattered radiation and focuses it onto the film plate. The optics are arranged such that there is a magnification of four at the film plane for an object a half meter from the collimating lens. The imaging characteristics of the lens were checked with small particle slides to gain some cognizance of the modulation transfer function of the lens.

Once the apparatus was arranged in Tunnel F, small particle slides were again placed in the field of view inside the tunnel and a hologram was taken. Inspection of the hologram revealed that diffraction patterns for even the small particles were evident. Furthermore, these particle fields reconstructed quite well. The small particle slides were removed from the tunnel, and holograms were made of the tunnel test section with no flow before each tunnel firing. As expected, there were no particle diffraction patterns present. A number of holograms were then made across the test section with the tunnel in operation. Since the flow in Tunnel F lasted only 0.5 sec, particles were in the field of view for only a fraction of this time. It was, therefore, difficult to obtain holograms with any particles in the field; they were so small (less than 20 microns) that the resolution of the camera was insufficient to record them. Under these conditions the results were negative, as the holograms were completely void of diffraction patterns.

Although the results of this experiment are inconclusive, the basic technique is sound and should be of interest to the rocket exhaust plume analyst involved in the development of instrumentation capable of quantitative velocity field information and sizes of individual particles.

SECTION VI
SUMMARY

6.1 TEMPERATURE

The necessity for an accurate determination of the thermodynamic state of a flowing gas at supersonic and subsonic velocities has become of utmost importance in the environmental testing of rocket propulsion systems. Physical probes, probably the first of which was the common mercury thermometer, have developed into elaborate and sophisticated devices that are usually designed for a specific type of temperature measurement. Recently a considerable amount of research and development work has been expended to develop suitable noninterfering techniques of temperature measurement.

Two principal temperature states for a rapidly moving gas are defined as: the static temperature which is the temperature that would be observed by a thermometer moving with the gas, and the total temperature which is the temperature detected by a stationary thermometer in a flowing gas at the instant the gas is brought to a complete rest, the kinetic energy being converted adiabatically into a temperature rise.

As far as theory is concerned, the stagnation temperature, T_0, which is the result of an adiabatic reduction of the velocity of the gas from free-stream velocity to zero is functionally related to the flow Mach number M_∞ and the static temperature T_∞ by the equation

$$T_0/T_\infty = 1 + \frac{\gamma - 1}{2}(M_\infty)^2$$

where γ represents the ratio of the specific heats of the gas.

Using existing physical temperature probes a direct measurement of static temperature cannot be accomplished at gas flow velocities where compressibility effects are appreciable. These effects occur at a Mach number of approximately 0.3. The reasoning associated with this phenomenon is that when a stationary probe is placed in a flow field the gas velocity will be reduced in the boundary layer. An indirect determination of static temperature is possible by measuring the static pressure in addition to either the gas density, the index of refraction, or the velocity of sound.

If radiation errors can be minimized, the total temperature can be measured at the stagnation point of a temperature probe within an acceptable tolerance. Probes that measure total temperature are more desirable than probes designed to measure other temperatures. This is largely attributable to their insensitivity to small changes in probe configuration which is a direct result of the stagnation region created in front of the temperature sensing element. Experience indicates that the calibration of a probe of this type exhibits a greater degree of repeatibility than calibrations produced by a probe for which the recovery factor is determined by the flow characteristics in the boundary layer.

In general, a conventional temperature probe operating in a high velocity flow field will indicate a temperature between the static temperature and the total temperature.

Physical temperature probes are capable of producing valid data throughout the flow field with the exception of the extreme near field where the high enthalpy content of the gas precludes their direct use. Careful attention should be given to probe design, radiation, orientation, and various other factors which affect the environment-sensor interface.

Noninterfering probe techniques eliminate the uncertainty associated with disturbances created by the physical probe interference with the ambient environs. Unfortunately, none of these techniques measure the bulk gas temperatures directly. In most cases a single temperature related parameter is monitored. Doubtful measurements are most often the result of a vague theoretical understanding of the complicated mechanism involved.

Recent theoretical and experimental work has advanced the state of the art in noninterfering temperature measuring techniques to a degree where accuracies on the order of 2 or 3 percent are commonplace for such methods as spectroscopy and excitation-emission phenomena.

In addition to the noninterfering property, so-called probeless techniques offer a solution to the measurement of various ultra-high temperatures in situations where the operation of a physical insert or the extraction of an electrical signal would be impossible.

If the flow is to be probed within its boundaries a constraint must be placed on the opacity of the flowing gases. Background radiation is often a problem when applying these techniques, but can usually be alleviated by proper filtering. The test environment should be considered and fully integrated into the overall system design for each individual application of probeless temperature diagnostic techniques.

An excellent example of a spectral method which measures both gas and particle temperatures in rocket exhaust plumes is presented in Ref. 127.

6.2 PRESSURE

Since pressure is a measurement of force per unit area, a direct pressure measurement requires introducing the sensor, directly, into the environment to be measured. For flowing gases such as those encountered in rocket exhaust plumes this is most often accomplished by means of a sampling device such as the impact tube. For this particular configuration the pressure recovered by the pressure sensor connected to the impact tube, except at very low free-stream pressures, is the average of the forces acting on a unit surface of gaseous matter located at the stagnation point of the probe or total pressure. Insertion of a pressure probe of this type into the flow field introduces various interactions with the environment which must be considered if representative measurements are to be obtained. Important phenomena which fall in this category are: the viscous effect, the thermal transpiration effect, the orifice effect, and the compressibility effect. Since the probe is necessarily constructed of material substance, a survival factor concerned with the probe-flow interface enters into the design and application of a particular system.

The most common pressure measuring instruments use a bellows or Bourdon element which senses pressure directly and produces a functional deflection as a result. Other instruments, usually of small physical size, rely on the direct pressure displacement of a very small, tightly stretched diaphragm which is measured by means of strain gages. The outputs of these instruments are often nonlinear, but, if correctly calibrated, they can be very accurate and produce good frequency response. As a word of caution, this type of instrument is, in most cases, quite sensitive to temperature and requires temperature compensation or correction.

The capacitance manometer offers an increase in sensitivity, expanded low pressure range, and greater accuracy over the strain-gage transducers. These direct sensing instruments also are sensitive to temperature.

A significant fact is that all of the mechanical sensing elements measure pressure directly without regard to gas composition.

The most sensitive direct pressure measuring devices (diaphragm capacitance manometers) become inaccurate at pressures less than 10^{-4} torr. This necessitates the use of indirect pressure measuring instruments that are capable of monitoring a specific gas property which has a functional pressure dependence. In general, these devices are sensitive to both gas temperature and composition. A competent understanding of the operation and application of these devices is required for valid results.

Existing spectroscopic pressure measuring techniques which associate the small shifts of wavelength of resonance spectral lines with changes in pressure suffer from the fact that the shift is also inversely proportional to the square root of the absolute temperature and depends on the kind of foreign gas in which the emitting atoms are located. The only data generated thus far are for sodium vapor in gases such as hydrogen, nitrogen, and argon.

It is recommended when making a pressure measurement that a direct pressure measuring device be utilized if at all possible. If this choice is impossible or undesirable as a result of range or other parameter, then a reliable instrument of proven worth from the class of indirect pressure sensing devices should be chosen, keeping in mind the ambient operating conditions. The operator should then thoroughly familiarize himself with the operation and application of the chosen instrument as it applies to his particular requirements.

6.3 DENSITY

Upon considering the existing and practical gas density measuring techniques, in almost every case the density measurements can be made without introducing probes into the volume measured. The vast majority of these density measurements are based on a large body of theory and technique having to do with the behavior of individual particles and their effect on the collection or macroscopic system. Before attempting to apply one of these methods a thorough understanding of the physics involved is highly recommended.

Optical density measuring techniques comprise a large percentage of the older methods that have been developed over many years of careful refinement. Most of the optical density procedures employed in the investigation of gaseous flow fields are based on a common fundamental concept: density gradients within the transluminated medium induce variations in the absolute local index of refraction which in turn modulate the traversing light. The data are recorded as intensity variations on a photographic plate. The level of interpretation of the data depends on how well the system can be described theoretically. The theory consists primarily of the concepts of geometric optics. Individual systems should be examined from a standpoint of physical optics to determine the ranges and conditions of operation.

Conventional optical methods (shadowgraphs, schlieren, and interferometry) of measuring densities or observing flow characteristics in high velocity gases approach the limits of feasibility if the product of test section width and absolute density becomes smaller than about 10^{-4} gm/cm^2. This is equivalent to pressures on the order of 10^{-3} atm and lower.

Excitation-emission or scatter techniques of density measurement such as the electron beam, metastable beam, gamma-ray beam or X-ray beam configurations allow measurements to be acquired at lower densities as compared to the optical methods. The corresponding pressure range for this type of measurement spans from several atmospheres, in the case of the gamma-ray or X-ray probe, to approximately 10^{-8} torr for the metastable beam system.

The source strength or beam intensity will not determine the accuracy of the method, but it does determine the length of time required to get a density measurement with a given probable error. All of these techniques are quite sensitive to geometry and in this regard care must be taken in the overall system design. Background radiation should always be considered as a problem when applying these methods. The beam generating apparatus is also a major intergration factor which must be considered in the overall system design.

Techniques which measure densities other than gas densities, for example, electron-ion densities, in most instances require the analysis of complicated physical phenomena. Therefore, a careful study of the technique as applied to a particular environment should be completed before the actual instrumentation phase is undertaken.

6.4 VELOCITY

The measurement of gas velocities in hot supersonic rocket exhausts by means of a physical insert is very difficult. Probes of any kind placed within the exhaust expansion set up strong shock waves which modify the flow field being measured, and are subjected to the forces and extremely high temperatures presented by the high velocity gases. This environment destroys all but the most elaborately designed probes. Consequently much work has been done concerning probeless or noninterfering techniques of velocity measurement. One of the earliest methods resorted to is the measurement of the thrust force and mass flow rate of the rocket motor; however, recent developments have extended the measurement of velocity directly to the gases and condensates within the flow itself.

The Doppler shift phenomenon has been exploited in applicable self-radiating characteristics of the flow media in addition to the scattering of foreign radiation. A large number of methods based on this principle have been developed. The span of velocities for which these techniques are suited range from a small fraction of a cm/sec to the neighborhood of 8000 m/sec. Resolution varies from a fraction of a cm/sec to approximately 50 m/sec. The velocity range and resolution is a direct function of the capabilities of a particular system. The sensitive optical equipment necessary to obtain these measurements requires that the system be well isolated from mechanical disturbances.

Accurate velocity distributions have been obtained using a time-of-flight technique applied to impulse functions along a collimated molecular beam which is extracted from the gaseous flow field. Because of the large probe necessary to contain the apparatus, the system is constrained to the far field region of an exhaust plume.

One of the latest techniques, holography, is still yet unproved as a method for measuring particulate velocities above approximately 2000 ft/sec for characteristic diameters below 100 microns. At this writing an attempt is under way to measure particulate matter by holographic means, at velocities of approximately 4000 ft/sec, by personnel at AEDC. The characteristic diameter of the particles averages approximately 50 microns.

REFERENCES

1. Chapman, S. and Cowling, T. G. The Mathematical Theory of Non-Uniform Gases. Cambridge University Press, 1952 (Second Edition).

2. Schrodinger. Statistical Thermodynamics. Cambridge University Press, London, 1948.

3. Allis and Herlin. Thermodynamics and Statistical Mechanics, McGraw-Hill, New York, 1952.

4. Fowler and Guggenheim. Statistical Thermodynamics. Cambridge University Press, New York, 1952.

5. Dale. Statistical Thermodynamics. Prentice-Hall, Englewood Cliffs, N. J., 1954.

6. Sommerfield. Thermodynamics and Statistical Mechanics. Academic Press, New York, 1956.

7. Wilson. Thermodynamics and Statistical Mechanics. Cambridge University Press, New York, 1957.

8. Lee, Sears, and Turcotte. Statistical Thermodynamics. Addison-Wesley, Reading, Massachusetts, 1963.

9. Aston and Fritz. Thermodynamics and Statistical Thermodynamics. John Wiley and Sons, New York, 1959.

10. Baker, Ryder, and Baker. Temperature Measurement in Engineering. Vol. II, John Wiley and Sons, New York, 1961.

11. Temperature Its Measurement and Control in Science and Industry. Herzfeld, C. M., Editor-in-Chief, Vol. II, Parts 1 and 2, Reinhold, New York, 1962.

12. Broida, H. P. "Experimental Temperature Measurements in Flames and Hot Gases." Temperature, Its Measurement and Control in Science and Industry, Vol. II (Edited by H. C. Waolfe), Reinhold, New York, 1962-1963.

13. Powell, H. M. and Heald, J. H. "A System for the Measurement of Velocity Distributions of Molecular Beams." AEDC-TR-68-151 (AD675306), September 1968.

14. Muntz, E. P. "Measurement of Rotational Temperature, Vibrational Temperature, and Molecular Composition in Non-Radiating Flows of Low Density Nitrogen." University of Toronto Institute of Aerophysics, Report 71, AFOSR-TN 60-499, April 1961.

15. Muntz, E. P. and Softley, E. J. "An Experimental Study of Laminar Near Wakes." The General Electric Space Sciences Laboratory, GE-TIS-R65SD6, April 1965.

16. Zempel, R. E. and Muntz, E. P. "Slender Body Near Wake Density Measurements at Mach Numbers Thirteen and Eighteen." The General Electric Space Sciences Laboratory, GE-MSD-TIS-R63SD55, July 1964.

17. Softley. E. J., Muntz, E. P. and Zempel, R. E. "Experimental Determination of Pressure, Temperature, and Density in Some Laminar Hypersonic Near Wakes." The General Electric Space Sciences Laboratory, GE-MSD-TIS-R64SD35, May 1964.

18. Petrie, S. L., Pierce, G. A. and Fishburne, E. S. "Analysis of the Thermo-Chemical State of an Expanded Air Plasma." Ohio State University Research Foundation, AFFDL-TR-64-191, August 1965.

19. Sebacher, D. J. and Duckett, R. F. "A Spectrographic Analysis of a 1-Foot Hypersonic Air-Tunnel Airstream Using an Electron Beam Probe." NASA TR-R-214, December 1964.

20. Marsden, D. J. "The Measurement of Energy Transfer in Gas-Solid Surface Interactions Using Electron Beam Excited Emission of Light." University of Toronto Institute of Aerophysics Report 101, November 1964.

21. Robben, F. and Talbot, L. "Some Measurements of Rotational Temperature in a Low Density Wind Tunnel Using Electron Beam Fluorescence." University of California Report No. AS-65-5, May 1965.

22. Marrone, P. V. "Rotational Temperature and Density Measurements in Underexpanded Jets and Shock Waves Using an Electron Beam Probe." University of Toronto Institute of Aerophysics Report 113, April 1966.

23. Askenas, H. "Rotational Temperature Measurements in a Free Jet and in a Static Gas." NASA-JPL Space Programs Summary No. 37-41, Vol. IV, October 1966, p. 196.

24. Hickman, R. S. "Rotational Temperature Measurement in Nitrogen Using an Electron Beam." University of Southern California, USCAE 104. September 1966.

25. Merrit, G. E. "Velocity Measurements in the University of Southampton Gun Tunnel." A.A. S.U. Report No. 172, April 1961.

26. Bowman, J. E. "Determination of Stagnation Temperatures in the RARDE Hypersonic Gun Tunnel from Streak Camera Measurements of Flow Velocity." A.R.C. 27, February 1966, p. 768.

27. Kilburg, R. F. "A High Response Probe for the Measurement of Total Temperature Profiles through a Turbulent Boundary Layer with High Heat Transfer in Supersonic Flow." AIAA Paper No. 68-374, April 1968.

28. Perry, J. H. and East. R. A. "A Miniature Total Temperature Probe for Boundary Layer Measurements in Short Running Time Hypersonic Facilities." Proceedings 1969 International Congress on Instrumentation in Aerospace Simulation Facilities, May 1969, p. 295.

29. Grey, J. "Thermodynamic Methods of High-Temperature Measurement." ISA Transactions, Vol. 4, April 1965, pp. 102-115.

30. Halbach, C. R. and Freeman, L. "The Enthalpy Sensor—A High Gas Temperature Measuring Probe." Report MR 20, 331, The Marquardt Corporation, June 1965.

31. Huber, F. J. A. "Probes for Measuring Mass Flux, Stagnation Point Heating and Total Enthalpy of High-Temperature Hypersonic Flows." AIAA Preprint No. 66-750, September 21-23, 1966.

32. Incropera, F. P. and Leppert, G. "Investigation of Arc Jet Temperature-Measurement Techniques." ISA Transactions, Vol. 6, January 1967, pp. 35-41.

33. Folck, J. L. and Heck, R. R. "Operational Experiences and Preliminary Results of Total Enthalpy Probe Measurements in the AFFDL 50-Megawatt Electrogasdynamics Facility." FDM-TM-68-2, April 1968.

34. Softley, E. J. "Use of a Pulse Heated Fine Wire Probe for the Measurement of Total Temperature in Shock Driven Facilities." AIAA Paper No. 68-393, April 1968.

35. Langmuir, I. and Mott-Smith, H. M. "Positive Ion Currents from the Positive Column of the Mercury Arc." G. E. Review, Vol. 26, 1923, p. 731.

36. Langmuir, I. and Mott-Smith, H. M. "Positive Ion Currents from the Positive Column of Mercury Arcs." Science, Vol. 58, 1923, p. 290.

37. Langmuir, I. and Mott-Smith, H. M. "The Pressure Effect and Other Phenomena in Gaseous Discharges." Journal of the Franklin Institute, Vol. 196, 1923, p. 751.

38. Mott-Smith, H. M. and Langmuir, I. "The Theory of Collectors in Gaseous Discharges." Physical Review, Vol. 28, 1926, pp. 727-763.

39. Talbot, L. "Theory of the Stagnation-Point Langmuir Probe." Physics of Fluids, Vol. 3, 1960, pp. 289-298.

40. Talbot, L. " A Note on the Stagnation-Point Langmuir Probe." Physics of Fluids, Vol. 5, 1962, pp. 629-630.

41. Brundin, C. L. and Talbot, L. "Free Molecule Langmuir Probes in a Flowing Plasma." Proceedings of the First International Congress on Instrumentation in Aerospace Simulation Facilities, 1964.

42. Brundin, C. L. and Talbot, L. "The Application of Langmuir Probe Techniques to Flowing Ionized Gases." North Atlantic Treaty Organization Advisory Group for Aeronautical Research and Development Report No. 478, September 1964.

43. Kawashima, N. "Ion Temperature Measurement of a Streaming He Plasma by a Double Probe Method." Applied Physics Letters, Vol. 7, No. 12, December 1965, pp. 324-325.

44. Muntz, E. P., Harris, C. J. and Kaegi, E. M. "Techniques for the Experimental Investigation of the Properties of Electrically Conducting Hypersonic Flow Fields." The Second National Symposium on Hypervelocity Techniques, Denver Research Institute, Denver, Colorado, March 1962.

45. Potter, J. L., Kinslow, M. and Boylan, D. E. "An Influence of the Orifice on Measured Pressures in Rarefied Flow." AEDC-TDR-64-175 (AD447734), September 1964, and Rarefied Gas Dynamics, Edited by J.H. de Leeuw, Volume II, Academic Press, 1966.

46. Ashkenas, H. and Sherman, F. S. "The Structure and Utilization of Supersonic Free Jets in Low Density Wind Tunnels." Rarefied Gas Dynamics, Edited by J. H. de Leeuw, Volume II, Academic Press, 1966.

47. Rogers, K. W., Wainwright, J. B. and Touryan, K. J. "Impact and Static Pressure Measurements in High Speed Flows with Transitional Knudsen Numbers." Rarefied Gas Dynamics, Edited by J. H. de Leeuw, Volume II, Academic Press, 1966.

48. Pressure Handbook, Aronson, Milton H., Editor, Rimbach Publications Division of Chilton Company, Pittsburgh, 1963.

49. Perino, Peter R. "Characteristics of Thin Film Strain Gage Transducers." Instrument Society of America 21st Annual Conference and Exhibit, New York, October 24-27, 1966.

50. Hecht, Richard. "Study of New Methods to Measure Low Pressure." NASA CR-1120, August 1968.

51. Utterback, N. G. and Griffith, Thomas, Jr. "Reliable Submicron Pressure Readings with Capacitance Manometer." The Review of Scientific Instruments, Vol. 37, Number 7, July 1966.

52. Lamers, K. W. and Rony, P. R. "The Design, Construction, and Operation of a Differential Micromanometer." UCRL-11218, October 1965 and April 1965.

53. Sherrell, F. G. "Vacuum Measuring Instruments and Calibration Techniques." Paper presented at The Cryogenic Engineering Conference, Boulder, Colorado, June 18, 1970.

54. Leck, J. H. Pressure Measurements in Vacuum Systems. Reinhold, New York, 1957.

55. McKay, E. M. "The Output and Sensitivity of Vacuum Gauges Using a Heated Element in a Wheatstone Bridge." Journal of Scientific Instruments (Journal of Physics E), Series 2, Vol. 2, April 1969, pp. 305-310.

56. Dushman, Saul. Scientific Foundations of Vacuum Technique. Lafferty, J. M., Editor, John Wiley and Sons, New York, 1962 (Second Edition).

57. Ramsauer, C. "About the Temperature in the Electric Arc." Elektrotechnik und Maschinenbau, Vol. 51, 1933, p. 189.

58. Von Engel and Steenbeck. "Measurements of the Time Dependence of the Gas Temperatures in the Column of an AC Arc." Wiss. Veroeff. des Siemens-Konzerns, Vol. 12, 1933, p. 74.

59. Venable, D. and Kaplan, D. E. "Electron Beam Method of Determining Density Profiles across Flash Waves in Gases at Low Densities." Journal of Applied Physics, Vol. 26, 1955, p. 639.

60. Hurlbut, F. C. "An Electron Beam Density Probe for Measurements in Rarefied Gas Flows." WADC Technical Report 57644 (AD155537), January 1958.

61. Schultz-Grunow, F. and Frohn, A. "Density Distribution in Shock Waves Traveling in Rarefied Monatomic Gases." Rarefied Gas Dynamics, J. H. de Leeuw, editor, Vol. 1, Academic Press, New York, 1965, p. 250.

62. Russell, D. A. "Electron-Beam Measurements of Shock-Wave Thickness." Rarefied Gas Dynamics, J. H. de Leeuw, editor, Vol. 1, Academic Press, New York, 1965, p. 265.

63. Wada, I. "Experimental Study of Low Pressure Hypersonic Flow by Using an Electron Beam Densitometer." Rarefied Gas Dynamics, J. H. de Leeuw, editor, Vol. 1, Academic Press, New York, 1965, p. 535.

64. Ballard, H. N. and Venable, D. "Shock-Front-Thickness Measurements by an Electron Beam Technique." Physics of Fluids, Vol. 1, No. 3, 1958, p. 225.

65. Schumacher, B. W. and Gadamer, E. O. "Electron Beam Fluorescence Probe for Measuring the Local Gas Density in a Wide Field of Observation." Canadian Journal of Physics, Vol. 36, 1958, p. 659.

66. Muntz, E. P. and Marsden, D. J. "Electron Excitation Applied to the Experimental Investigation of Rarefied Gas Flows." Rarefied Gas Dynamics, J. A. Laurmann, editor, Vol. 2, Academic Press, New York, 1963, p. 495.

67. Petrie, S. L. "Density Measurements with Electron Beams." AIAA Journal, Vol. 4, No. 9, September 1966, p. 1679.

68. Robben, F. and Talbot, L. "Measurement of Shock Wave Thickness by the Electron Beam Fluorescence Method." Physics of Fluids, Vol. 9, No. 4, 1966, p. 633.

69. Gadamer, E. O. "Application of an Electron Gun to Density Measurements in Rarefied Gas Flow" UTIA Bulletin and Progress Report, 1960.

70. Rothe, D. E. "Electron Beam Studies of the Diffusive Separation of Helium-Argon Mixtures." Physics of Fluids, Vol. 9, No. 9, 1966, p. 1643.

71. Cunningham, J. W. and Fisher, C. H. "Measurement of Gas Density by Electron Scattering." AEDC-TR-66-212 (AD646590), February 1967.

72. Grodski, J. J. and Schumacher, B. W. "Local Density Determinations in Rarefied Gas Flows by Measuring the Large-Angle Single-Scattering from an Electron Beam." ISA Transactions, Vol. 6, No. 2, April 1967.

73. Camac, M. "Argon Shock Structure." Rarefied Gas Dynamics. J. H. de Leeuw, editor, Vol. 1, Academic Press, New York, 1965, p. 240.

74. Heitler, W. Quantum Theory of Radiation, Oxford University Press, Oxford, 1948.

75. Kosh, H. W. and Matz, J. W. "Bremsstrahlung Cross-Section Formulas and Related Data." Review of Modern Physics, Vol 31, No. 4, October 1959, p. 920.

76. Ziegler, C. A., Bird, L. L., Olson, K. H., Hull, J. A., Morreal, J. A. "Technique for Determining Density Distribution in Low Pressure, High Temperature Gases." The Review of Scientific Instruments, Vol. 35, No. 4, April 1964, p. 450.

77. Rossi, B. and Greisen, K. "Cosmic Ray Theory." Review of Modern Physics, Vol. 13, October 1941, p. 240.

78. Loeb, L. B. Fundamental Processes of Electrical Discharge in Gases. John Wiley and Sons, New York, 1939.

79. Loeb, L. B. "Secondary Processes Active in the Electrical Breakdown of Gases." British Journal of Applied Physics. Vol. 3, 1952, p. 341.

80. French, J. B. "Langmuir Probes in a Flowing Low Density Plasma." UTIA Report 79, 1961.

81. Allen, J. E., Boyd, R.L.F. and Reynolds, P. "The Collection of Positive Ions by a Probe Immersed in a Plasma." Proceedings of the Phys. Society, Vol. 70, Section B, London, 1957, p. 297.

82. Bernstein, I. B. and Rabinowitz, I. N. "Theory of Electrostatic Probes in a Low-Density Plasma." Physics of Fluids, Vol. 2, 1959, p. 112.

83. Brundin, C. L., Talbot, L. and Sherman, F. S. "Flow Studies in an Arc-Heated Low Density Supersonic Wind Tunnel." Univ. of Calif. Institute of Engineering Research Report HE-150-181, April 15, 1960.

84. Talbot, L., Katz, J. E. and Brundin, C. L. "A Comparison between Langmuir Probe and Microwave Electron Density Measurements in an Arc Heated Low Density Supersonic Wind Tunnel." Univ. of Calif. Institute of Engineering Research Report HE-150-186, January 27, 1961.

85. Muntz, E. P., Harris, C. J. and Kaegi, E. M. "Techniques for the Experimental Investigation of the Properties of Electrically Conducting Hypersonic Flow Fields." The Second National Symposium on Hypervelocity Techniques, Denver Research Institute, Denver, Colorado, March 1962.

86. Aerophysics Wing Staff, "CARDE-ARPA Re-entry Physics Research Program on Turbulent Wakes." CARDE TN 1727/66, Period 1 January–30 June 1966 and CARDE TN 1747/67 Period 1 July–31 December 1966.

87. Philco-Ford Corporation Space and Re-Entry Systems. Final Report–Advanced Penetration Problems–Wake Structure Measurements. Publication No. UG-4201, 16 July 1966–15 January 1967.

88. Sutton, George W. "On the Feasibility of Using a Langmuir Probe to Measure Electron Densities in Turbulent Hypersonic Wakes." AVCO Everett Research Laboratory Report 276, June 1967.

89. Sutton, Emmett A. "The Chemistry of Electrons in Pure Air Hypersonic Wakes." AVCO Everett Research Laboratory Report 266, July 1967.

90. Center, R. E. "Measurement of Electron Density behind Shock Waves by Free-Molecular Langmuir Probes." SAMSO-TR-69-369 (AVCO Everett Research Laboratory Report 292), December 1969.

91. Heckman, D., Emond, A. and Seviguy, L. "Some Results of Electrostatic Probe Studies of Turbulent Hypersonic Wake Plasmas." AIAA Paper No. 68-689, AIAA Fluid and Plasma Dynamics Conference, Los Angeles, California, June 24-26, 1968.

92. Belland, P. "Mesure de la Densite Electronique D'un Plasma Par Interferometrie Laser He-Ne." Thesis, Faculte des Sciences de l'Universite de Paris, December 15, 1967.

93. Drawin, H. W., Henning, H., Herman, L. and Nguyen-Hoe. "Stark-Broadening of Hydrogen Balmer Lines in the Presence of Strong Magnetic Fields in Plasmas." Journal of Quantitative Spectroscopy and Radiative Transfer, Vol. 9, March 1969, pp. 317-331.

94. Berg, O. E. and Richardson, F. F. "The Pioneer 8 Cosmic Dust Experiment." The Review of Scientific Instruments, Vol. 40, No. 10, October 1969, pp. 1333-1337.

95. Kerker, Milton. The Scattering of Light and Other Electromagnetic Radiation. Academic Press, New York, 1969.

96. Prinsen, H. W. and Tripp, B. R. "Investigation of the Feasibility of a Doppler Radar Technique to Measure Free Stream Velocity in the AFFDL Electrogasdynamics Facility." AFFDL-TR-68-78, June 1968.

97. Peters, T. Printed remarks in discussion section, Low Pressure Aerodynamic Facilities Proceedings of the Round Table Conference. Smolderen, J. J., Editor, TCEA TM 12, October 1960, p. 43.

98. Funk, B. H. "A Direct Measurement of the Most Probable Preferred Angular Velocity of Turbulent Structures by Optical Correlation of Laser Schlieren Signals." NASA TM X-53870, August 1969.

99. Benek, J. A. and Powell, H. M. "Investigation of Performance Parameters of a Mass Spectrometer Sampling Probe in Rarefied Flows." AEDC-TR-70-79, June 1970.

100. Van de Hulst, H. C. Light Scattering by Small Particles. John Wiley and Sons, New York, 1957.

101. Rudd, M. J. "A New Theoretical Model for the Laser Dopplermeter." Journal of Scientific Instruments, Series 2, Vol. 2, January 1969, pp. 55-58.

102. Yeh, Y. and Cummins, H. Z. "Localized Fluid Flow Measurements with a He-Ne Laser Spectrometer." Applied Physics Letters, Vol. 4, No. 10, May 1964, pp. 176-178.

103. Foreman, J. W., Jr., George, E. W., and Lewis, R. D. "Feasibility Study of a Laser Flowmeter for Local Velocity Measurements in Gas Flow Fields." Brown Engineering Technical Note R-149 (AD616719), May 1965.

104. Foreman, J. W., Jr., George, E. W. and Lewis, R. D. "Measurement of Localized Flow Velocities in Gases with a Laser Doppler Flowmeter." Applied Physics Letters, Vol. 7, No. 4, August 1965, pp. 77-78.

105. Foreman, J. W., Jr., et al. "Fluid Flow Measurements with a Laser Doppler Velocimeter." IEEE J. Quantum Electronics, Vol. QE-2, No. 8, August 1966, pp. 260-266.

106. Huffaker, R. M., Kinnard, K. F. and Rolfe, E. "Laser Doppler System for Measuring Three-Dimensional Vector Velocity." NASA Case MFS-20386, April 22, 1969.

107. Welch, N. E. and Tomme, W. J. "The Analysis of Turbulence from Data Obtained with a Laser Velocimeter." NASA-TM-X-53703, February 5, 1968.

108. Lewis, R. D., Chatterton, N. E. and Watson, H. J. "Investigation of Two-Dimensional Flow Measurements Using the Laser Doppler Technique." Brown Engineering Technical Note AST-284 (AD685249), December 1968.

109. Lewis, R. D., Foreman, J. W., Jr., Watson, H. J., and Thornton, J. R. "Laser Doppler Velocimeter for Measuring Flow-Velocity Fluctuations." Physics of Fluids, Vol. 11, February 1968, pp. 433-435.

110. Brayton, D. B. "A Laser Doppler-Shift Velocity Meter with Self-Aligning Optics." Proceedings of the Technical Program, Electro-Optical Systems Design Conference, September 16-18, 1969, New York City Coliseum.

111. Huffaker, R. M. "Laser-Doppler Gas Velometer." NASA Tech Brief 70-10143, April 1970.

112. Lennert, A. E., Brayton, D. B., Goethert, W. H. and Smith, F. H. "Laser Applications for Flow Field Diagnostics." Presented at 2nd National Laser Industry Association Meeting, October 20-22, 1969. Published in Laser Journal, March-April 1970, and Industrial Research, February 1970.

113. Vasudevan, M. S. and Jansson, R.E.W. "Optical Methods of Measuring Turbulence." University of Southampton Department of Aeronautics & Astronautics Report No. 288, July 1969.

114. Grant, G. R. and Donaldson, R. W. "A Laser Velocity Measurement System for High-Temperature Wind Tunnels." NASA TM X-1976, April 1970.

115. James, R. N., Babcock, W. R. and Seifert, H. S. "A Laser-Doppler Technique for the Measurement of Particle Velocity." AIAA Journal, Vol. 6, No. 1, January 1968, pp. 160-162.

116. James, R. N., Babcock, W. R. and Seifert, H. S. "Application of a Laser-Doppler Technique to the Measurement of Particle Velocity in Gas-Particle Two-Phase Flow." AFRPL-TR-66-119, June 1966.

117. Morse, H. L., Tullis, B. J., Babcock, W. R. and Seifert. H. S. "Development, Application and Design Specifications of a Laser-Doppler Particle Sensor for the Measurement of Particle Velocities in Two-Phase Rocket Exhausts." Vol. I & II, AFRPL-TR-68-153, September 1968.

118. Shofner, F. M., Menzel, R. W., Gee, T. H. and Webb, R. O. "Fundamentals of Holographic Velocimetry." Proceedings 1969 International Congress on Instrumentation in Aerospace Simulation Facilities, May 1969, pp. 126-135.

119. Shofner, F. M., Menzel, R. W., Gee, T. H. and Webb, R. O. "Processing Holographic Velocimetry Data." Proceedings 1969 International Congress on Instrumentation in Aerospace Simulation Facilities, May 1969, pp. 136-144.

120. Trolinger, J. D., Farmer, W. M., and Belz, R. A. "Multiple Exposure Holography of Time Varying Three-Dimensional Fields." Applied Optics, No. 8, August 1968.

121. Belz, R. A. "Analysis of the Techniques for Measuring Particle Size and distribution from Fraunhofer Diffraction Patterns." AEDC-TR-68-125 (AD674741), September 1968, and Masters Thesis, University of Tennessee, June 1968.

122. Farmer, W. M. "Dynamic Holography of Small Particle Fields Using a Q-Spoiled Laser." Masters Thesis, University of Tennessee, August 1968.

123. Trolinger, J. D., Farmer, W. M. and Belz, R. A. "Applications of Holography in the Environmental Sciences." Invited Paper National Symposium of the Institute of Environmental Sciences April 20, 1969, published in the IES Journal, October 1969.

124. Trolinger, J. D. and O'Hare, J. E. "Aerodynamic Holography." AEDC-TR-70-44 (AD709764), August 1970.

125. Trolinger, J. D. "A Wide View Angle Holo-Camera." Applied Optics, August 1969.

126. Farmer, W. M., Belz, R. A., Trolinger, J. D., and O'Hare, J.E. "Holographic Flow Visualization." AIAA Tennessee Section Weekend Workshop Manual on Applied Measuring Techniques, February 1969.

127. Adams, J. M. "The Measurement of Gas and Particle Temperatures in Rocket Motor Chambers and Exhaust Plumes." Pyrodynamics, Gordon and Breach, Science Publishers Ltd., Ireland, Volume 6, No. 1, January 1968, pp. 1-28.

128. Jen, Teh-Sen, Hoyaux, M. F. and Frost, L. S. "A New Spectroscopic Method of High Pressure Arc Diagnostics." Journal of Quantitative Spectroscopy and Radiative Transfer, Vol. 9, No. 4, April 1969, pp. 487-498.

129. Gusinow, M. A., Gerardo, J. B. and Hill, R. A. "Spectral Temperatures of Nonuniform Plasmas," Journal of Quantitative Spectroscopy and Radiative Transfer, Vol. 9, No. 3, March 1969, pp. 383-389.

130. Blom, A. P. and Pratt, N. H. "A Theoretical Study of the Interpretation of Emission-Absorption Intensity Ratio Temperature Measurements in the Absence of Thermal Equilibrium." Journal of Quantitative Spectroscopy and Radiative Transfer, Vol. 9, No. 3, March 1969, pp. 423-442.

131. Rixom, P. J. and Townsend, W. G. "The Silicon Integrating Light Detector Applied to Optical Pyrometry." Journal of Scientific Instruments (Journal of Physics E), Series 2, Vol. 2, February 1969, pp. 153-154.

132. Unger, H. J., Hill, F. K. and Paul, N. G. "Spectroscopic Determination of High Velocity Flow Field Static Temperatures." Proceedings 1969 International Congress on Instrumentation in Aerospace Simulation Facilities, May 1969, pp. 303-308.

133. Jolls, K. R. and Sforza, P. M. "A New Ferroelectric Transducer for Use in Heat Transfer and Flow Studies." Proceedings 1969 International Congress on Instrumentation in Aerospace Simulation Facilities, May 1969, pp. 278-286.

134. Petrie, S. L. and Lazdinis, S. S. "Ion Excitation Applied to the Measurement of the Properties of Molecular Oxygen in High Speed Flows." AFFDL-TR-68-153, December 1968.

135. Anderson, J. B., Andres, R. P., Fenn, J. B. and Maise, G. "Studies of Low Density Supersonic Jets." Rarefied Gas Dynamics, Edited by J. H. de Leeuw, Vol. II, Academic Press, 1966.

136. Beck, H. "Temperature Measurements in Hot, Fast-Moving Gases with Special Consideration of Their Application to Aircraft and Spacecraft Propulsion." Astronautik, Vol. 5, March-April 1968, pp. 36-42 (in German).

137. Rochelle, W. C. and Kooker, D. E. "Heat-Transfer and Pressure Analysis of Rocket Exhaust Impingement on Flat Plates and Curved Panels." Journal of Spacecraft and Rockets, Vol. 6, No. 3, March 1969, pp. 248-256.

138. Sheeran, W. J., Hendershot, K. C. and Llinas, J. "A Short Duration Experimental Technique for Investigating High-Altitude Rocket Plume Effects." Proceedings of the Rocket Plume Specialists' meeting TOR-0200 (S4960-10)-1, Vol. II, July 1968, pp. 4-135 to 4-190.

139. Newcomer, J. C. "A Pressure Transducer of the Strain-Gauged Diaphragm Type." Journal of Scientific Instruments (Journal of Physics E), Series 2, Vol. 2, February 1969, pp. 218-219.

140. Iglesias, G. E., Santochi, O. R. and Puparelli, M. "Convection Pirani Vacuum Gauge." The Review of Scientific Instruments, Vol. 40, No. 10, October 1969, pp. 1291-1203.

141. Mori, H. and Suminokura, T. "Interferometric Method for Measuring Ultrasonic Light Diffraction Spectra." Japanese Journal of Applied Physics, Vol. 7, No. 12, December 1968, pp. 1518-1522.

142. Akaishi, K. "Measurement of Extreme High Vacuum by Negative Potential Modulation Method with a Modulated Bayard-Alpert Gauge." Japanese Journal of Applied Physics, Vol. 8, No. 8, August 1969, pp. 1061-1062.

143. Martens, A. E. and Keller, J. D. "An Instrument for Sizing and Counting Airborne Particles." American Industrial Hygiene Association Journal, Vol. 29, May-June 1968.

144. Gloersen, P. "Density Profile Measurements." AFOSR 67-2364 (AD660588), September 1967.

145. Schmidt, Conrad. "Measurement of Atomic and Molecular Beam Intensities with a Torsion Balance." The Review of Scientific Instruments, Vol. 40, No. 10, October 1969, pp. 1327-1329.

146. Bunting, W. D. and Heikkila, W. J. "Observations on the Effect of Surface Conditions on Langmuir Probes." Journal of Applied Physics, Vol. 41, No. 5, April 1970, pp. 2263-2264.

147. Dewey, J. M. and Anson, W. A. "Density Measurements in a Value Driven Shock Tube." The Review of Scientific Instruments, Vol. 40, No. 3, 1969, pp. 451-455.

148. Oliver, B. M. and Clements, R. M. "Radio-Frequency Floating Double Probe as a Plasma Diagnostic." Journal of Applied Physics. Vol. 41, No. 5, April 1970, pp. 2117-2122.

149. Schneiderman, A. and Itzkan, I. "Interferometric Gas-Flow Studies with a Pulsed 5501-Å Neon Laser." Journal of Applied Physics, Vol. 41, No. 5, April 1970, pp. 2253-2256.

150. O'Hare, J. E. and Trolinger, J. D. "Holographic Color Schlieren." Applied Optics, Vol. 8, No. 10, October 1969, pp. 2047-2050.

151. Measures, R. M. "Spectral Line Interferometry: A Proposed Means of Selectively Measuring the Change in the Density of a Specific Atomic Population." Applied Optics, Vol. 9, No. 3, March 1970, pp. 737-741.

152. Lederman, S. and Dawson, E. F. "An Application of a Modified Mass Spectrometer to Shock Tube Diagnostics." Polytechnic Institute of Brooklyn, Farmingdale, New York, Nonr-839(38 .)

153. Howlett, L. C. and Swigart, J. I. "Rocket-Borne Rayleigh Scattering Instrumentation to Measure Atmospheric Density." The Review of Scientific Instruments, Vol. 40, No. 1, January 1969, pp. 28-32.

154. Vriens, L., Boers, A. L. and Smit, J. A. "Measurements on a Molecular Beam Apparatus for Mass Spectrometric Study of Reactions in Flames." Applied Scientific Research, Section B, Vol. 12, December 1965, pp. 65-73.

155. Brook, J. W. "Far Field Approximation for a Nozzle Exhausting into a Vacuum." Journal of Spacecraft and Rockets, Vol. 6, No. 5, May 1969, pp. 626-628.

156. Chivian, J. S., Claytor, R. N. and Eden, D. D. "Infrared Holography at 10.6μm." Applied Physics Letters, Vol. 15, No. 4, 15 August 1969, pp. 123-125.

157. Maguire, B. L., Muntz, E. P. and Mallin, J. R. "Quantitative Visualization of Low Density Flow Fields Using the Electron Beam Excitation Technique." Proceedings 1969 International Congress on Instrumentation in Aerospace Simulation Facilities, May 1969, pp. 79–85.

158. Hannah, B. W. and Dale, R. G., Jr. "Quantitative Schlieren Measurements by the Photomultiplier Technique." Proceedings 1969 International Congress on Instrumentation in Aerospace Simulation Facilities, May 1969, pp. 223-228.

159. Oertel, F. H. and Spurk, J. H. "Two-Wavelength Laser Interferometry of Hypersonic Ionized Flows." Ballistic Research Laboratories Report No. 1435, May 1969.

160. Dix, R. E. "Sampling Probe for Instantaneous Mass Spectrometric Analysis of Rarefied High Enthalpy Flow." AEDC-TR-69-37 (AD686405), April 1969.

161. Chamberlain, J., Gebbie, H. A., George, A. and Beynon, J.D.E. "A 337 μm CW Maser Interferometer for Plasma Diagnostics." Journal of Plasma Physics, Vol. 3, Part 1, February 1969, pp. 75-79.

162 Fisher, M. J. and Johnston, K. D. "Turbulence Measurements in Supersonic, Shock-free Jets by the Optical Crossed-Beam Method." NASA TN D-5206, February 1970.

163. Alcalay, J. A. and Knuth, E. L. "Molecular-Beam Time-of-Flight Spectroscopy." The Review of Scientific Instruments, Vol. 40, No. 3, March 1969, pp. 438-447.

164. Fuhs, A. E. "Development of a Device for Measuring Electrical Conductivity of Ionized Air during Re-Entry." STL/TR-60-0000-09256, September 1960.

165. Fuhs, A. E. "Additional Comments on a Technique for Obtaining the Electrical Conductivity/Velocity Profile." DCAS-TDR-62-52, Report No. TDR-930(2230-03) TN-5, March 1962.

166 Owens, J. C. "Optical Doppler Measurement of Microscale Wind Velocity." Proceedings of the IEEE, Vol. 57, No. 4, April 1969, pp. 530-536.

167. Pigott, J. C. and Rittenhouse, L. E. "Noninterference Velocity Measurements in a Supersonic Seeded Plasma Using Tracers Produced by a Spark Discharge and a Focused Pulsed Laser." AEDC-TR-68-235 (AD678521), November 1968.

168. Karamcheti, K. et al. "Measurements of Pressure and Speed of Flow in a Spark-Heated Hypersonic Wind Tunnel." AEDC-TR-62-218 (AD288668), November 1962.

169. Jacobson, A. D., Evtuhov, V. and Neeland, J. K. "Motion Picture Holography." Applied Physics Letters, Vol. 14, No. 4, 15 February 1969, pp. 120-122.

170. Hall, W. D. and Champagne, E. B. "A Technique for Particle Sizing in Moving Streams." Proccedings 1969 International Congress on Instrumentation in Aerospace Simulation Facilities, May 1969, pp. 168-172.

171. Fourney, M. E., Matkin, J. H. and Waggoner, A. P. "Aerosol Size and Velocity Determination via Holography." The Review of Scientific Instruments, Vol. 40, No. 2, February 1969, pp. 205-213.

APPENDIXES
I. ILLUSTRATIONS
II. TECHNICAL BRIEFS

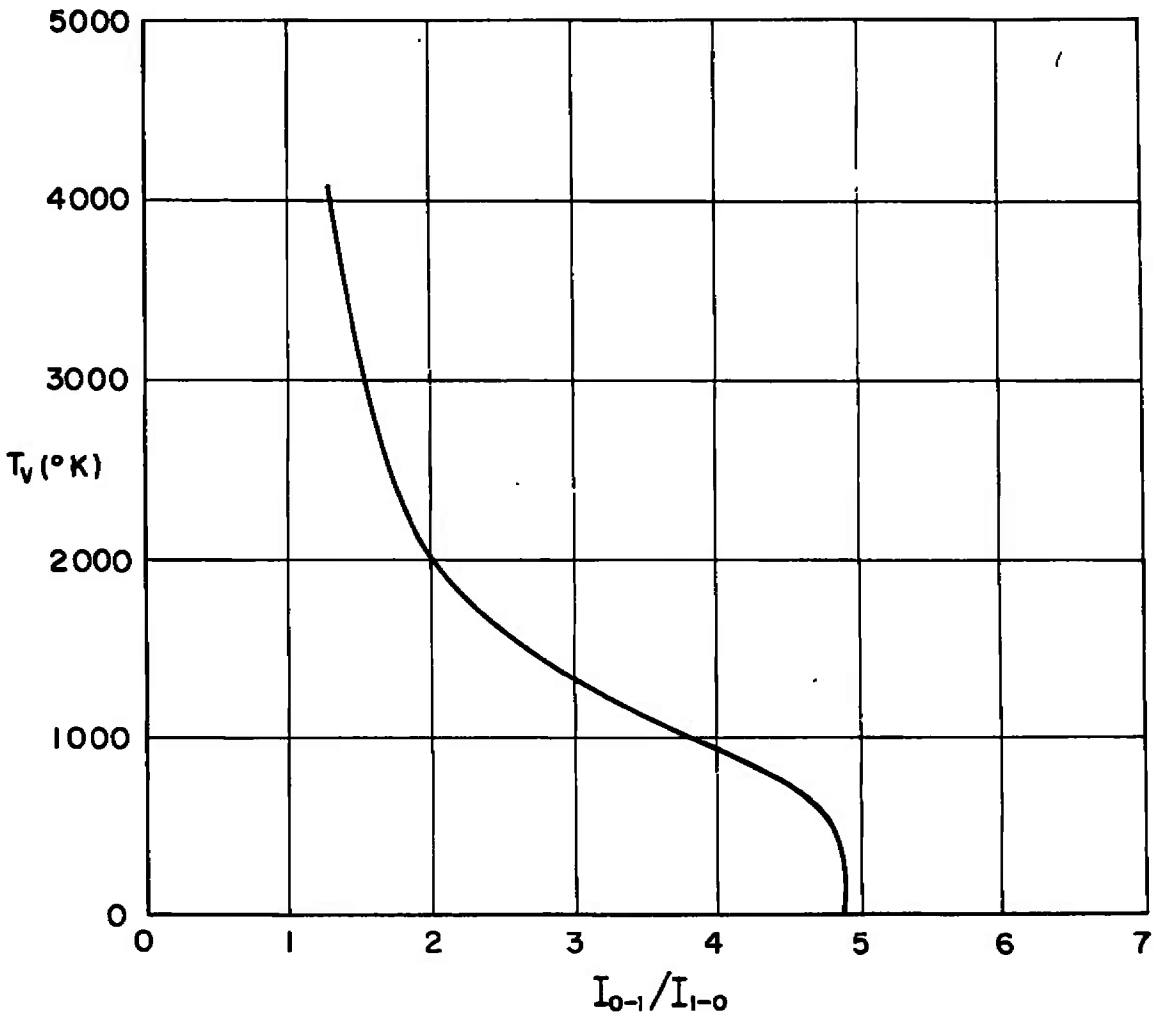

Fig. 1 Intensity of (0,1) and (1,0) Bands versus T_{vib}

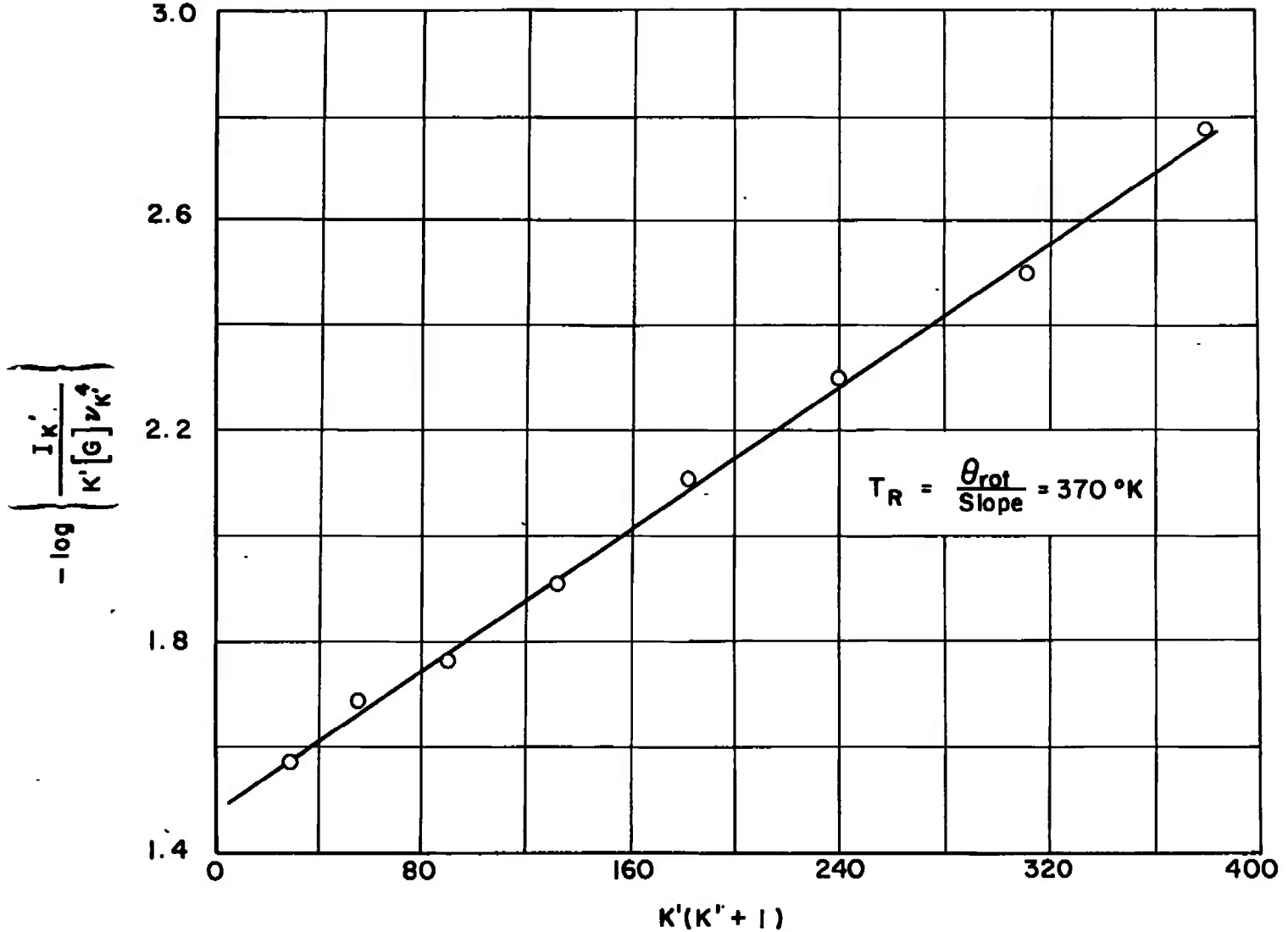

Fig. 2 Sample Log $I_{K'}$ Plot

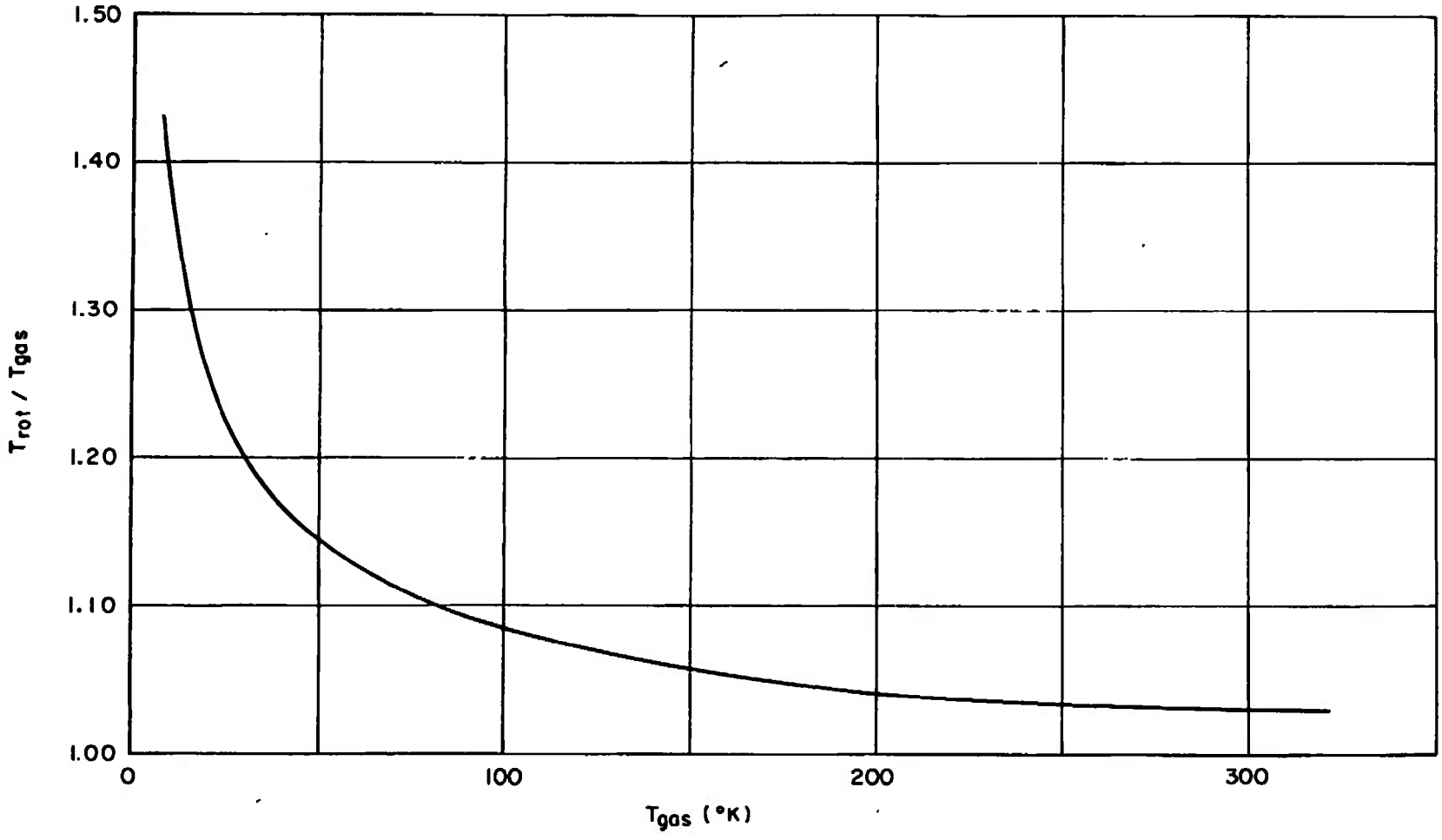

Fig. 3 Robben/Talbot Calibration Curve

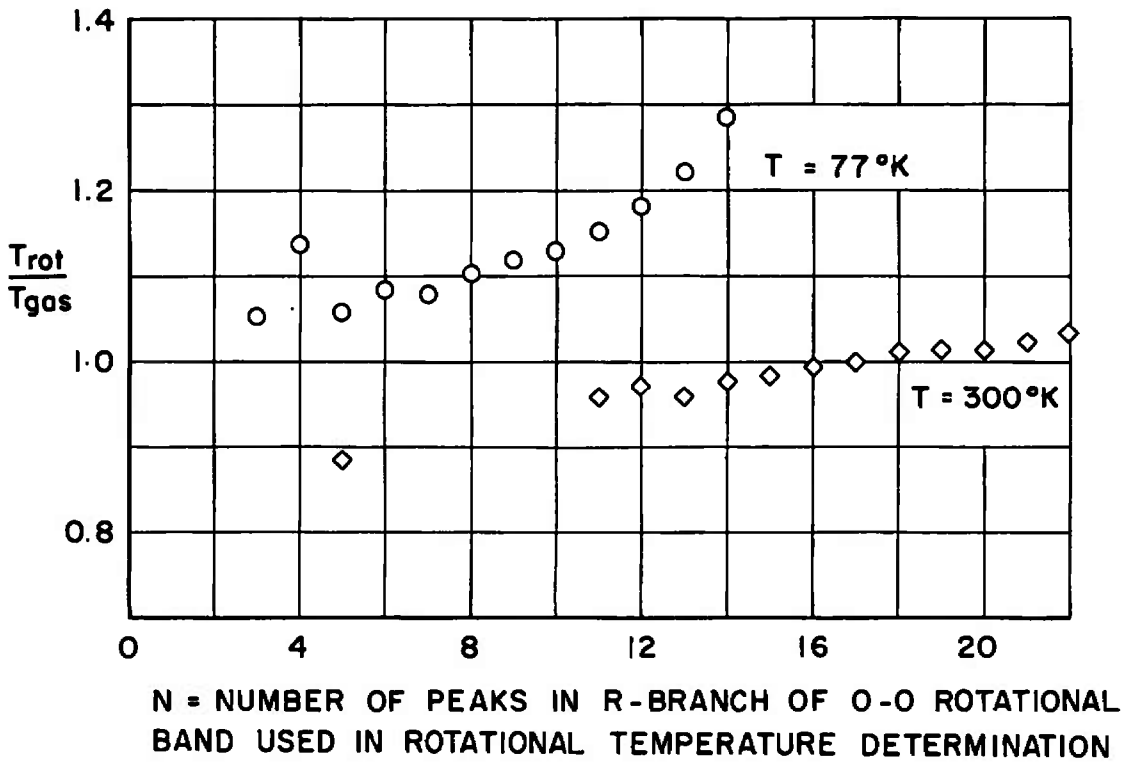

Fig. 4 Effect of Nonlinear Log I_K' Plot

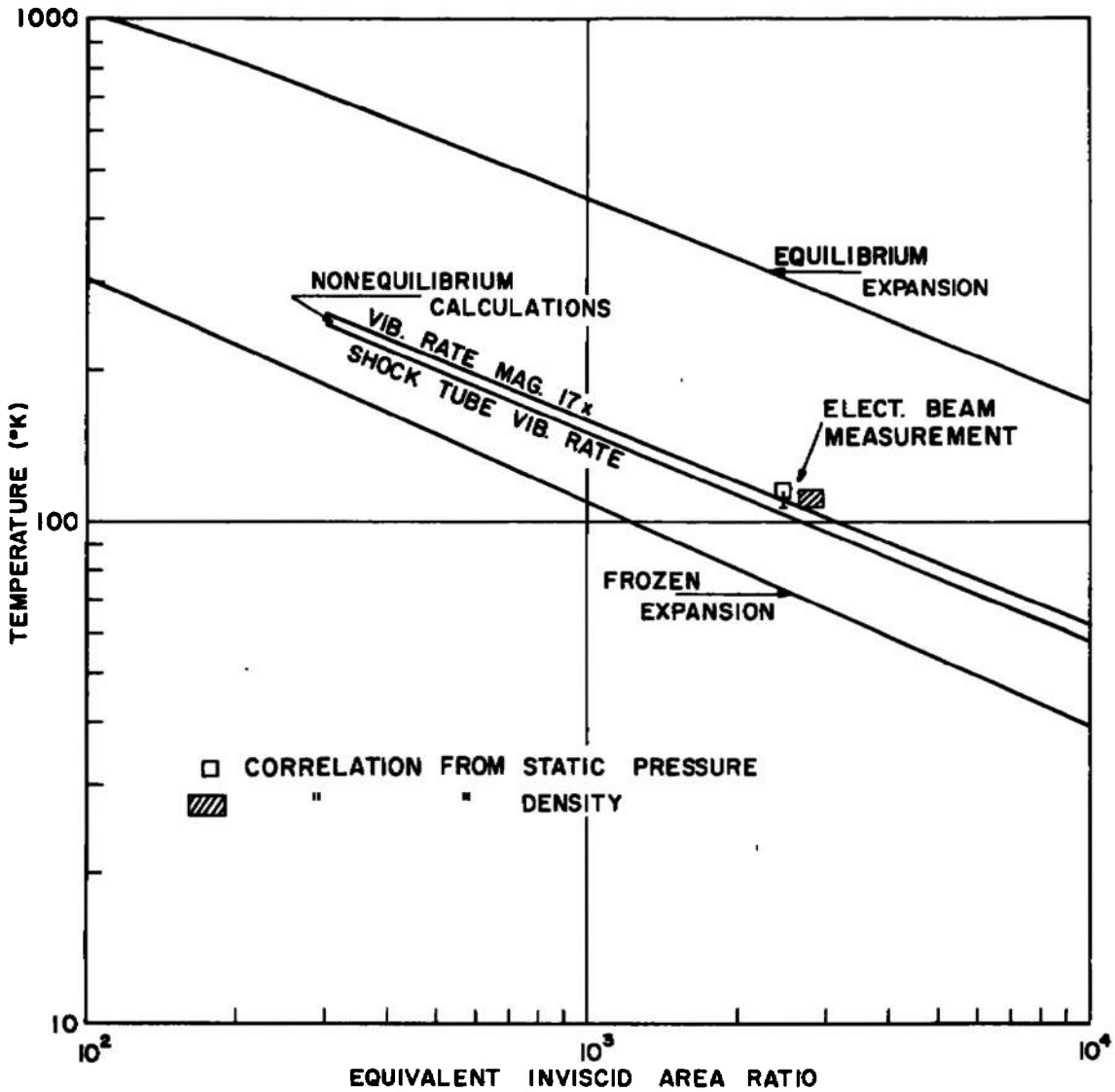

Fig. 5 Static Temperature in Hypersonic Nozzle for p_o = 10 atm and T_o = 4000°K

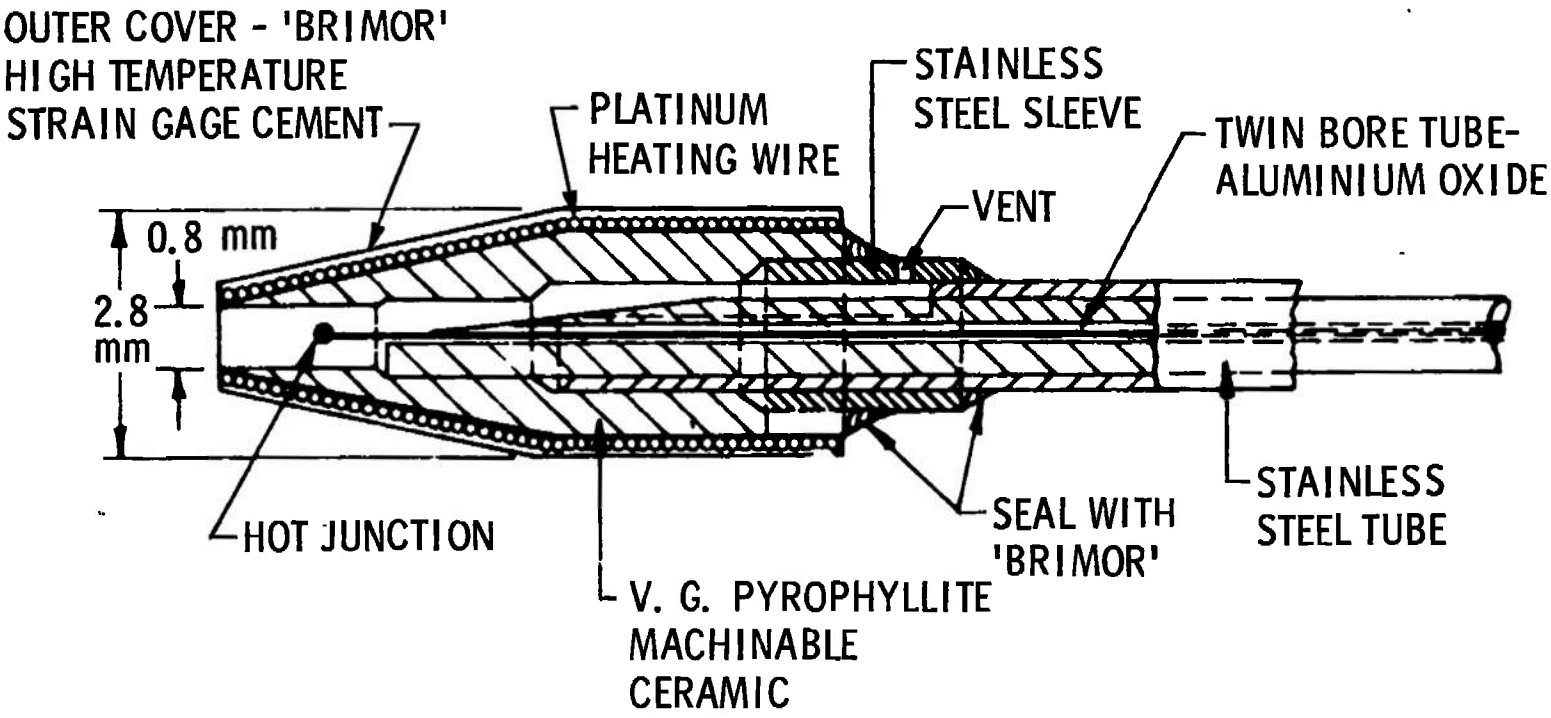

Fig. 6 Construction Details of the Boundary-Layer Total Temperature Probe

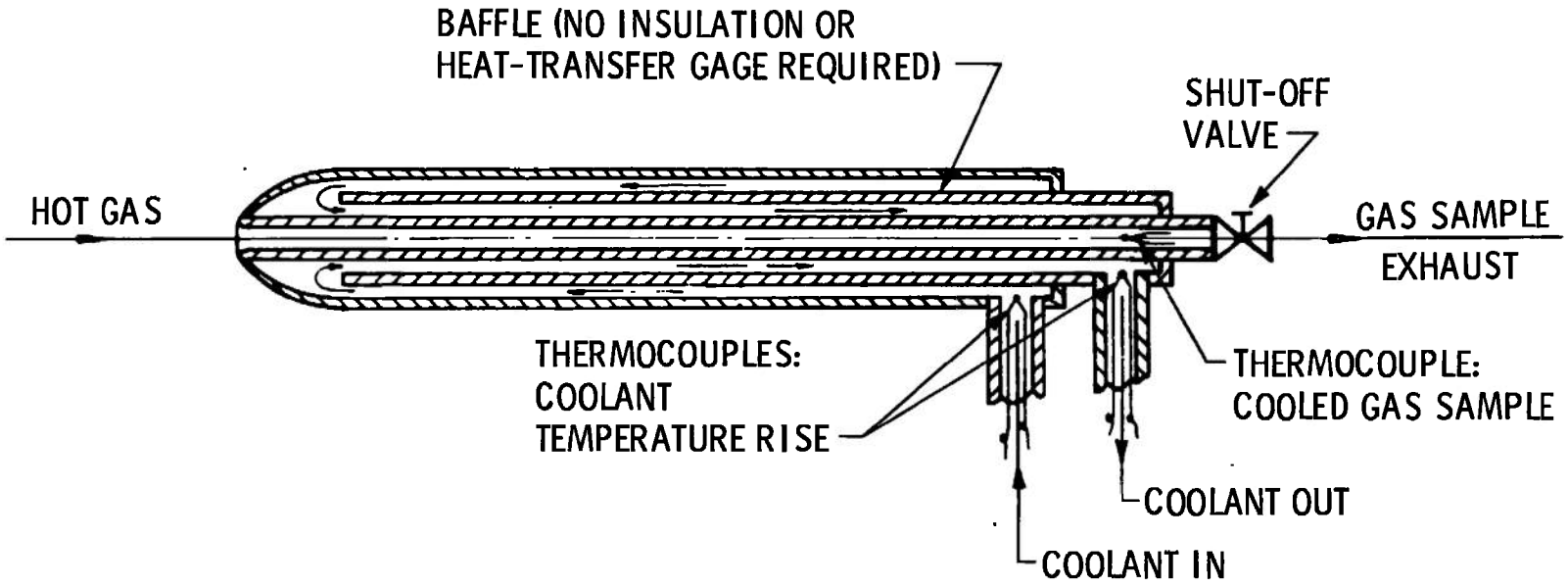

Fig. 7 Simple Tare-Measurement Probe for Enthalpy, Impact Pressure and Gas Composition in Extremely High Heat-Flux Environments

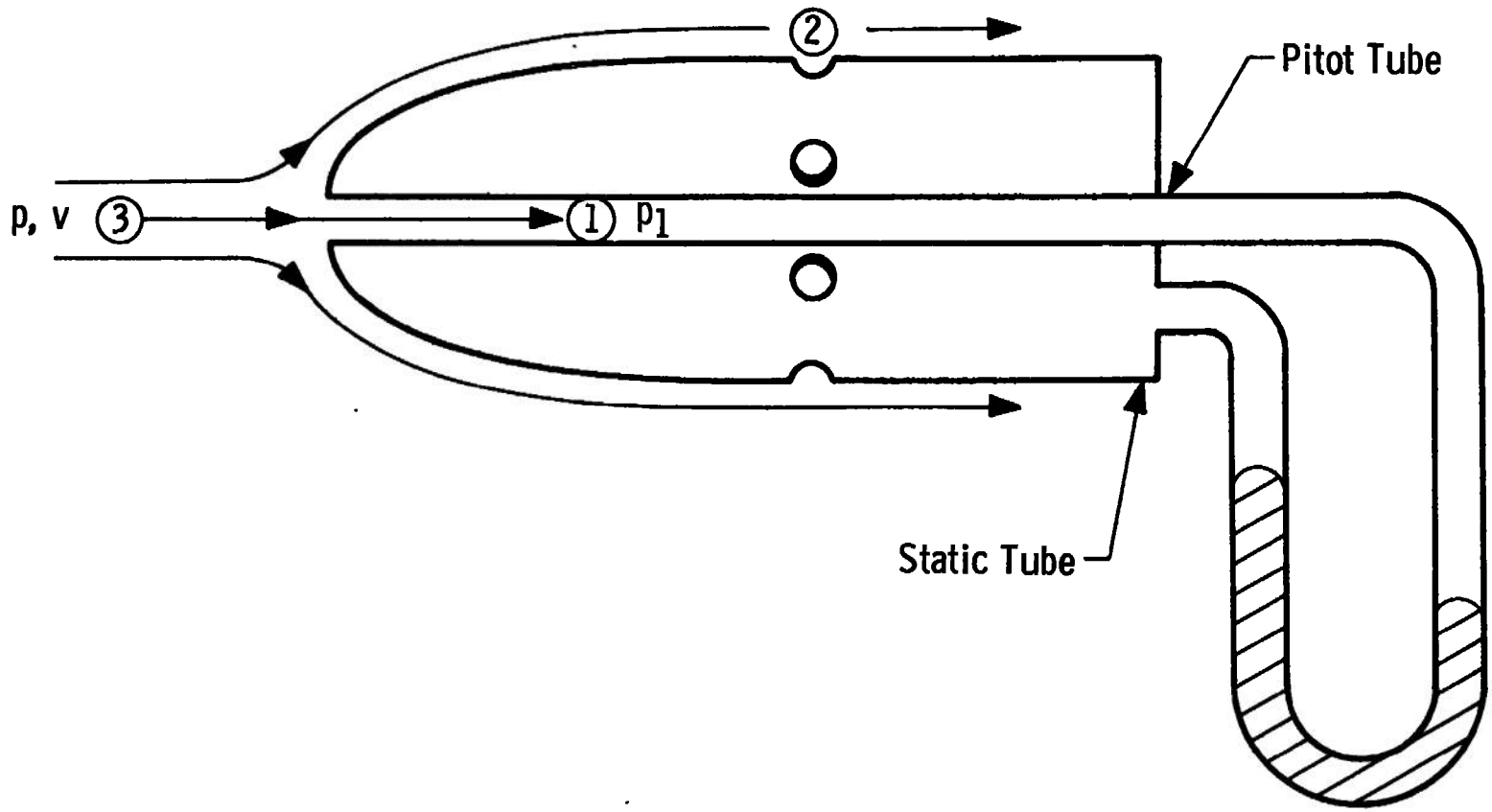

Fig. 8 Cross Section of Pitot-Static Tube

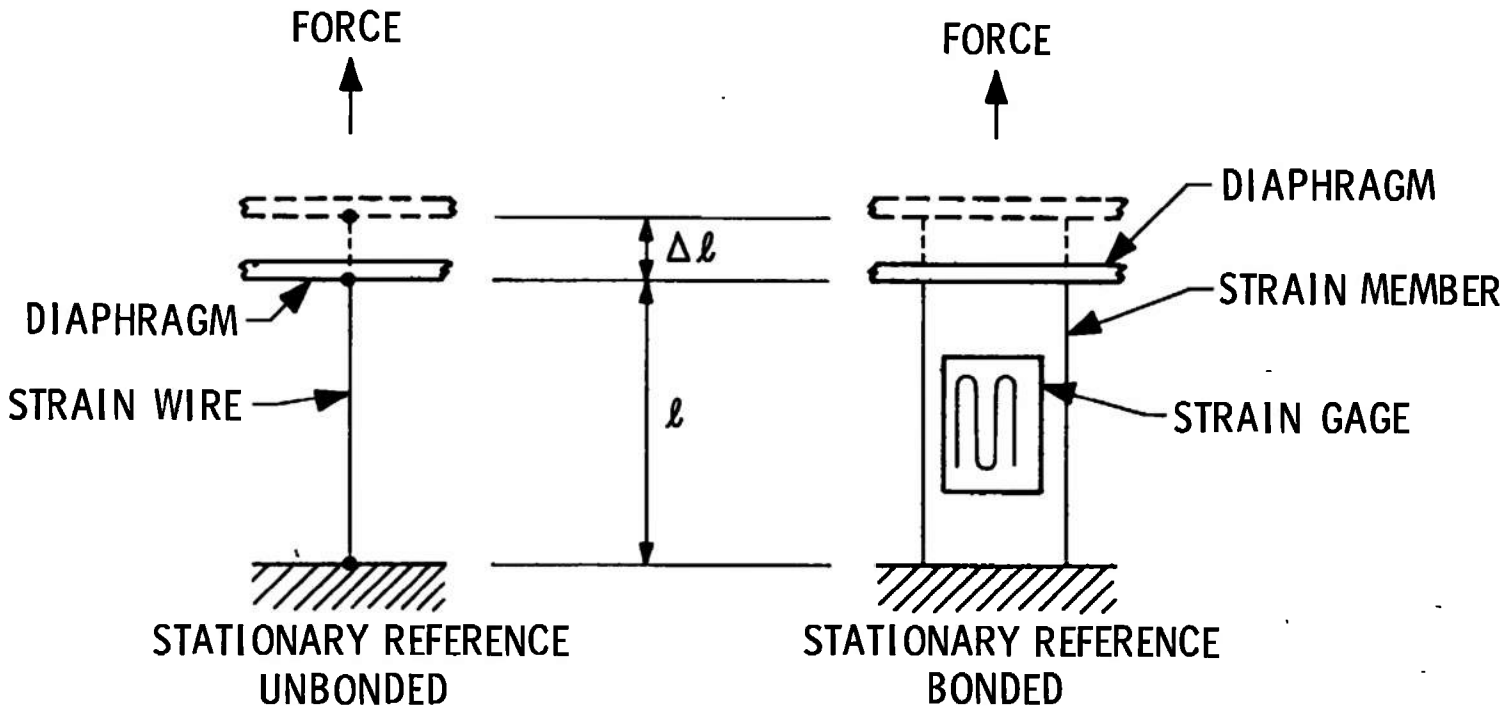

Fig. 9 Strain-Gage Transducers

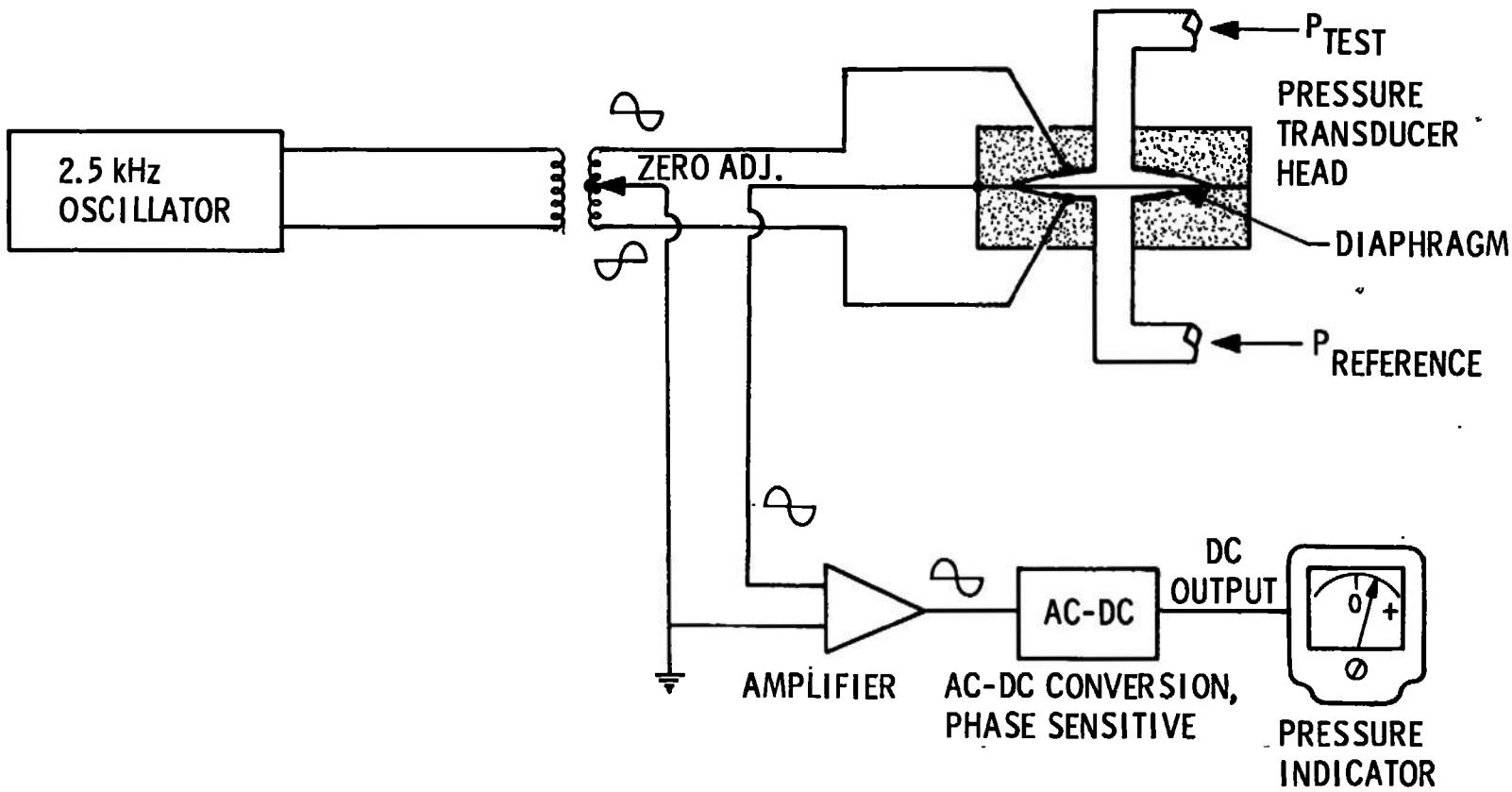

Fig. 10 Simplified Schematic of a Differential Capacitance Diaphragm Pressure Sensor

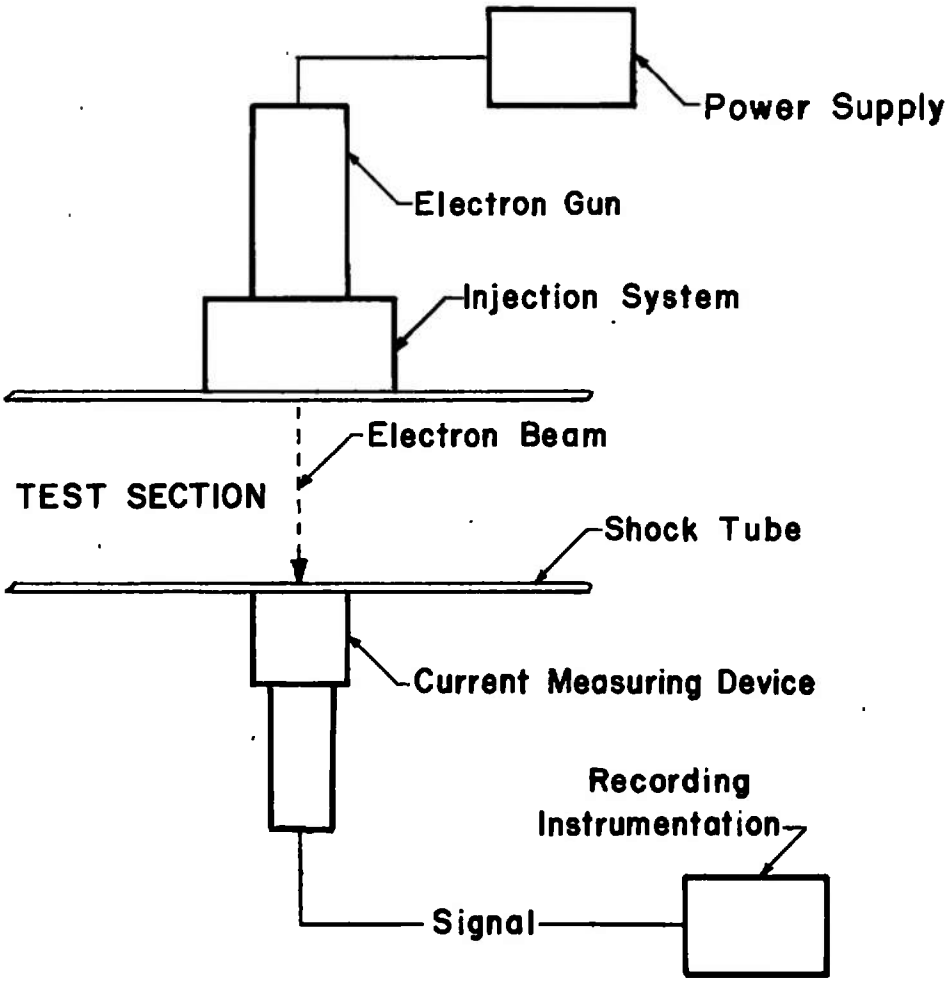

Fig. 11 Schematic Arrangement for Attenuation or Absorption Measurements

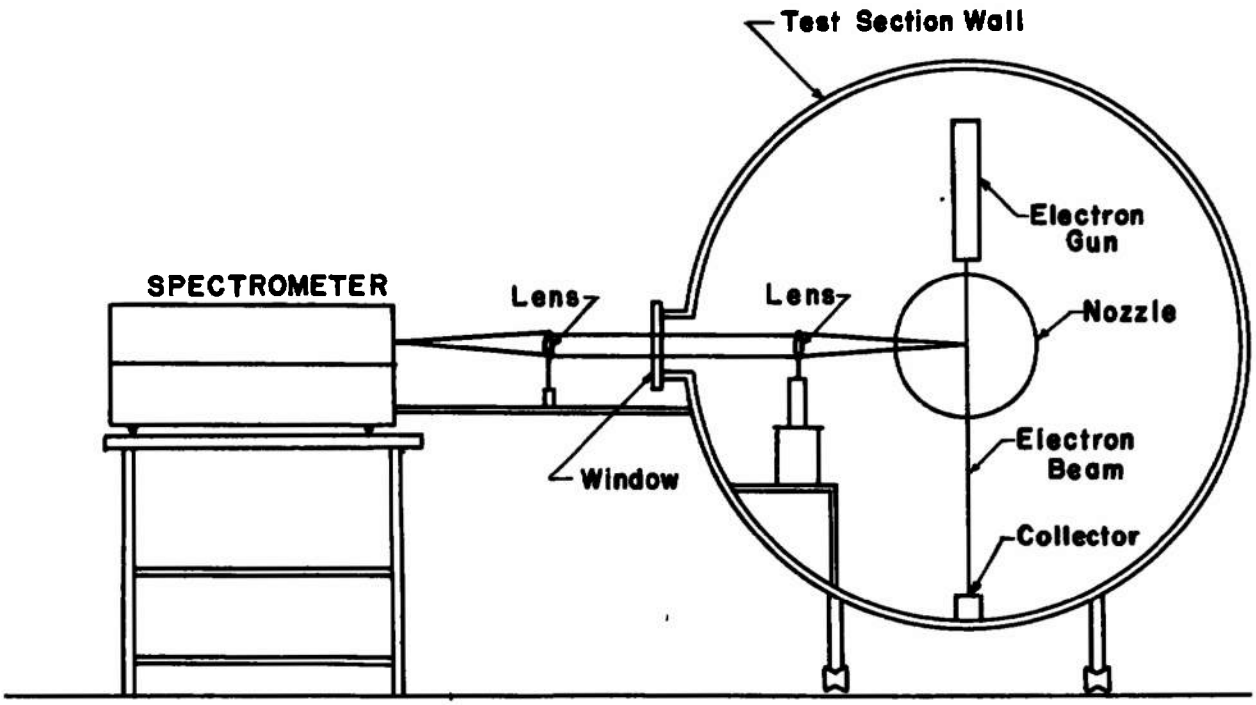

Fig. 12 Typical Component Arrangement for Measuring Electron-Beam-Induced Fluorescence

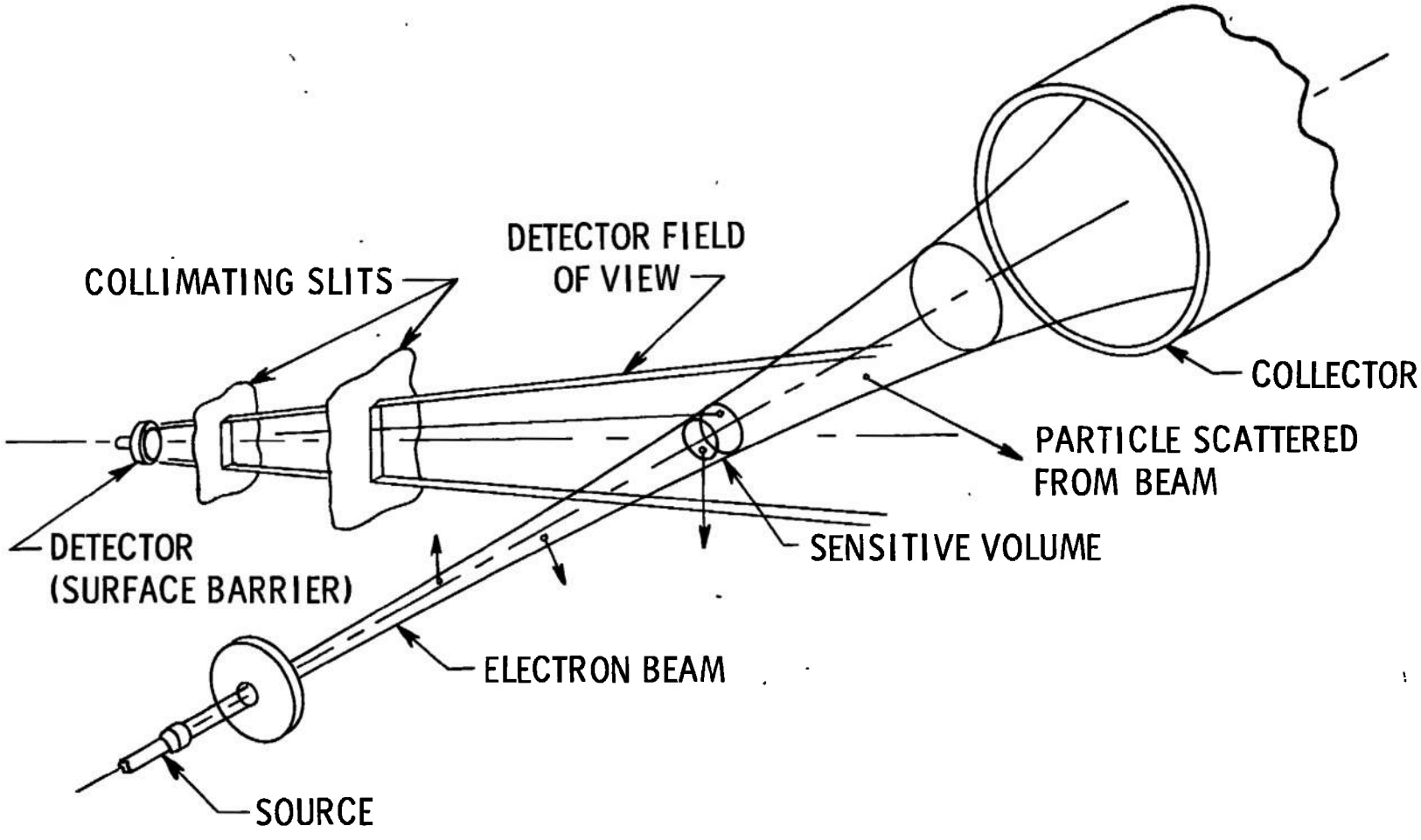

Fig. 13 Principle of Density Measurement by Electron Scattering

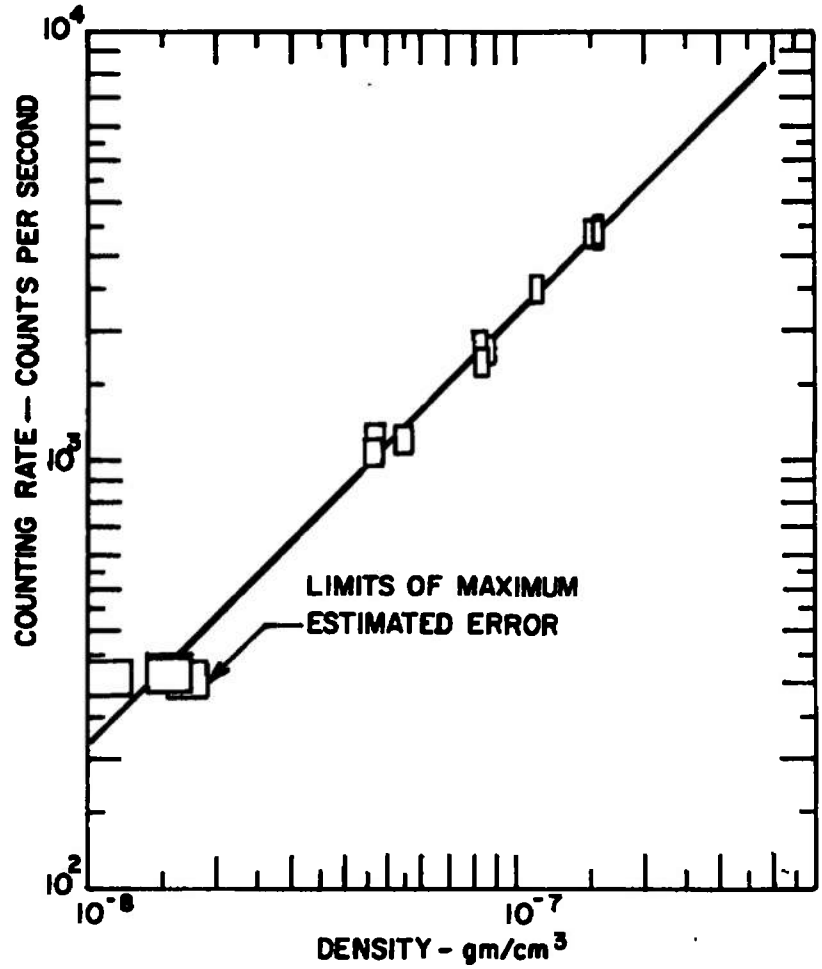

Fig. 14 Calibration Curve Obtained in the Low Density Wind Tunnel

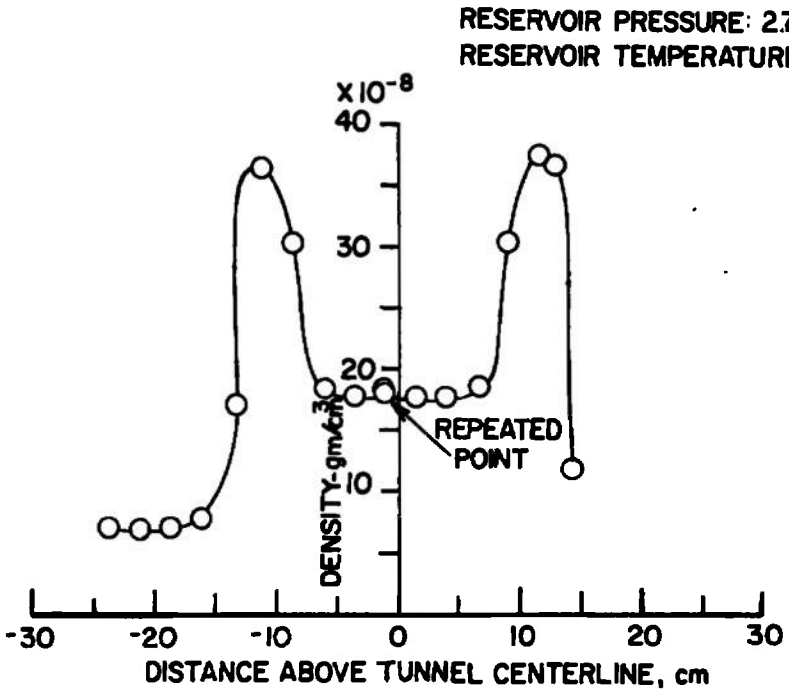

a. Cold Flow

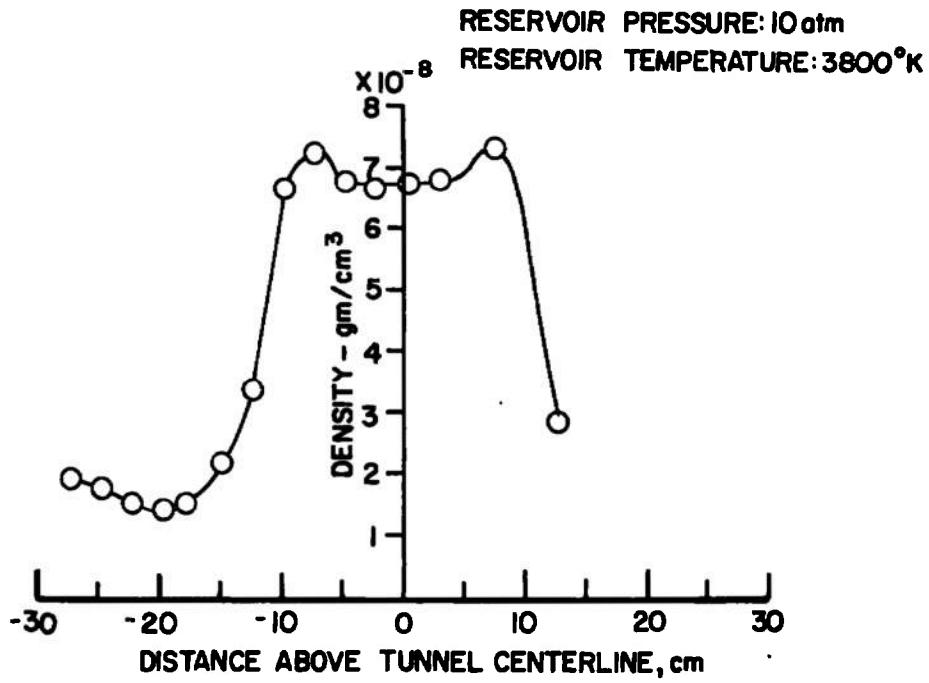

b. Hot Flow

Fig. 15 Density Profile Measured in the Low Density Wind Tunnel

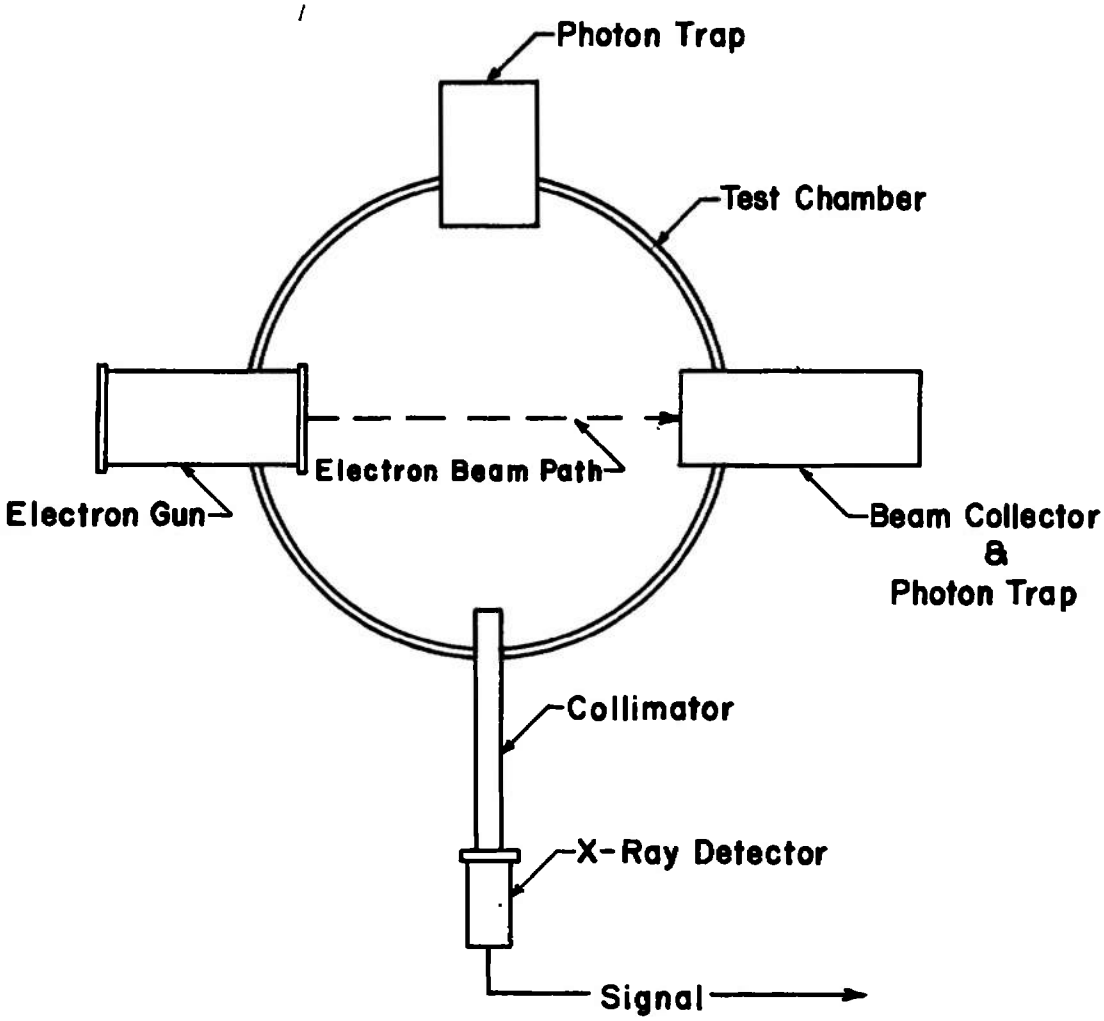

Fig. 16 Typical Measuring Arrangement for the Bremsstrahlung Technique

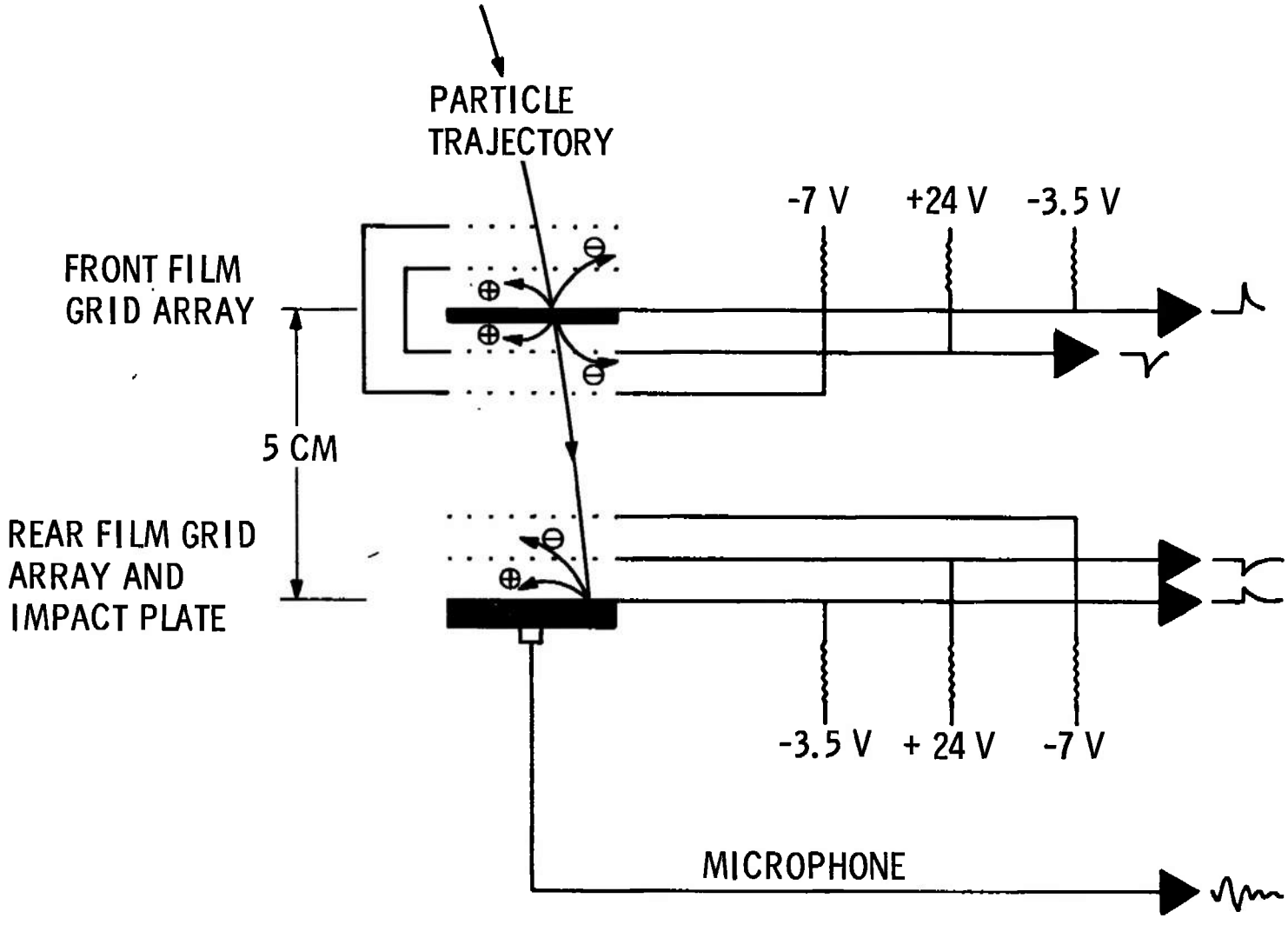

Fig. 17 Basic Cosmic Dust Sensor Schematic

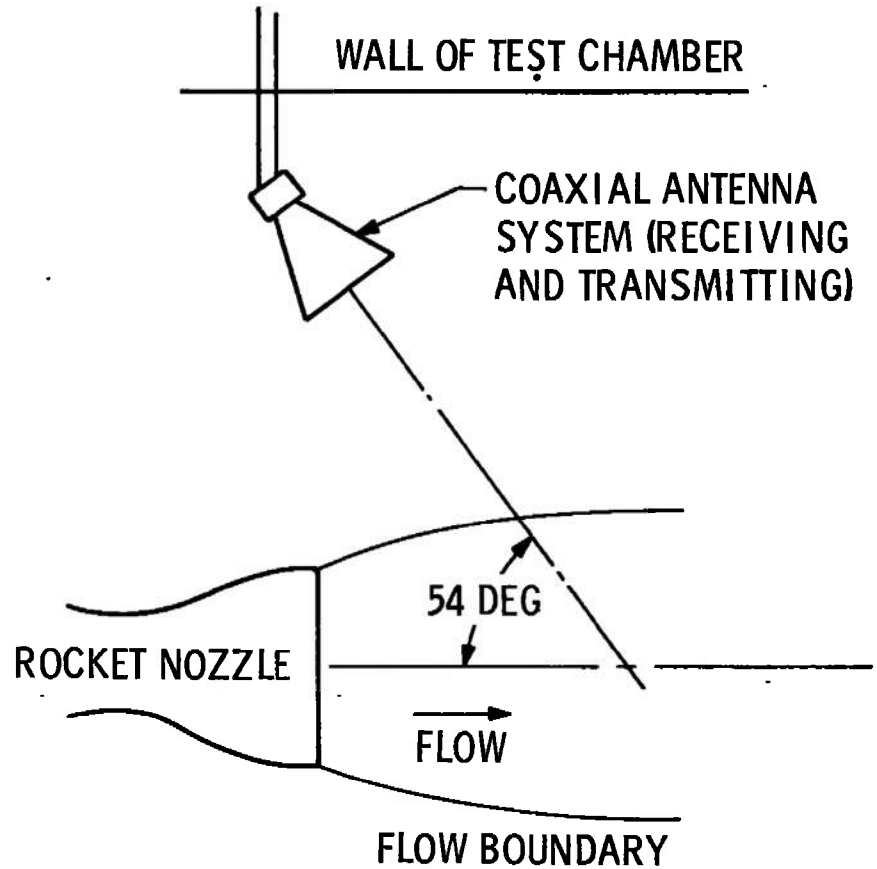

Fig. 18 Antenna Geometry for Free-Stream Velocity Measurement Using the Doppler Radar Technique

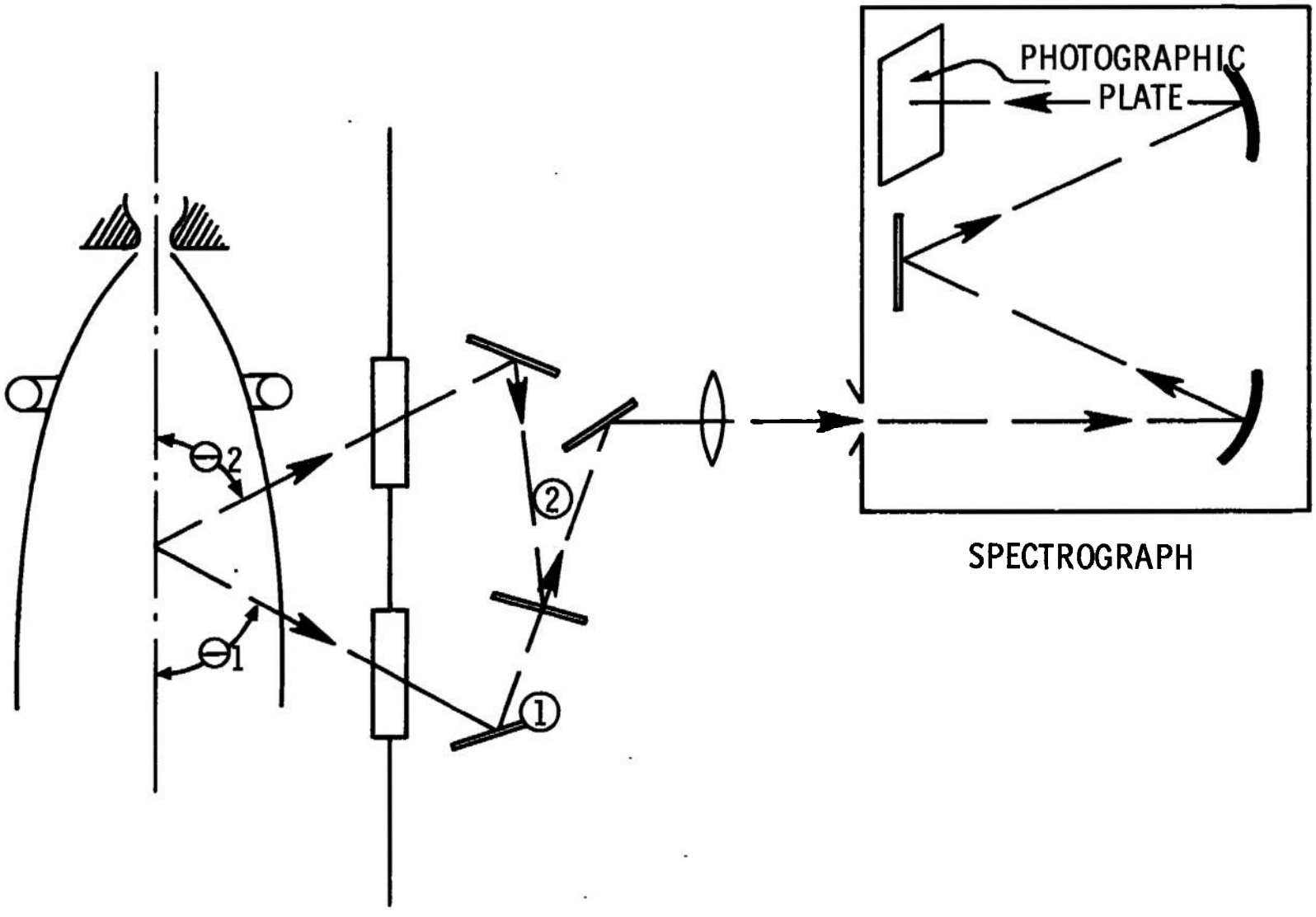

Fig. 19 Line Broadening

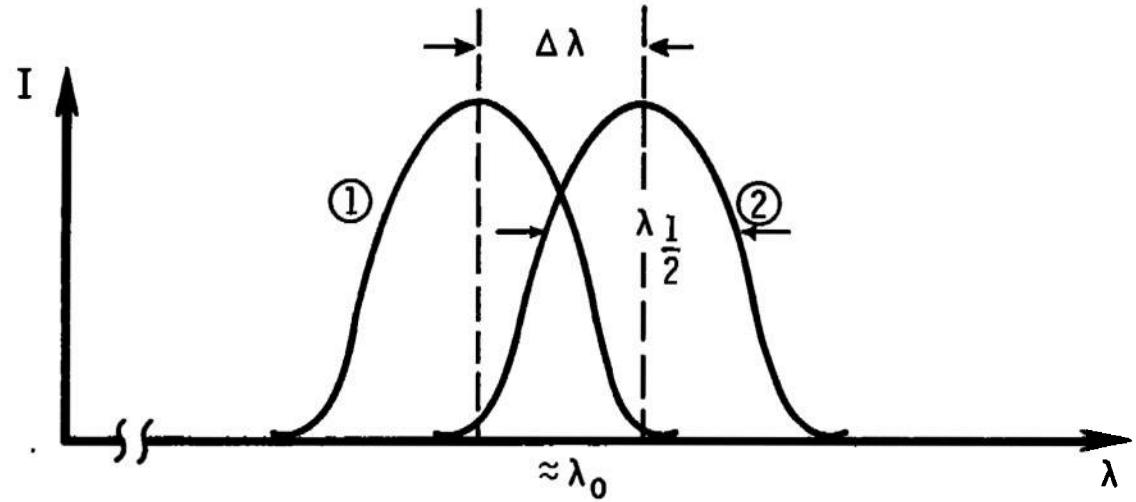

a. Two Single Lines

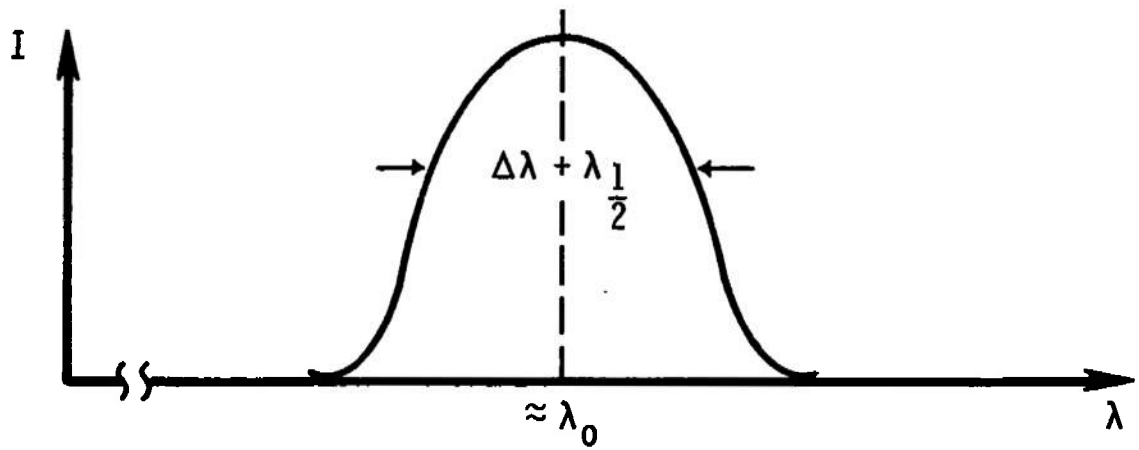

b. Composite of Lines 1 and 2

Fig. 20 Display of Typical Doppler-Shifted Lines

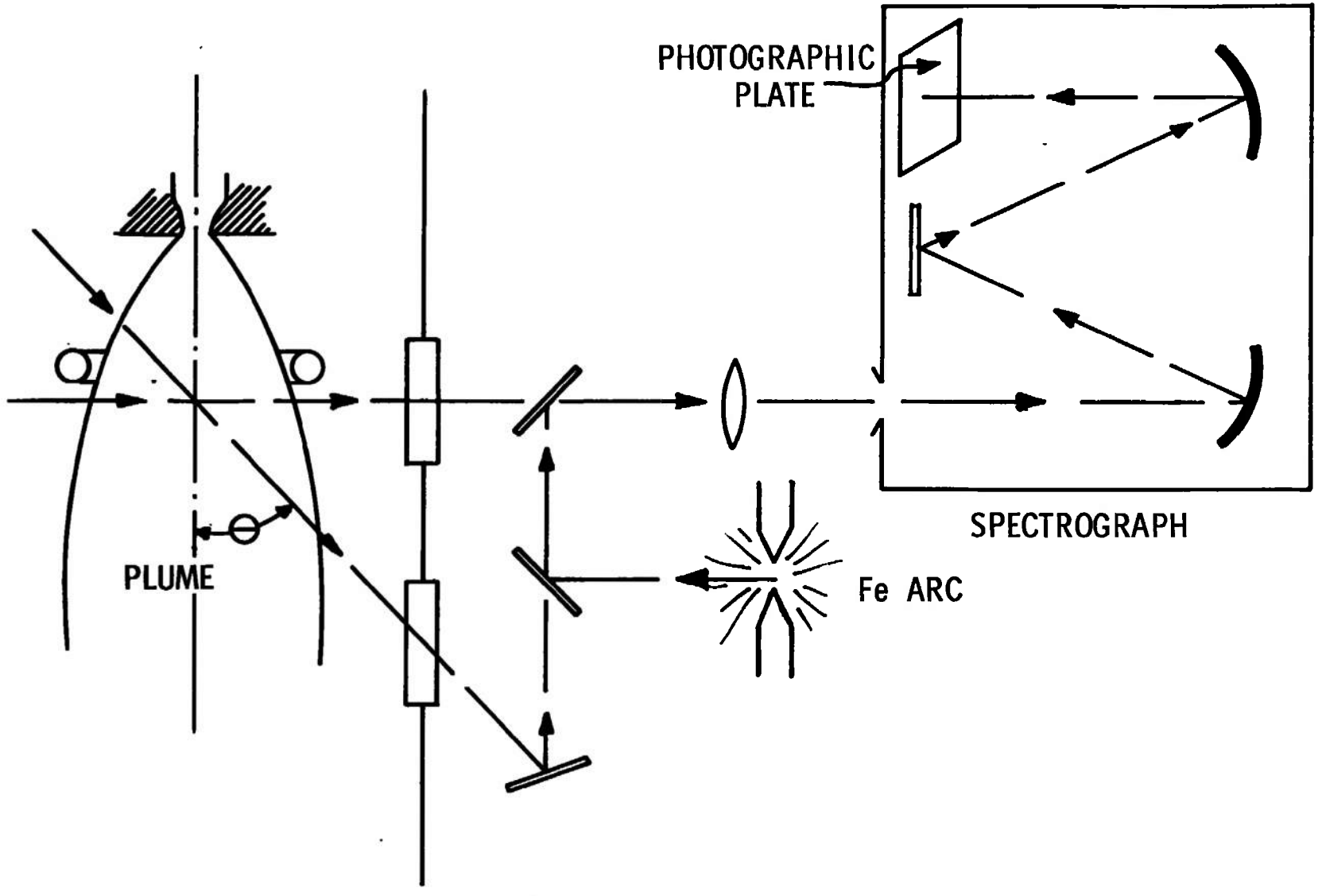

Fig. 21 Absolute Line Shift

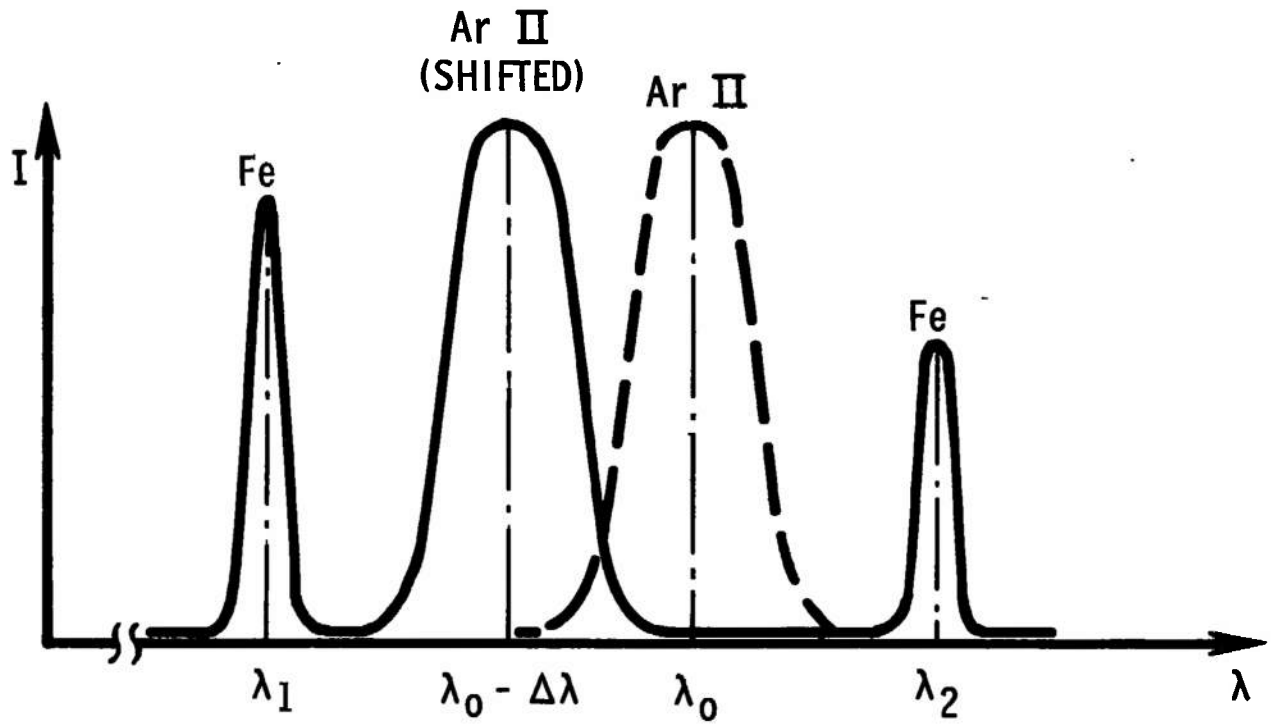

Fig. 22 Comparison of the Shifted and Unshifted Argon Line as Recorded with Standard Iron Lines

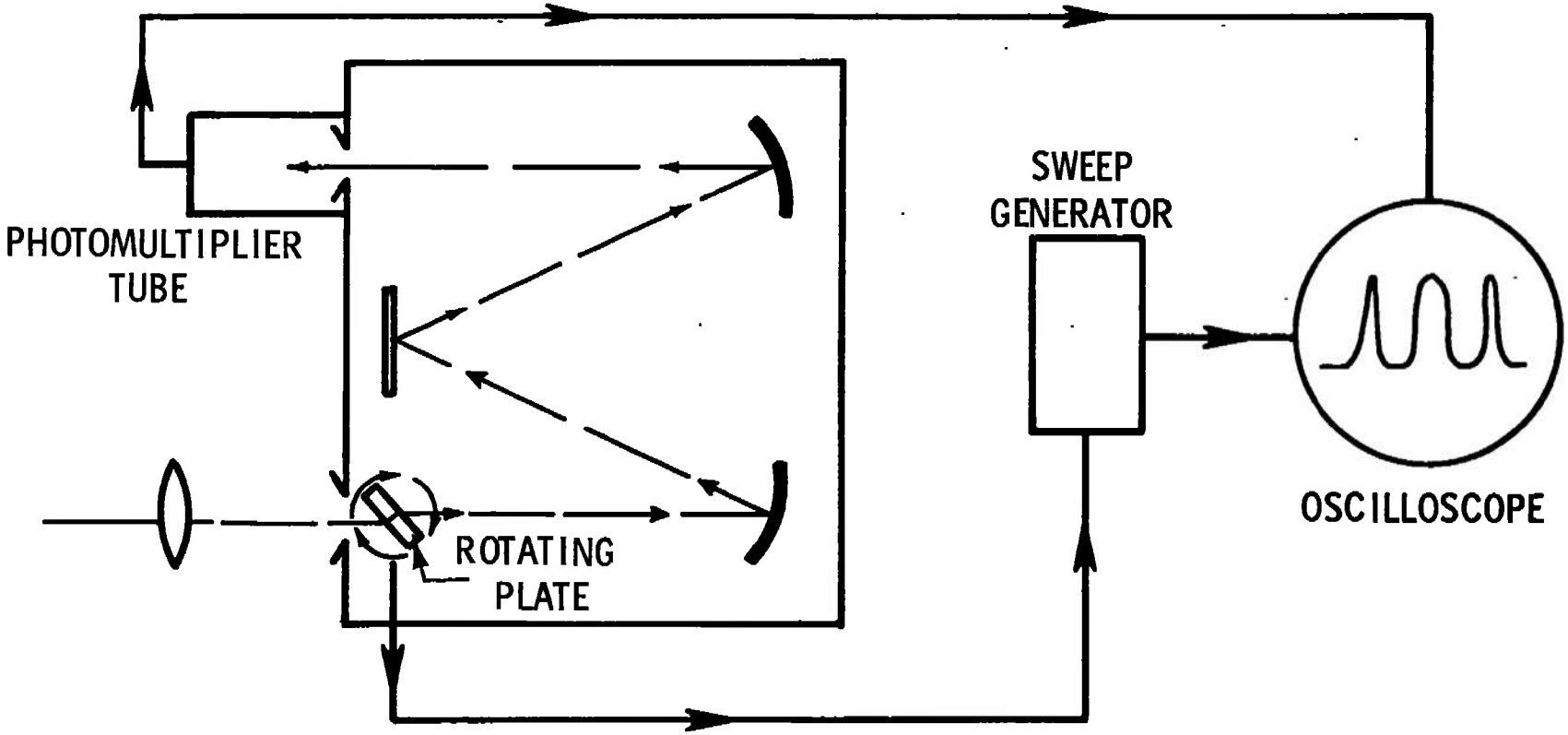

Fig. 23 Rotating Refractory Plate

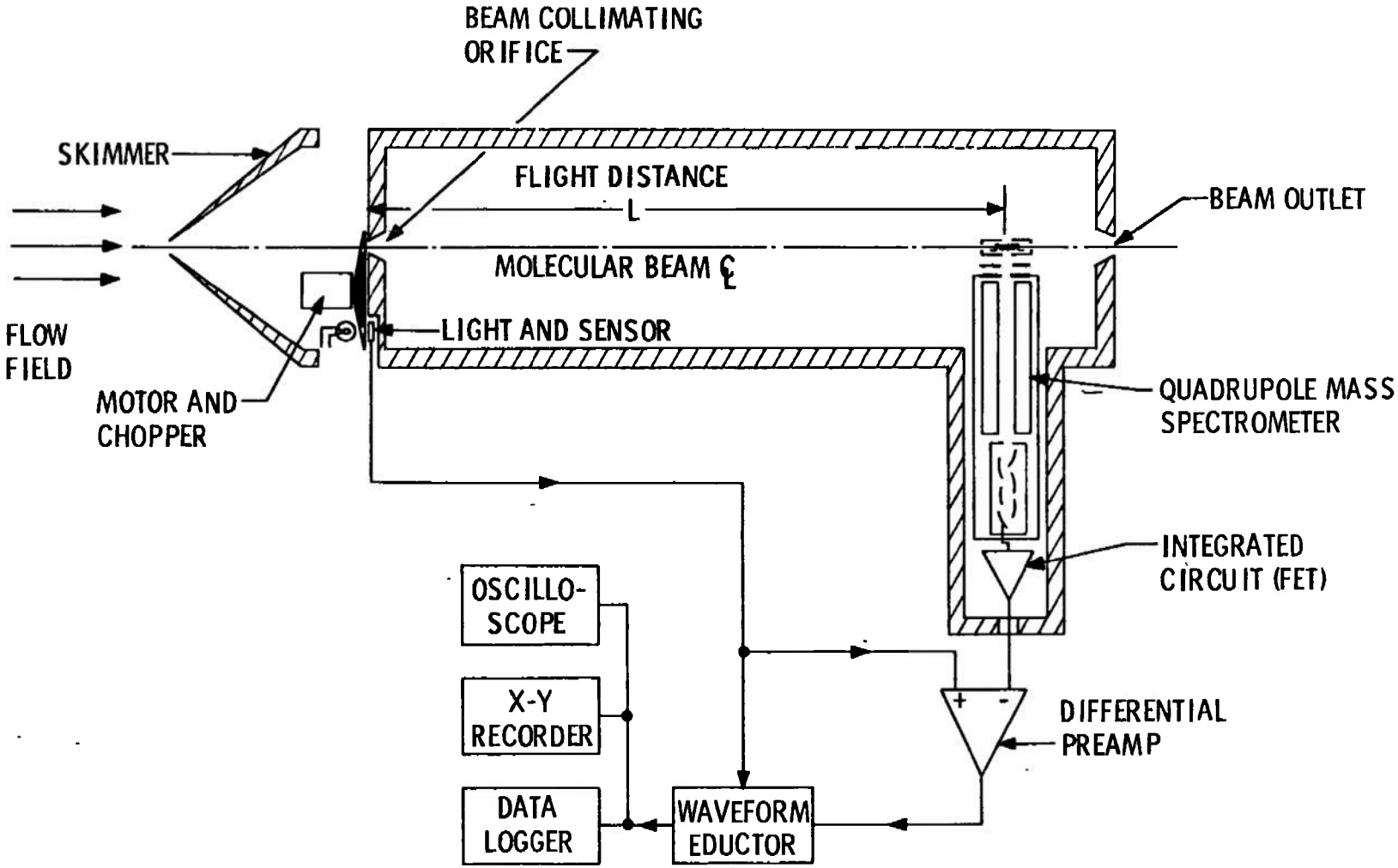

Fig. 24 Block Diagram for System for Measurement of Velocity Distributions in a Highly Expanded Plume

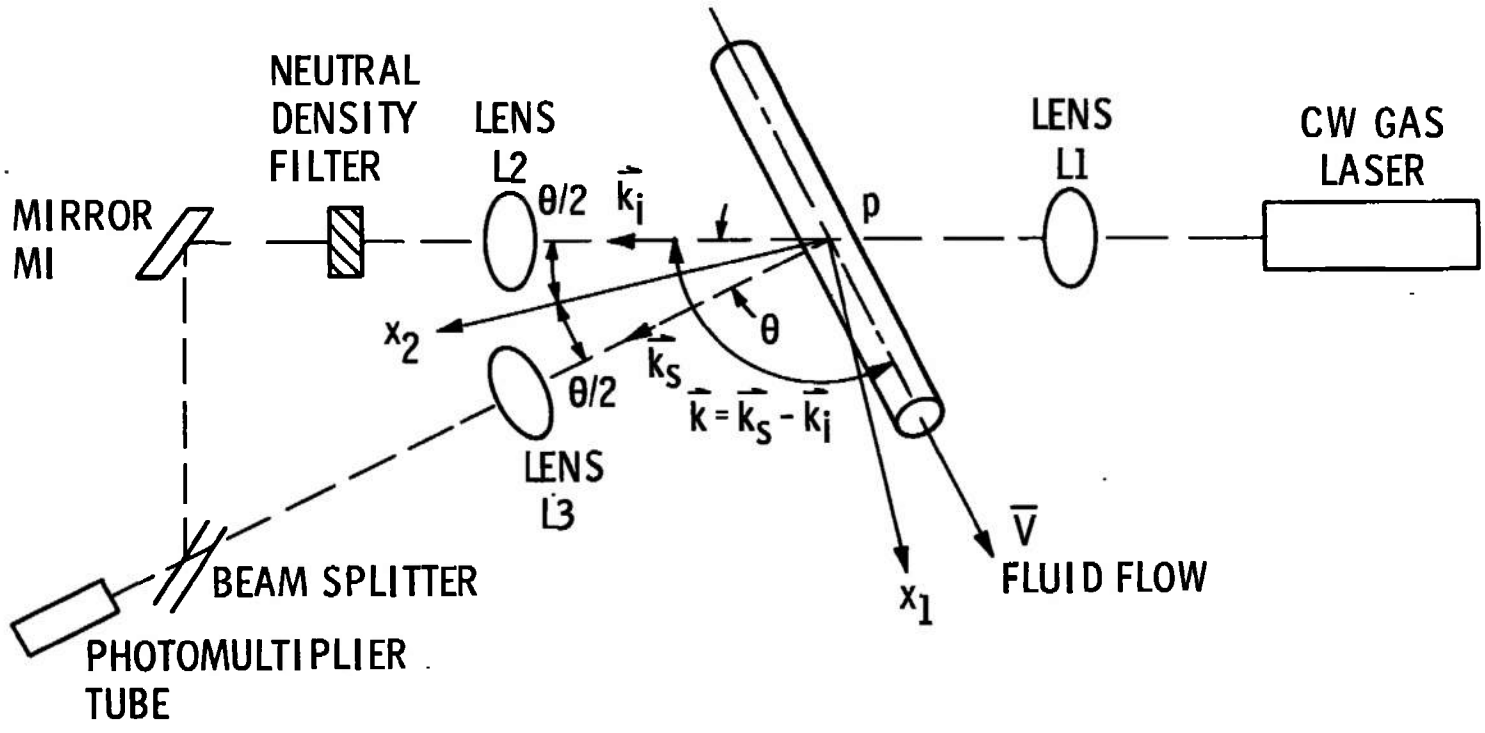

Fig. 25 Schematic Diagram of Typical Single Component Laser Anemometer System

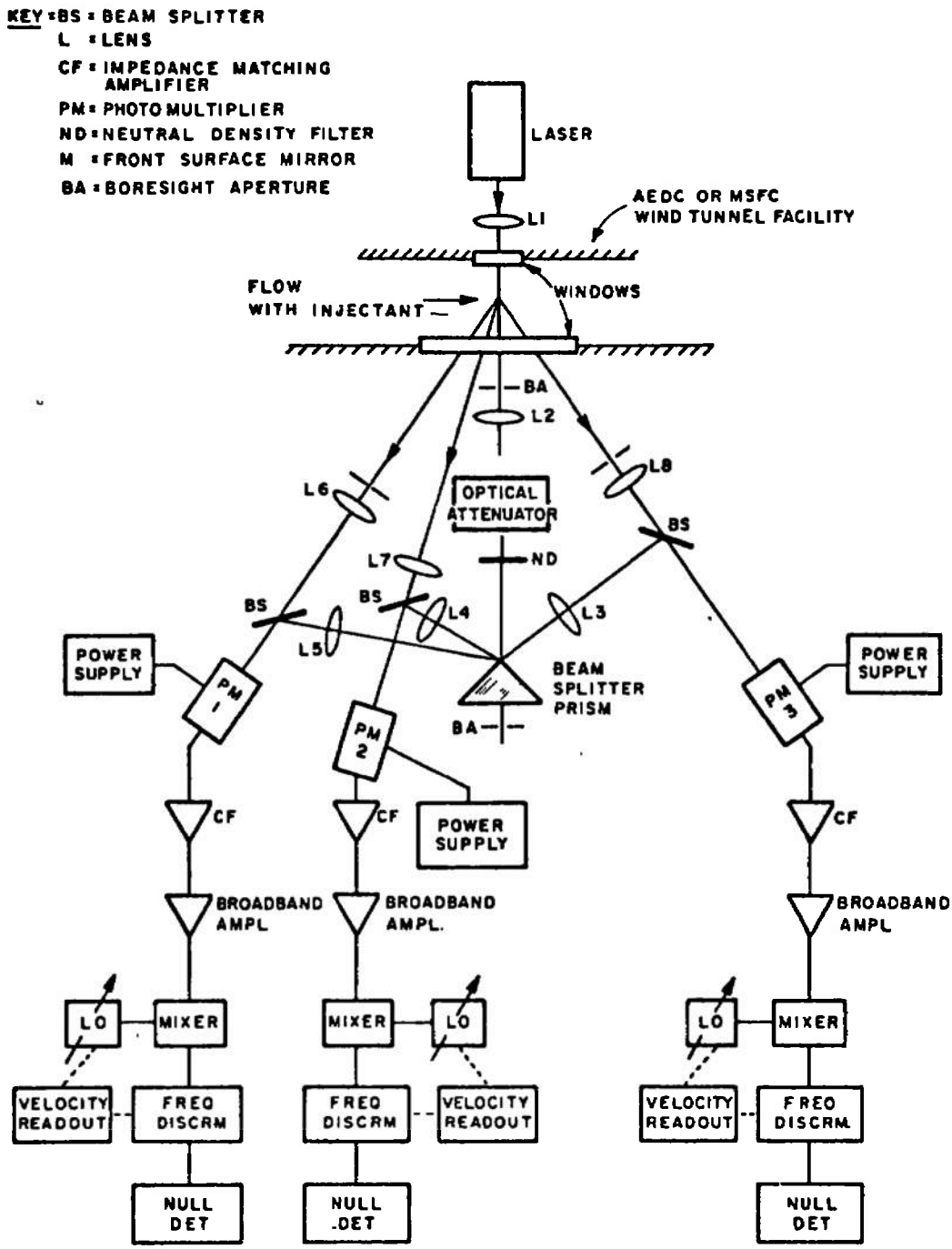

Fig. 26 Typical Three-Dimensional Laser Doppler Anemometer

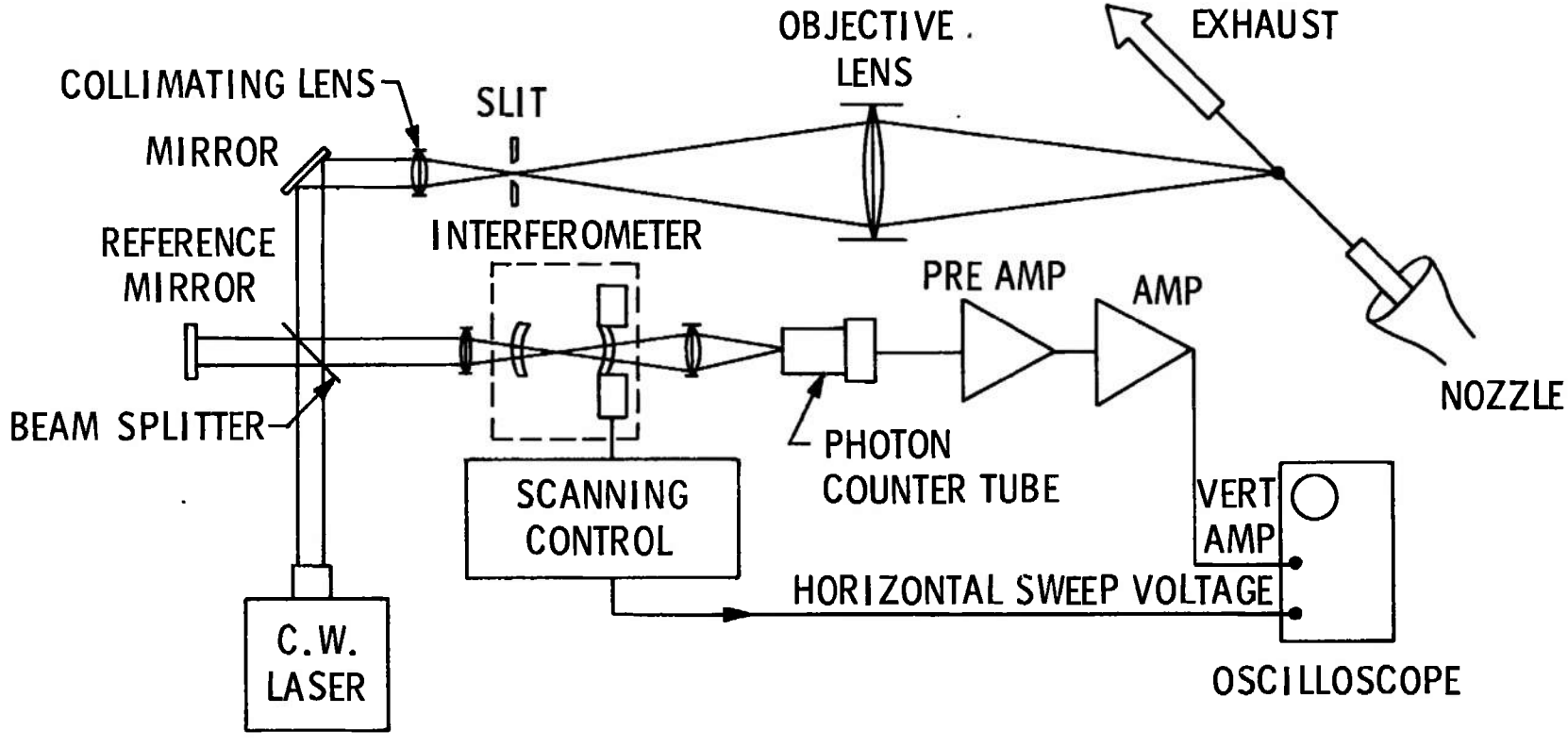

Fig. 27 Laser Doppler Particle Velocity System with Fabry-Perot Interferometer

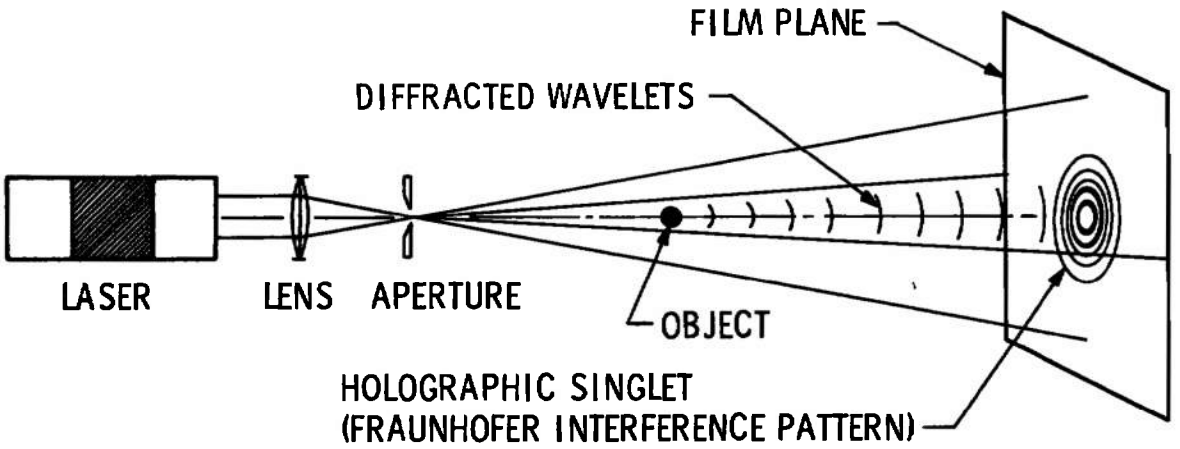

a. In-Line

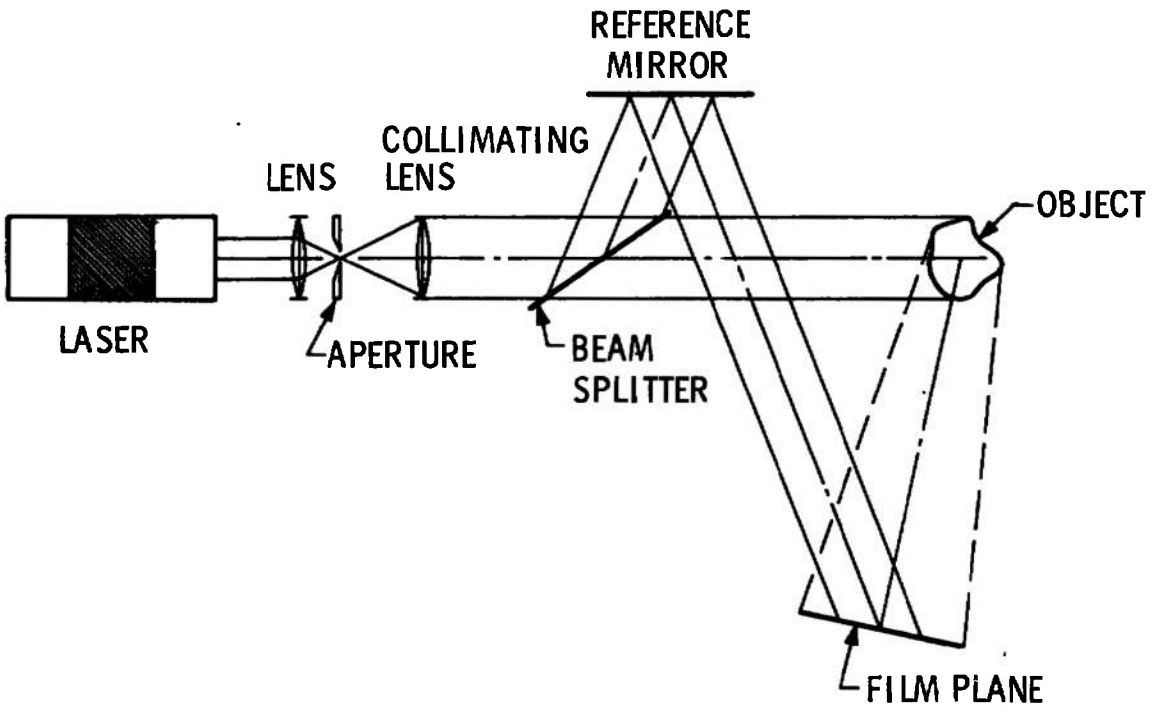

b. Off-Axis

Fig. 28 Typical Holography (Recording Phase)

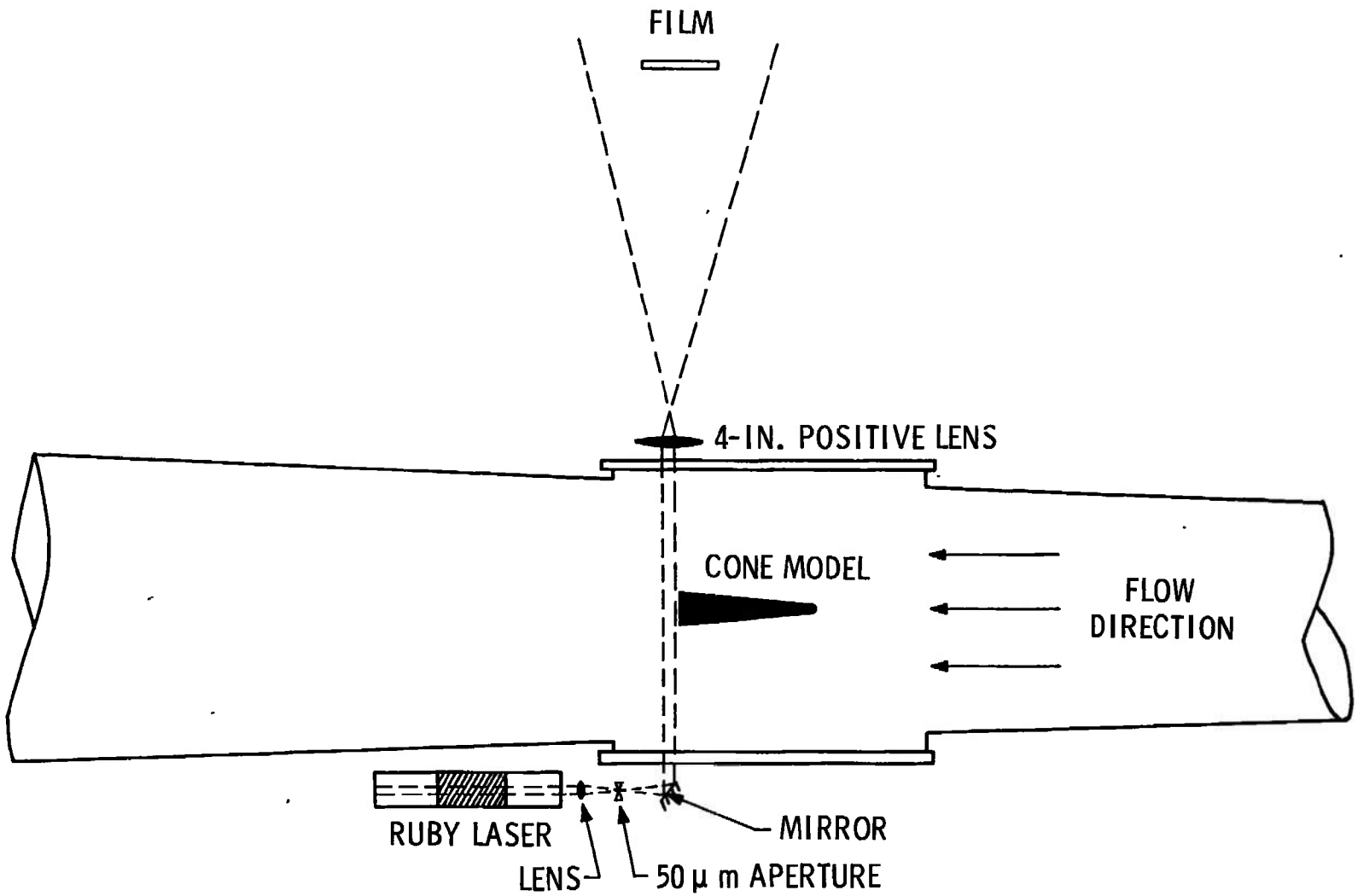

Fig. 29 VKF Tunnel F Holocamera Arrangement

APPENDIX II
TECHNICAL BRIEFS

TEMPERATURE

PARAMETER: Central temperature and pressure of a high pressure alkali metal vapor arc.

REFERENCE: 128

ABSTRACT: Although additional experimental justification is needed, a set of self-consistent methods of high pressure arc diagnostics based on the resonance line spectral profile are presented. The methods offer fairly simple ways to obtain the central temperature and the pressure if a good line profile can be obtained. These diagnostic methods were developed to study alkali metal vapor arcs; however, the results indicate a potentially productive approach to plasma investigations.

LIMITATIONS: (1) The resonance profile should be isolated from other radiation in the frequency range of interest. (2) The absorption oscillator strengths of the resonance lines are high enough so that they are primarily broadened by the resonance broadening mechanism. (3) The gas is monatomic, and the simple power approximation for the temperature profile of the arc is valid.

MEASURING TIME: Dependent on scan rate, but also primarily on the recording mechanism.

ACCURACY: Approximately 10-percent agreement with published experimental results.

PARAMETER: Spectral Temperatures

REFERENCE: 129

ABSTRACT: Boltzmann plots derived from spatially integrated spectral line intensities emitted from nonuniform gaseous plasmas are investigated. Emphasis is placed on the measuring of temperatures inferred from these Boltzmann plots and also on the effect of relaxing the local thermodynamic equilibrium (LTE) requirement. It is shown that for plasmas with

sufficiently small electron density and electron temperature gradients, the line-of-sight Boltzmann temperature is nearly equal to the spatially averaged electron temperature if sufficient LTE restrictions are applied.

LIMITATIONS: Boltzmann plots of line-of-sight spectral line intensities emitted from a nonuniform plasma are meaningful only if a sufficiently large portion of the spatially integrated intensity is emitted from the LTE region of the plasma.

MEASURING TIME: Dependent on scanning rate and recording method or methods used.

PARAMETER: Rotational and Vibrational Temperatures

REFERENCE: 130

ABSTRACT: Emission-absorption intensity ratio temperature measurements of diatomic molecules under thermal nonequilibrium conditioning are investigated theoretically. It is shown that the rotational population distribution must be taken into account when a small part of a vibration-rotation band is viewed in experiments for measuring a vibrational temperature. An emission-absorption intensity ratio of unity does not always mean equality of effective brightness temperature of background source and a vibrational temperature. Such an assumption could lead to errors of several percent in experimentally deduced vibrational temperatures, particularly in situations where the ratio of rotational and vibrational temperatures is less than unity. The rotational temperature dependence is explained in terms of transitions taking place in vibration-rotation bands and this dependence decreases when a larger part of a band is viewed. Emission-absorption measurements are also investigated for cases where the vibrational population distribution deviates from Boltzmann for polyatomic and for molecular electronic spectra. Finally it is shown that, in principle, both rotational and vibrational temperatures may be determined from two simultaneous emission-absorption measurements.

PARAMETER: Color temperature measurement

REFERENCE: 131

ABSTRACT: The application of a commercially available solid-state integrating light detector to optical pyrometry is considered. Two systems using the detector for color temperature measurement are described: one giving a digital output on a frequency meter has an accuracy to better than ±5°C and the second giving a less accurate reading on a moving-coil voltmeter. A temperature range from 800 to 2000°C is considered.

LIMITATIONS: Calibration necessary.

PARAMETER: Static temperature measurements in high velocity flow fields.

REFERENCE: 132

ABSTRACT: A duplex-scanning infrared spectrometer, with spatial and wavelength scanning modes, has been used to measure static temperatures in arc-tunnel tests producing high velocity air streams. Conditions at the exit of a contoured nozzle included a velocity of ≈ 9000 ft/sec at a static temperature level ≈ 1200°R. The power input of the arc source was about 7 Mw. The local air temperature was changed by inserting simple models in the flow and continuous spectrographic records were made. In each test, 40 to 80 spectra were obtained in the 4- to 6-μ region at five arbitrarily separated locations in the flow field. The spectral sweep time at each position was approximately 0.4 sec. Temperatures were obtained from measurement of the separation of the peak intensity of the P and R branches of the 5.35-μ NO band; the thermal levels have been confirmed by simultaneous records on CO at 4.67 μ. Because of the large number of independent temperature determinations, the maximum error was calculated to be ±70°R in the 1200 to 2400°R range. A description is given of the spectrometer and equipment, and typical spectra are shown to illustrate the applications to high-speed flow studies.

PARAMETER: Heat-Transfer Rates

REFERENCE: 133

ABSTRACT: A transducer is described for the measurement of heat-transfer rates in gaseous systems. Based on the ferroelectric properties of triglycine sulphate $(CH_2NH_2COOH)_3 \cdot H_2SO_4$, the device autostabilizes its operating temperature so that external heat-transfer depends linearly upon the ambient temperature and the film coefficient. An analysis of temperature stability in several heat-sensitive transducers is presented and the fundamental improvement in stability offered by the ferroelectric probe is demonstrated both in the analysis and experimentally. Data are presented in reference to possible applications of the device as a linear heat-transfer gage and a binary gas analyzer. A qualitative discussion of transient response is given and a comparison is made to a similar technique for the linear detection of diffusion-controlled processes in convected mass-transfer systems.

PARAMETER: Rotational and Vibrational Temperature

REFERENCE: 134

ABSTRACT: The flourescence stimulated by a high energy ion beam is examined for application in the determination of the rotational temperature, vibrational temperature. and species concentration of molecular oxygen in high enthalpy wind tunnel flows. The theoretical analysis of the relevant excitation-emission process is discussed. An ion generator which delivers a beam of hydrogen ions with energy up to 30 kev and beam currents near 50 μamp is described and the operating characteristics of the system are summarized. Results of a spectroscopic study of the light emitted from ion impact on molecular oxygen at pressures up to 0.200 torr are presented. The predominant radiation is from 0^+ and from the first negative emission system of $0_2{}^+$. Calibrations of the variation of the intensities of the bands in the (2,0) and (1,0) progressions in the first negative system near 5500 Å are discussed. It is shown that the band intensity-pressure variation is linear at pressures less than 0.040 torr; at higher pressures, collision quenching and the loss of ions through charge exchange with 0_2 cause severe nonlinearity in the variation of progression

intensity with pressure. However, examination of the ratio of the band intensities indicates no preferred quenching of the vibrational energy levels in the upper electronic energy state of the 0_2 ion at pressures up to 0.200 torr. The results of this study indicate that the determination of the concentration of molecular oxygen in an arbitrary gas mixture by measuring the intensity of the 0_2^+ first negative emission induced by high-speed ions is limited to densities less than that corresponding to 0.040 torr at room temperature. However, O_2 vibrational temperature measurements appear to be possible at much higher density levels.

PARAMETER: Stagnation Temperature

REFERENCE: 135

ABSTRACT: A single stagnation temperature probe is described which eliminates the conduction loss problem and promises to be a useful investigative tool. The probe consists of a 6.35-mm-diam copper shell, a 1.59-mm-diam fiber glass insert, a 0.64-mm-diam Chromel®-Alumel® thermocouple junction in the fiber glass insert at the stagnation point, and a second thermocouple in the copper shell at the shoulder of the probe. When the probe is inserted in the flow the shoulder temperature is lower than the tip temperature because of the variation of the recovery factor in the probe vicinity. This temperature gradient would result in heat loss by conduction from the stagnation point if it were not for a resistance heater located in the probe which is capable of equalizing the shoulder and tip temperature. Therefore, as long as radiation can be neglected, the thermocouple at the tip will then give the true adiabatic recovery temperature.

PARAMETER: Temperature Measuring Techniques in General

REFERENCE: 136

ABSTRACT: Suitable methods for making temperature measurements in fast-moving gas streams are discussed along with the fundamental

problems involved. Various factors which affect the reliability of thermocouple data—e.g., flow stagnation, protection against radiation, and suitable selection of materials—are evaluated. The possibility of extending the upper measuring range of thermocouples is discussed. It is suggested that the pneumatic pyrometer is well suited to measuring temperatures which are above the limits of thermocouples. Optical spectroscopic temperature measurements are covered with emphasis on procedures that give satisfactory results in aircraft and spacecraft propulsion under adverse environmental conditions. Included in the study are emission-absorption systems and a method by which the temperature can be determined from the peak intensity of a spectral line.

PRESSURE

PARAMETER: General Experimental and Theoretical Rocket Exhaust Impingement Analysis

REFERENCE: 137

ABSTRACT: Experimental and theoretical correlations of pressure and heating rate were obtained under a wide variety of test conditions for rocket exhausts impinging on flat plates and curved panels. Axisymmetric real-gas exhaust plumes were generated using the method of characteristics and equilibrium chemistry to provide input to the heating and pressure analysis. Impingement pressures were calculated using both a relieved-boundary approach and the Newtonian impact theory for strong- and weak-shock interaction regions. Heating rates in the weak-shock region were obtained using various methods, including a turbulent iteration method and the Spalding and Chi turbulent skin-friction method. A modification of an equation given by Fay and Riddell was used in the strong-shock region. The results showed that pressures and heating rates can be predicted satisfactorily.

PARAMETER: Low Pressure Measurement as the Result of Rocket Exhaust Expansions Impinging upon a Surface at High Altitudes

REFERENCE: 138

ABSTRACT: Model surface impingement pressure levels attributable to expanding rocket exhaust plumes at high altitude are measured with CAL-fabricated piezoelectric pressure transducers. Although several different transducer designs exist, all of these instruments are approximately the same size, measuring 3/8 in. in diameter by about 1/4 in. deep. The transducers are internally acceleration compensated by means of a second diaphragm and crystal assembly not exposed to the pressure input. For pressure on the order of 0.0005 psia. the signal level for this instrument is about 1 mv.

RANGE: Pressures on the order of 0.0005 psia

NOMINAL PRESSURE SENSITIVITY: 2000 mv/psi

RESPONSE TIME: 200 μsec

PARAMETER: Direct Pressure Measurement

REFERENCE: 139

ABSTRACT: Design and fabrication details of a pressure transducer are given, with particular attention to the sensing element—a strain-gaged diaphragm. The transducer is inexpensive and easily made, and incorporates a simple means of changing its range.

LIMITATIONS: Calibration necessary. For fluctuating pressures the static calibration is applicable if the frequency of the applied pressure is well below the fundamental natural frequency of the diaphragm, otherwise a dynamic calibration should be made.

RANGE: 0-100 lb/in.^{2} (overloads to 200 lb/in.^{2})

ACCURACY: Approximately 3 percent of full scale

PARAMETER: Indirect Pressure Measurement

REFERENCE: 140

ABSTRACT: A convection Pirani vacuum gage covering the 1- to 1000-millibar range is described. It works in forced convection and Pirani modes for the high and low pressure ranges, respectively. Both effects combine in the intermediate zone. Light weight, small power consumption, low temperature shift, and easy telemetering of information have been considered essential in the design.

LIMITATIONS: Calibration necessary

PARAMETER: Pressure and Velocity Amplitudes of Sound Waves in Media

REFERENCE: 141

ABSTRACT: An interferometric method for measuring light diffraction spectra of phase gratings produced by ultrasonic sound waves traveling in media is described. The diffracted light beam is heterodyned by the reference light beam coming from the same He-Ne gas laser as for the diffracted beam. Since the frequency of the diffracted beam is shifted according to that of the ultrasonic waves and the spectral order, the spectra are obtained by measuring the beats between two beams.

Clear spectra were obtained for the waves traveling in water and the method will have various applications, such as exact measurements of the velocities and the pressure amplitudes of sound waves in media.

LIMITATIONS: Laser must operate in a single resonant mode. Any nonuniformity of the reference light intensity on the focal plane cannot be tolerated.

PARAMETER: Indirect Gas Pressure Measurement

REFERENCE: 142

ABSTRACT: Two (positive and negative) modulation methods are investigated as a means to reduce the lower pressure measurable with a Bayard-Alpert gage. It is concluded from the results that the negative potential modulation method is considerably better than the positive one, since the x-ray photocurrent is not modulated and pressure burst is decreased in the change of modulator potential.

RANGE: The measurements were carried out from 10^{-9} to 10^{-12} torr.

DENSITY

PARAMETER: Particle size and count

REFERENCE: 143

ABSTRACT: An electro-optical instrument for detecting and counting airborne dust particles is described. The instrument operates by measuring the light scattered from individual particles passing within a continuous air sample flow through the view-volume of an optical system. The design of the optics makes the size detection relatively independent of particle shape or material properties. Particles from 0.3 to over 10 microns can be detected and sized. The instrument is capable of monitoring concentrations to 10^6 particles per cubic foot. Performance and experimental data are reviewed. This instrument as described is presently being produced by Bausch and Lomb as Dust Counter Model 40-1.

SAMPLING RATE: 0.01 ft^3 in 100 sec (0.17 liter/min)

PARTICLE SIZE RANGE: 0.3, 0.5, 1.0, 2.0, 3.0, 5.0, 10 microns

MAXIMUM CONCENTRATION MEASURABLE: 10^6 particles/ft^3 (35 x 10^3 particles/liter)

MEASURING TIME: Once the sample draw or flow is initiated, monitoring is continuous.

ACCURACY: 10 percent

PARAMETER: Number Density of Ions and Neutrals Within a Flowing Plasma

REFERENCE: 144

ABSTRACT: Plasma densities were measured in the exhaust stream of a repetitively fired coaxial plasma gun. Species in the exhaust were identified and their density and velocity profiles were obtained. The experimental results were compared with those anticipated on the basis of existing theoretical models. The results also were

found to be in substantial agreement with conclusions reached from other measurements such as thrust. mass flow, and total energy in the exhaust stream. The measuring techniques that were involved were as follows: For the xenon neutral atoms, vacuum ultraviolet (VUV) absorption spectroscopy: for the xenon ions (and also impurity ions), a Langmuir probe biased to collect ions; and for particle identification of luminous species in the exhaust. emission spectroscopy in the VUV region. The number density of the xenon ions turned out to be marginally low for optical detection and. furthermore. the background light source produced ion lines of sufficiently low intensity so that pulse sampling would have been required to obtain the desired results.

A principal result was the observation that a large pulse of xenon atoms (energy range, 1 to 10 ev; density $\approx 2 \times 10^{19}$ m^{-3}) emerged under two different operating conditions when xenon ions (density $\approx 5 \times 10^{18}$ m^{-3}) emerged at energies of about 24 ev and 1000 ev, respectively.

PARAMETER: Atomic and Molecular Beam Intensities

REFERENCE: 145

ABSTRACT: The two methods most often used in molecular and atomic beam experiments to determine beam intensities are a measure of the pressure increase in a small volume or the use of a mass spectrometer. The latter method is most often used (Ref. 99) but requires frequent calibration because of the sensitivity changes. Condensable beams can be detected by weighing the condensed matter.

This technique offers a new and different approach to this measurement. The beam intensity is measured by the momentum the particles give to a target on a sensitive tension balance. Accommodation coefficients need not be known.

RANGE: Beam intensities of 10^{14} particles $\cdot$ cm^{-2} $\cdot$ sec^{-1} have been measured.

SENSITIVITY OF THE BALANCE: 21.1 rad/dyne (in a dynamic mode the sensitivity can be increased by a factor of 50)

ACCURACY: 3 percent

PARAMETER: Electron Density and Temperature

REFERENCE: 146

ABSTRACT: It is observed that probe surface conditions are very important in low-density. low-temperature ($Ne < 10^7$ cm^{-3}, $T_c < 10^3$°K) plasmas. Errors are caused by variations of the work functions over the probe surface and by insulating layers such as oxides or hydrocarbons. It is the purpose of this communication to show that reliable Langmuir probe measurements can be obtained if the probe surface is carefully cleaned. The method found most successful is a discharge cleaning which sputters off the contaminants.

PARAMETER: Gas Density

REFERENCE: 147

ABSTRACT: A gage for the measurement of the density variation in a shock wave is described. It is based on the absorption of low energy beta radiation from an ^{169}ER source. The gage was used to study the density variation through the contact zone between the expansion chamber gas and the driver gas of a value driven shock tube.

LIMITATIONS: Source material has a relatively high degree of radioactivity and oxidizes in the presence of moisture; also, the half-life of ^{169}ER is only 9.5 days. Calibration is necessary.

RANGE: Several atmospheres

MEASURING TIME: On the order of nanoseconds depending on electronics

ACCURACY: Approximately 5 percent

PARAMETER: Ionization Density and Electron Temperature

REFERENCE: 148

ABSTRACT: A floating double probe operating at radio frequencies in the megahertz range has been developed which relies on measurements of sheath capacitance and resistance to yield values for plasma ionization density and electron temperatures. The experimental technique used supersedes previous methods in that it enables sheath capacities as low as 10^{-2}pf to be measured. The analysis of the results has been extended to cover the important nonplasmas (cylindrical) sheath case. As a result of these two developments. the technique is now applicable to small diameter probes which are essential for measurements in most gas discharge plasmas. The performance of the probes has been checked over a range of plasma densities and working frequencies and has been found to give results which are in good agreement with microwave cavity and dc probe measurements. This type of measurement has various advantages over the usual dc probe methods in terms of complete isolation, but it is expected that its main application will be in situations where the use of the dc probe is suspect because of probe surface contamination effects.

MEASURING TIME: Microseconds

ACCURACY: Plasma ionization density ≈ 8 percent
Electron temperature ≈ 16 percent

PARAMETER: Density Gradients

REFERENCE: 149

ABSTRACT: A superradiant pulsed neon laser operating at 5401 Å was used to obtain interferograms of the flow through nozzles in a shock tunnel. This laser has a number of unique features which make it particularly convenient to use in such an application. First, it has a 3-nsec pulse duration and sufficient energy to expose film with a single pulse (30μ J). This provides a stop-action capability that is useful in studying time-varying systems, such as gas flows, and also makes it insensitive to laboratory vibrations in static system studies. In contrast to other pulsed laser systems, however, it can also be pulsed repetitively at up to 100 pulses/sec, thereby giving an apparently continuous visual display of the system under study. In addition the pulsed neon laser has a 30-cm coherence length which permits interferometry with the need for extreme care in balancing the two optical paths; it is also useful in doing holography with scenes of moderate size.

SENSITIVITY: Sensitive to density variations of approximately 15 μ gm/cm^3

MEASURING TIME: Nanoseconds

PARAMETER: Density Gradients and Flow Visualization

REFERENCE: 150

ABSTRACT: A 20-in. (51-cm)-diam schlieren system was converted to a generalized holographic flow visualization system. The system has been used successfully in producing the following types of visualization from a single holographic plate: three-dimensional photography, variable focus shadowgraph, variable knife-edge position schlieren, color schlieren, and interferometry. All of these except for holographic color schlieren have previously been reported with varying degrees of success. This paper presents a technique for producing color schlieren photographs from holograms formed in the above system and shows preliminary results of the application. The method possesses a number of advantages over conventional color schlieren photography.

LIMITATIONS: Requires careful system maintenance for the prevention of interference and diffraction noise associated with the use of temporally coherent light. Interference also occurs between different parts of the wave as it traverses the field of interest, and a complete analysis of these effects must be completed before the full potential of coherent schlieren methods can be realized.

SENSITIVITY: Potentially, holographic schlieren offers a considerably higher sensitivity in practice, especially for larger systems, because the knife-edge is not required during the initial data recording.

PARAMETER: Species Concentration Variation

REFERENCE: 151

ABSTRACT: An extension of the two-wavelength interferogram technique is proposed that will enable selective measurements to be made of the variation in the density of a specific atomic population. One wavelength should be chosen to closely coincide with the wavelength associated with an absorption line of the species of interest, whereas the other wavelength should be displaced by several angstroms from the line. The difference between the fringe shifts on the two interferograms would then enable the density variation of the specific atomic population of interest to be measured with high sensitivity. Two criteria are established that ascertain for any system the minimum density that could be detected, and the range in density variation for which the interferograms should be discernible.

PARAMETER: Species Analysis—Ion Number Density

REFERENCE: 152

ABSTRACT: A quadrupole mass spectrometer was used to sample the gas in the precursor region of an advancing shock through a very small hole on the side of a shock tube. Because of the pressure difference in the shock tube, 2 torr as compared to 10^{-6} torr in the mass spectrometer chamber, a steady jet of particles will be issuing from the hole in the shock tube in the direction of the ionization chamber and analyzer. Since the gas in front of the shock is already ionized because of the radiation emanating from behind the shock, the ionizer of the mass spectrometer was eliminated by disconnecting the heating current from the filament. Thus a neutral particle issuing into the quadrupole

mass spectrometer would not cause any response. On the other hand, an incoming ionized particle would cause a response if the amplitudes of the dc and rf fields of the quadrupole analyzer were preset for the corresponding mass of the incoming ion. If, however, the amplitides were preset for a given mass number and no ions of this mass number were present in the jet issuing into the mass spectrometer, no response could be expected. In this way it is possible through repeated tests of the same initial conditions to scan through the whole mass range and determine the presence or absence of all ionized particles. If the mass spectrometer is also calibrated, it should be possible to determine quantitatively the contribution of each particular impurity to the total ion or electron number density.

PARAMETER: Gas or Molecular Density Measurements

REFERENCE: 153

ABSTRACT: A rocket-borne system to measure air density by detecting Rayleigh-scattered light from an onboard light source is described. The system utilized a high intensity mercury arc lamp to produce a modulated light beam. Light scattered from air molecules in a portion of the light beam beyond the disturbances caused by the sounding rocket was viewed by an optical system. Details of the instrumentation and flight results are discussed. Based on the findings of this flight a second proposed payload will utilize the 2537Å Hg line for increased scattering and reduced background light.

LIMITATIONS: In the optical band selected (3500 to 4500Å) the background noise level limited data accuracy along with the stability of the light intensity output of the mercury arc source.

RANGE (Covered in Experiment): Number density from 10^{22} to $10^{28}\,m^{-3}$

PARAMETER: Neutral Molecular Densities and Species Analysis

REFERENCE: 154

ABSTRACT: The formation of a molecular beam in sampling 1 torr to 1 atm gases (Ar or H_2) is studied for three diameters of the sampling orifice. To modulate the beam, use is made of a mechanical chopper placed very near the sampling orifice. This enables the measurement of the scattering of the beam by collisions between beam molecules. From the measurements it follows that these collisions are very important for sampling orifice diameters greater than 0.020 mm at an initial pressure of 1 atm. The consequences of the results are discussed for mass spectrometric studies of flames.

PARAMETER: An Analytical Study of Density Profiles

REFERENCE: 155

ABSTRACT: The prediction of forces resulting from plume impingement, in addition to knowledge of the gas-surface interaction properties, requires a reasonably accurate description of density profiles in the far field of the plume (i.e., tens of nozzle-exit radii downstream). This Note describes an analytical method for obtaining these profiles which is more accurate than those presently available.

PARAMETER: Particle Density, Size, and Size Distribution

REFERENCE: 156

ABSTRACT: In holography since motion tolerance is a function of incident radiation wavelength (the greater the wavelength the greater the motion tolerance, hence greater particle speeds can be resolved), it would be a distinct advantage to apply the technique at longer wavelengths. With this criterion in mind the following abstract should be considered:

Infrared holography at 10.6 μm has been accomplished by using a thermochromic material, cuprous mercuric iodide, to record an on-axis interference pattern. The pattern is subsequently reduced in a two-step photographic process, and reconstruction is accomplished in the visible spectrum with He-Ne laser light.

PARAMETER: Individual Molecular Specie Density Measurements

REFERENCE: 157

ABSTRACT: A beam of electrons is oscillated through a plane of the flow field using a magnetic deflection coil located downstream from the defining orifice of the electron gun. An image of the emission resulting from collisions between the beam electrons and the gas molecules which is passed through a narrow bandpass spectral filter is formed by a focusing lens onto the face of the image intensifier tube. A photograph of the output of the tube is analyzed to determine the individual specie density distribution throughout the plane of the flow field defined by the oscillating electron beam. The instrumentation requirements of the visualization technique include: (1) a method of deflecting the beam of electrons through the flow field, (2) a detector system with the necessary time resolution, sensitivity, spectral characteristics and linearity, and (3) controlled processing of the resulting photograph.

LIMITATIONS: Calibration procedure necessary to obtain the relationship between film blackening and light intensity. For meaningful results should be applied in the gas density region in which the fluorescence intensity is linearly proportional to the gas density and electron beam current.

RANGE: Free-stream nitrogen densities of 4×10^{16} to 2×10^{17} molecules/cm^3 were measured; also helium densities of 10^{15} to 10^{16} molecules/cm^3 were measured using this technique.

MEASURING TIME: Total exposure time of 5 msec

PARAMETER: Gas Density Measurements

REFERENCE: 158

ABSTRACT: A method is developed to obtain quantitative density data from a schlieren measurement system. The necessary hardware has been developed along with the complementary data reduction scheme. Present results are limited to axisymmetric flow outside the schlieren diffraction bands. A comparison of experimental data versus a Taylor-Maccoll analysis for a supersonic conical flow field is presented. The technique is presently being extended into the diffraction region to allow measurement of boundary-layer and other surface phenomena.

LIMITATIONS: Calibration is necessary.

PARAMETER: Electron Number Density in a Hypersonic Flow

REFERENCE: 159

ABSTRACT: An experiment to measure the electron concentration in a hypersonic flow is described. The experimental method, two-wavelength interferometry, is based on the fact that the refractivity of the heavy polarizable particles (atoms and ions) is practically independent of wavelength, whereas the refractivity for free electrons is proportional to the square of the wavelength and negative. A Mach-Zehnder optical interferometer backlighted by a giant pulse ruby laser is used. In this particular application the flow is a hypersonic high energy flow of argon over a 2-in.-diam spherical body.

RANGE: The free-stream velocity was 5180 m/sec. At a free-stream density of approximately 0.024 kg/m^3 and a free-stream pressure of approximately 3.64×10^3 N/m^2, the electron number density at the stagnation point was approximately $4 \times 10^{17}/cm^3$.

PARAMETER: Mass Spectrometric Analysis

REFERENCE: 160

ABSTRACT: An aerodynamically shaped probe has been developed for instantaneous mass spectrometric analyses of gas samples taken from low density, high enthalpy, hypersonic flows. The requisite 10^{-5} torr operating pressure for a quadrupole mass spectrometer mounted in the water-cooled probe was established and maintained by a liquid-hydrogen cryopump. During an initial series of 5-min tests, the detected composition of an arc-heated airflow with a stagnation condition of approximately 10 atm at 3000°K agreed well with a nonequilibrium flow expansion calculation. The probe admitted a chemically undisturbed rarefied hypersonic flow sample to its interior by assuring an attached shock.

RANGE: The test environment (nozzle exit conditions) were static pressure, about 1.4×10^{-2} torr; static temperature, approximately 80°K; and static density, 1.08×10^{-4} amagats. The flow velocity was 2680 m/sec, with a Mach number of 14.85.

MEASURING TIME: The sweep time, or display time, for the desired range of mass-to-charge ratio values could be set from 50 msec to 30 min.

PARAMETER: Measurement of Electron Density and Collision Frequency in a Plasma

REFERENCE: 161

ABSTRACT: It is demonstrated that the electron density and the collision frequency in a plasma can be determined by using a 337-m CW maser as a source for a Mach-Zehnder interferometer containing the plasma in one of its arms. Plasmas having electron densities ranging from 10^{19} to $10^{21}/m^3$ and electron collision frequencies from 3×10^{10} to 3×10^{12}/sec are shown to be particularly suitable for diagnosis in this manner.

MEASURING TIME: A Golay cell detector was used with a response time of about 10 msec, but a Putley indium antimonide detector can be used which has a temporal resolution of a microsecond.

PARAMETER: Turbulence Properties

REFERENCE: 162

ABSTRACT: A new optical crossed-beam technique was used to measure the turbulence properties of two supersonic, shock-free, cold air jets. The method as used here is based on the absorption of ultraviolet radiation by air. The measurements were highly successful in that reasonable and consistent values of the turbulence properties such as convection speeds, length scales, and spectra were obtained, and the data generally followed the trends set by hot-wire measurements in subsonic jets. The most interesting feature of the crossed-beam technique which was investigated in these experiments is the possibility of a direct measurement of three-dimensional spectral density. However, the demonstration that the crossed-beam technique can be used for turbulence measurements in supersonic flow is considered to be the major accomplishment of these experiments.

VELOCITY

PARAMETER: Speed Distribution and Density of a Molecular Beam

REFERENCE: 163

ABSTRACT: A method for determining the speed distribution and density of a molecular beam from time-domain measurements of propagated beam perturbations is examined. Algebraic relations between the moments of the measured time-of-flight signal, of the speed-distribution function, of the modulator gate function, and of the dynamic function of the detector and its electronics are derived. By extracting a sufficient number of moments, one can characterize any speed-distribution function to any desired accuracy. For use in applications, moments and recursion relations of a general class of speed-distribution functions and moments of some typical gate functions are developed. Sufficient conditions for approximating a rectangular gate function by an impulsive gate function are presented. An application to time-of-flight measurements in an arc-heated supersonic molecular beam illustrates the use of the general method and emphasizes the need to consider the characteristic time of the gate function and the dynamic response functions of the detector and its electronics when interpreting time-of-flight signals.

PARAMETER: Velocity/Electrical Conductivity Profile

REFERENCES: 164 and 165

ABSTRACT: During the initial work an instrument was developed which has a linear response to the magnetic field induced by the flow of a conducting medium through the applied magnetic field. This meter was designed to measure the conductivity of ionized air. In a subsequent investigation measurement of the electrical conductivity/velocity profile of a plasma sheath appears possible by the use of transducers of suitable design. A transducer is characterized by a set of influence functions. Mathematical criteria are established to measure the degree of independence of these functions. Three transducers are described and the performance of each is analyzed. Results of the measurement of a known conductivity/velocity profile are discussed.

LIMITATIONS: Calibration necessary

RANGE: Typical nominal values are as follows: for the electrical conductivity, 50 mhos/m; for the velocity, 400 m/sec.

MEASURING TIME: Continuous readout—response to an impulse function could be on the order of nanoseconds depending on the associated electronics.

ACCURACY: 18 percent for the measurement of the product of electrical conductivity and velocity.

PARAMETER: Particulate Velocities

REFERENCE: 166

ABSTRACT: A system analysis of the feasibility of optical heterodyne measurement of Doppler shifts as a method for the remote determination of vector wind velocity is carried out. It is found that with a 50-mw laser at 6328 Å, naturally occurring aerosols in clear air will permit measurements at distances of only a few tens of centimeters, but haze and dust will extend this range to a few tens of meters and fog to 75 meters. By generating smoke to enhance the scatter, a range of about 40 meters will be achievable. The use of a 1-watt argon laser will extend the clear-air and smoke-plume ranges by a factor of 48 and the ranges in uniform dust or fog by smaller amounts. Excellent condensed treatment of the practical aspects of the optical heterodyne measurement of the frequency shift of scattered light using the Doppler effect.

LIMITATIONS: Particle size lower limit is 0.1 μm.
Particle velocity is approximately 3000 ft/sec maximum.

RANGE: 0 to 30 miles/hr wind velocities considered in text. Technique should extend to 3000 ft/sec with existing electronics.

SENSITIVITY: Volumes as small as 10^{-6} cm^3 can be examined at a distance of a meter or more. Particle size considered is from 0.1 to 3 μm

PARAMETER: Plasma Velocity

REFERENCE: 167

ABSTRACT: Experimental results are presented from a program conducted to develop a noninterference method for obtaining the velocity of a supersonic high enthalpy plasma seeded with an alkali metal. The technique used was the time-of-flight measurement of a tracer spark produced in the plasma by an electric spark discharge (two pointed electrodes) and by a focused pulse laser. The tracer spark was photographed with a streak and framing camera or an image-converter camera at preselected delay times to obtain the time-of-flight velocity measurements. The experimental work was accomplished in air and nitrogen plasmas at a static pressure of about 1 atm and at total enthalpies up to 2700 Btu/lb. Velocities were measured up to 2600 m/sec. The techniques are described, and the problems and results are discussed.

LIMITATIONS: There is apparently no practical upper velocity limit, but a lower velocity limit of approximately 1000 ft/sec exists because of the spark duration. High values of plasma conductivity produce spark diffusion for the electric spark discharge technique.

MEASURING TIME: On the order of microseconds

ACCURACY: Electrode spark, ±5 percent
Laser spark, ±3 percent

PARAMETER: Longitudinal Gas Flow Velocity

REFERENCE: 168

ABSTRACT: The speed of flow in a capacitance-driven, spark-heated, hypersonic wind tunnel was measured by means of schlieren pictures of the rate of displacement of a disturbance produced by a spark discharge in the gas stream.

RANGE (over which technique was applied): Velocity: 5000 to 10,000 ft/sec
Density: 4.6×10^{-4} to 2.77×10^{-3} amagats
Temperature: 30 to 80°K

MEASURING TIME: On the order of microseconds

ACCURACY: Approximately 8 percent

PARAMETER: Time-Resolved Studies of Particle Dynamics

REFERENCE: 169

ABSTRACT: An experiment to record a holographic motion picture is described. The source of illumination is a CW ruby laser operated in the repetitively Q-switched mode. The film was recorded at the rate of 20 frames per second on 100 ft of 70-mm film, transported by a convential 70-mm sequential-still camera. Other applications for the technique are: motion-picture holomicroscopy and time-resolved holographic interferometry.

PARAMETER: Velocity, Size, and Position of Particulate Matter in a Low Density Flow

REFERENCE: 170

ABSTRACT: This article describes a new technique for determining the size, velocity, and position of particles in a moving stream of restricted flow volume. The system is based on the use of an afocal tilted film plane optical arrangement using a pulsed light source for imaging. The technique described is based upon a particular device, but detailed investigations are required in certain areas to determine the characteristics of the light source and imaging system for various applications.

LIMITATIONS: The particle velocity limitations are imposed by the available pulse repetition frequency and pulse length of the light source. Particle size limitations are constrained by the modulation transfer function of the combined optical system and recording media.

RANGE: Particle size: 5 μm to several millimeters
Particle velocity: several cm/sec to over 10^6 cm/sec (providing the energy density required for exposure of the recording media can be maintained)

MEASURING TIME: On the order of microseconds

ACCURACY: 5 to 10 percent

PARAMETER: Particle Velocity and Size

REFERENCE: 171

ABSTRACT: An experimental technique for obtaining the spatial size and velocity distributions for liquid or solid aerosols suspended in an air flow is described. The technique leaves the flow undisturbed and allows a large range of particle sizes and velocities. The successful combination of a Q-spoiled ruby laser and holography was employed to record the desired information. A helium-neon laser was used to reconstruct the magnified image which was analyzed using closed-circuit television.

UNCLASSIFIED

Security Classification

DOCUMENT CONTROL DATA - R & D

(Security classification of title, body of abstract and indexing annotation must be entered when the overall report is classified)

1. ORIGINATING ACTIVITY *(Corporate author)*
Arnold Engineering Development Center
ARO, Inc., Operating Contractor
Arnold Air Force Station, Tennessee 37389

2a. REPORT SECURITY CLASSIFICATION
UNCLASSIFIED

2b. GROUP
N/A

3. REPORT TITLE
SURVEY OF INSTRUMENTATION APPLICABLE TO THE STUDY OF ROCKET EXHAUST PLUMES

4. DESCRIPTIVE NOTES *(Type of report and inclusive dates)*
Final Report, November 1969 to March 1970

5. AUTHOR(S) *(First name, middle initial, last name)*
C. H. Fisher, ARO, Inc.

6. REPORT DATE	7a. TOTAL NO. OF PAGES	7b. NO. OF REFS
May 1971	119	171

8a. CONTRACT OR GRANT NO.	9a. ORIGINATOR'S REPORT NUMBER(S)
F40600-71-C-0002	
b. ~~XXXXXXXX~~. Program Element 921E	AEDC-TR-71-45
c. NASA-Defense Purchase Request No. H-58562A.	9b. OTHER REPORT NO(S) *(Any other numbers that may be assigned this report)*
d.	ARO-VKF-TR-70-295

10. DISTRIBUTION STATEMENT
This document has been approved for public release and sale; its distribution is unlimited.

11. SUPPLEMENTARY NOTES	12. SPONSORING MILITARY ACTIVITY
Available in DDC.	NASA-MSFC, S & E-AERO-AF, Huntsville, Alabama 35812

13. ABSTRACT

A review of measuring techniques and instrumentation which may be of use in the study of rocket exhaust plumes is presented in a twofold manner. The most practical techniques which have proven successful through actual application in rocket exhaust studies or related environments are treated in an integrated fashion within a plume analysis framework. An additional descriptive collection of appropriate techniques and instrumentation have been compiled into an appendix. This report is organized around those measurements considered most important: temperature, pressure, density, and velocity.

This document has been approved for public release and sale; its distribution is unlimited.

DD FORM 1 NOV 65 1473

UNCLASSIFIED

Security Classification

14. KEY WORDS	LINK A		LINK B		LINK C	
	ROLE	WT	ROLE	WT	ROLE	WT
plumes						
electron beams						
temperature						
pressure						
density						
hypersonic flow						
instrumentation						
velocity						

AFSC
Arnold AFS Tenn